Characterization of Pathway Specific Inhibitor Response in Pancreatic Ductal Adenocarcinoma *in vitro* Models with Different Genetic Backgrounds

Cumulative Dissertation

to obtain the academic degree

Doctor of Medical Sciences (Dr. rer. hum.)

of Rostock University Medical Center

aus der Universitätsmedizin Rostock

Zentrum für Innere Medizin

Medizinische Klinik III – Hämatologie, Onkologie und Palliativmedizin

Direktor: Prof. Dr. med. Christian Junghanß

Submitted by

Yixuan Ma,

born on 24 June 1991, Zhumadian, Henan, China

from Rostock

Rostock, 26 September 2022

https://doi.org/10.18453/rosdok_id00004330

Erster Gutachter: Prof. Dr. Christian Junghanß
Universitätsmedizin Rostock
Medizinische Klinik III - Klinik für Hämatologie, Onkologie, Palliativmedizin
Universität Rostock
18057 Rostock

Zweiter Gutachter: PD Dr. Matthias Sendler
Universitätsmedizin Greifswald
Klinik und Poliklinik für Innere Medizin A
Universität Greifswald
17475 Greifswald

Dritter Gutachter: Prof. Dr. med. Robert Jaster
Universitätsmedizin Rostock
Klinik für Innere Medizin II - Abteilung Gastroenterologie und Endokrinologie
Universität Rostock
18057 Rostock

Eingereicht am: 29.10.2022

Datum der Verteidigung: 06.06.2023

Original work of the cumulative dissertation

The results of the dissertation presented here have been published in peer-reviewed journals with impact factor points.

Work I

Inhibitory Response to CK II Inhibitor Silmitasertib and CDKs Inhibitor Dinaciclib Is Related to Genetic Differences in Pancreatic Ductal Adenocarcinoma Cell Lines

Ma, Y.; Sender, S.; Sekora, A.; Kong, W.; Bauer, P.; Ameziane, N.; Krake, S.; Radefeldt, M.; Al-Ali, R.; Weiss, F.U.; Lerch, M.M.; Parveen, A.; Zechner, D.; Junghanss, C.; Murua Escobar, H.

Int. J. Mol. Sci. **2022**, *23*, 4409. https://doi.org/10.3390/ijms23084409

Impact Factor 2022: 5.924

Work II

The Inhibitory Response to PI3K/AKT Pathway Inhibitors MK-2206 and Buparlisib Is Related to Genetic Differences in Pancreatic Ductal Adenocarcinoma Cell Lines

Ma, Y.; Sender, S.; Sekora, A.; Kong, W.; Bauer, P.; Ameziane, N.; Al-Ali, R.; Krake, S.; Radefeldt, M.; Weiss, F.U.; Lerch, M.M.; Parveen, A.; Zechner, D.; Junghanss, C.; Murua Escobar, H.

Int. J. Mol. Sci. **2022**, *23*, 4295. https://doi.org/10.3390/ijms23084295

Impact Factor 2022: 5.924

Work III

Inhibition of KRAS, MEK and PI3K Demonstrate Synergistic Anti-Tumor Effects in Pancreatic Ductal Adenocarcinoma Cell Lines

Ma, Y.; Schulz, B.; Trakooljul, N.; Al Ammar, M.; Sekora, A.; Sender, S.; Hadlich, F.; Zechner, D.; Weiss, F.U.; Lerch, M.M.; Jaster, R.; Junhanss, C.; Murua Escobar, H.

Cancers **2022**, *14*, 4467. https://doi.org/10.3390/cancers14184467

Impact Factor 2022: 6.575

Content

1 Introduction

Pancreatic ductal adenocarcinoma (PDAC) accounts for approximately 90% of malignancies of pancreatic origin [1]. The PDAC is originated within the part of the pancreatic cells that produce digestive enzymes, and then multiply out of control and form mass [2]. PDAC is conservatively estimated that in 2020, there were 446,000 newly diagnosed PDAC patients and 419,000 deaths worldwide [3]. Currently, PDAC remains one of the most aggressive human cancer types and is currently the fourth leading cause of cancer-related death in both men and women [4]. Without treatment, the median survival time of patients with metastatic pancreatic cancer is only 3 months and the overall 5-year relative survival rate for PDAC is only 10% [5-9]. Risk factors for PDAC include age, gender, area, blood group, diabetes, obesity, pancreatitis, smoking, *etc.* (Figure 1). [3, 10-17].

Figure 1

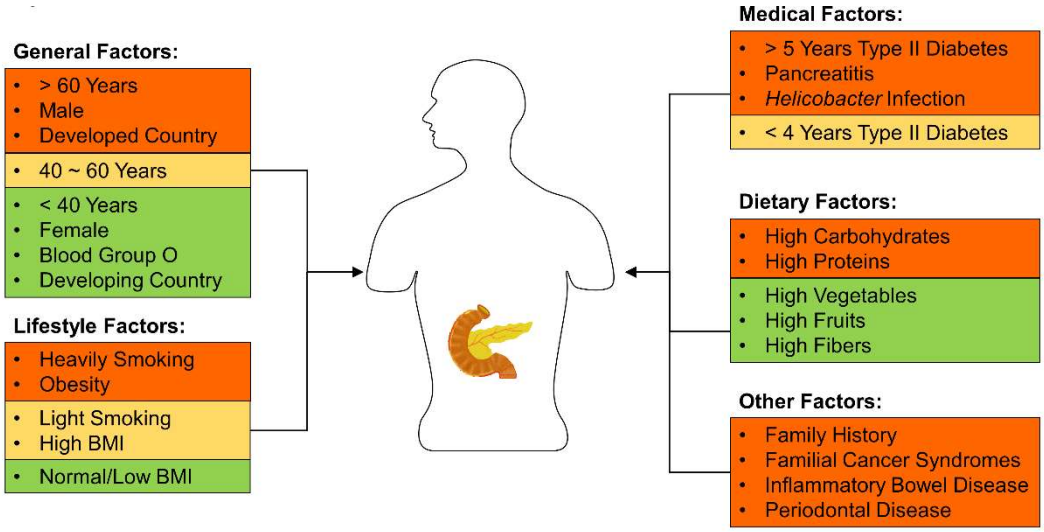

Figure 1: List of high (orange), moderate (yellow) and low (green) risk factors for PDAC.

1.1 Genetic Aberrations of PDAC

Genetic factor is an important risk factor for PDAC, about 5% - 10% of pancreatic cancers have a familial genetic background, and family history greatly increases the risk of first-degree relatives [18]. According to a prospective study, first-degree relatives of people with familial pancreatic cancer have a nine-fold higher risk of developing PDAC than the general population [19]. In addition, some germline or somatic mutations also contribute to the development of PDAC, the proto-oncogene *KRAS* and the tumor suppressor gene cyclin dependent kinase inhibitor 2A (*CDKN2A*) are present in more than 90% of PDAC [20-26]. Another tumor suppressor gene, tumor protein p53 (*TP53*), was also found to be mutated in about 70% of PDAC [27]. Furthermore, mutational inactivation of mothers against decapentaplegic homolog 4 (*SMAD4*) occurs in approximately 55% of PDAC [28]. As sequencing technology improved, more genetic mutations were identified, and whole-exome sequencing (WES) of PDAC revealed an average of 48 non-synonymous somatic mutations per tumor [20]. Twelve core

pathways (such as KRAS signaling, DNA damage control, and cell adhesion) are altered in most PDAC [20]. Moreover, 16 significantly mutated genes in PDAC were identified, in addition to the known *KRAS*, *TP53*, *CDKN2A*, *SMAD4*, *MLL3*, *TGFBR2*, *ARID1A*, and *SF3B1*, newly found genes to be related to chromatin modification (*EPC1* and *ARID2*), DNA damage repair (*ATM*) and other mechanisms (*ZIM2*, *MAP2K4*, *NALNC*, *SLC16A4*, *MAGEA6*) [22].

Genetic changes not only exist widely in PDAC, but even participate in the whole process of transformation from acinar cells to PDAC. The acinar cells of the pancreas are highly plastic, and this plasticity is considered to be a mechanism for maintaining pancreatic homeostasis and regeneration [29]. When stimulated by risk factors, acinar cells transdifferentiate into a more epithelial (duct-like) phenotype, and the process is called acinar-ductal metaplasia [30]. During metaplasia, acinar cells acquire stem-like features that make them more susceptible to proto-oncogenes, and ultimately transform into pancreatic intraepithelial neoplasia (PanIN), a transformation that is often considered the first step in PDAC progression [31]. According to the degree of dysplasia, PanIN is divided into 4 grades, namely PanIN-1A, PanIN-1B, PanIN-2, and PanIN-3 [32]. The genetic background of mutations in each of the different grades of the transformation of these acinar cells into adenocarcinoma cells also varied. Thanks to the rapid development of sequencing technology, a gene mutation evolution model from early PanIN to PDAC has been established (Figure 2) [33-35]. Thanks to the rapid development of sequencing technology, a gene mutation evolution model from early PanIN, which is often considered the first step in PDAC progression, to PDAC has been established (Figure 2) [33-35]. *KRAS* mutation was detected in 96.4% of pancreatic intraepithelial neoplasia (PanIN)-1a/b specimens, whereas normal pancreatic duct tissue did not contain this mutation. Moreover, the proportion of *KRAS* mutant cells in PanIN gradually increased with the grade [36]. In addition, guanine nucleotide binding protein, alpha stimulating complex locus (*GNAS*) mutations also frequently appear in early PanIN, and appear earlier than *KRAS* mutations. At the same time, *GNAS* mutations are also more often found in *KRAS* wild-type PanIN, suggesting that *GNAS*

Figure 2

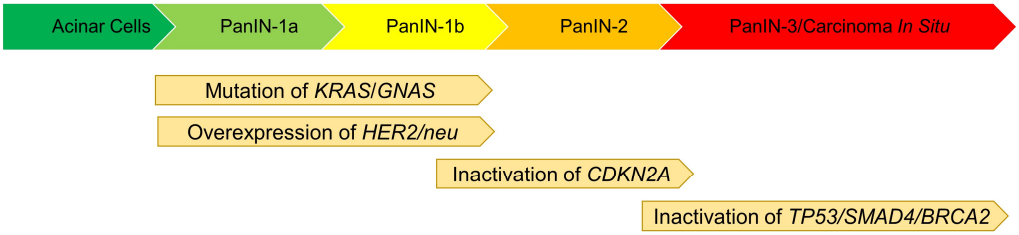

Figure 2: Gene mutation evolution model from acinar cells to PDAC.

mutations and KRAS mutations can also drive abnormal cell proliferation [31, 33]. Another gene that acts in the absence of *KRAS* mutations is human epidermal growth factor receptor 2 (*HER2/neu*). But unlike *GNAS*, which is often mutated, *HER2/neu* is often overexpressed in PanIN-1a/b [35]. Inactivation of the tumor suppressor gene *CDKN2A* appears to occur later, usually in late stage of PanIN-1b, throughout PanIN-2 and very early PanIN-3. Moreover, *CDKN2A* inactivation is often associated with severe cytological and structural atypia in ductal lesions [37, 38]. The subsequent stage is the inactivation of tumor suppressor genes *TP53*, *SMAD4* and breast cancer gene 2 (*BRCA2*) [37, 39-41]. The inactivation of these tumor suppressor genes is usually observed almost only in ductal lesions with obvious cytological and

structural, atypia (PanIN-3), or in the carcinomas *in situ* [35, 42, 43].
In addition, genetic background is also a major factor affecting the prognosis of PDAC. A study of the Cancer Genome Atlas (TCGA) database showed that a total of 1523 genes were associated with PDAC prognosis, of which 668 genes were associated with poor prognosis and another 855 genes were associated with favorable prognosis [44].

1.2 Kinases, Inhibitors and PDAC

Amplifications, deletions, translocations, inversions, frameshifts, and substitutions of genes can be identified in approximately 97% of PDAC patients [45-48]. These mutated genes in turn affect the function of proteins that lead to uncontrolled proliferation, motility and adhesion of cells, protection against apoptosis, autophagy, DNA repair problems, microsatellite instability and other processes that contribute to the development of PDAC [49]. The use of inhibitors targeting key kinases has been considered as a treatment option due to the development of small molecule inhibitors, but is not currently part of conventional chemotherapy regimens. In this section, several key kinases and their inhibitors involved in this doctoral study are presented, as well as their studies in PDAC.

1.2.1 Casein Kinase II (CK2)

Casein kinase II (CK2) consists of two catalytic subunits (α and α') and a regulatory β subunit, which typically assembles into tetrameric complexes with two catalytic and two regulatory subunits, it was first discovered in 1954 by Burnett and Kennedy [50]. CK2 are present in many cellular structures, including the nucleus, cytoplasm, plasma membrane, mitochondria, smooth endoplasmic reticulum, and Golgi apparatus [51-54]. CK2 is a highly conserved serine/threonine kinase, which is constitutively active and ubiquitously expressed in mammalian cells. CK2 has a wide range of candidate physiological targets and is involved in a series of complex cellular functions [55]. For example, CK2 activates protein kinase B (AKT) by direct phosphorylating AKT1 at Ser129 in the junction region or indirectly promotes increased AKT activity by inactivating PTEN [56-58]. The activated PI3K/AKT pathway further influences proliferation and survival [59]. In addition, CK2 upregulates JAK/STAT signaling pathway by activating JAK and RAS/MEK/ERK signaling pathway by activating ERK, providing cancer cells with survival advantage and proliferative capacity [60, 61]. Furthermore, CK2 is able to cooperate with MKK4/JNK pathway and promote the survival of PDAC cells [62]. The downregulation of CK2 via RNA interference enhances chemosensitivity to gemcitabine in PDAC cell lines [62, 63]. *In vitro* and *in vivo* experiments revealed anti-tumor activity of Silmitasertib, a CK2 inhibitor, in BxPc-3 cells [64]. CK2 specific-inhibitors also induce apoptosis of MIA PACA-2 and Dan-G cell lines [65]. However, in these experiments, different cell lines showed different responses to CK2 inhibitors. Therefore, studying the influence of genetic background on the efficacy of Silmitasertib is of considerable interest. In addition, although Silmitasertib has entered multiple clinical trials, target therapy for pancreatic cancer have not been reported [66].

1.2.2 Cyclin-Dependent Protein Kinase (CDK)

Cyclin-dependent protein kinases (CDKs) are a family of kinases containing a serine/threonine-specific catalytic core that cooperate with regulatory subunits of cyclins as critical regulators of cell cycle progression. The activity of CDKs is regulated by two families of inhibitors: INK4 family (INK4A, INK4B, INK4C, and INK4D) and the Cip and Kip family (p21, p27, and p57) [67]. The dysregulation of the cell cycle is the fundamental process of cancer growth and spread [67]. Within the CDK family, CDK1 and CDK2 regulate cell cycle progression by contributing to the phosphorylation and inactivation of the retinoblastoma (Rb) tumor suppressor gene product throughout late G1, S, and G2-M phases [68]. Another family member, CDK9, is involved in the regulation of RNA polymerase II and the control of cellular transcription [69]. CDK5 has been well characterized for its role in the central nervous system rather than the cell cycle [70]. In addition, studies have shown that CDK1 and CDK9 are also involved in the DNA damage repair process [71, 72]. Several CDK family members are highly expressed in different cancer types including PDAC [73]. Moreover, some studies indicated that CDKs play critical roles in cancer proliferation, migration, invasion, and metastasis [74, 75]. In addition, inhibition or knockdown of CDKs demonstrated satisfactory inhibition of cancer cells. Inhibition of CDK1, CDK2 and CDK9 caused cell cycle arrest [76, 77]. Activated CDKs induce resistance to cisplatin in cervical cancer and are involved in radiation resistance in lung cancer. In PDAC cell lines, inhibition of CDKs kinase activity significantly decreased the migration and invasion of cancer cells *in vitro* [74]. In addition, CDK5 inhibition promotes the chemosensitivity of PDAC cell lines to gemcitabine [74]. Combination of CDKs and AKT inhibitor showed dramatically blocked PDAC tumor growth and metastasis in animal models [75]. Moreover, based on the significant effects of CDKs inhibitors, several inhibitors Alcociclib (Flavopiridol), Dinaciclib, Ribociclib, and AT7519 have entered clinical trials against PDAC [73, 78, 79].Although the inhibition of CDKs has been shown to inhibit the viability of PDAC cell lines, the effect is highly variable depending on different cell lines and CDKs inhibitors. So far, the reasons for these differences are still not fully understood [80].

1.2.3 Phosphoinositide 3-Kinase (PI3K)

Phosphoinositide 3-kinase (PI3K) is a family of plasma membrane-associated lipid kinases, composed of three subunits: the p85 regulatory subunit, the p55 regulatory subunit, and the p110 catalytic subunit [81]. According to the different structures and functions, PI3Ks are divided into class I, class II and class III [82]. Class I PI3Ks are often closely associated with human cancers [83]. The PI3Ks involved in multiple cellular functions such as cell growth, proliferation, differentiation and intracellular trafficking [83]. PI3Ks can be activated by a variety of extracellular stimuli, such as growth factors, cytokines, and hormones, which subsequently result in phosphorylation of phosphatidylinositol 4,5-bisphosphate (PIP2) to phosphatidylinositol 3,4,5-bisphosphate (PIP3) [84, 85]. This in turn activates downstream kinases and affects cellular function. Dysregulation of the PI3K pathway, including loss or inactivation of the tumor suppressor PTEN, mutation or amplification of PI3K, and activation of tyrosine kinase growth factor receptors or oncogenes upstream of PI3K, often leads to

tumor transformation [86-88]. In PDAC, approximately 50% of the patients present increased activation of PI3K signaling, and this increase is often associated with poor tumor prognosis [89-91]. In particular, previous study revealed that detection of PIK3CA mutation status predicts improved drug response in a mouse model of PDAC [89]. A number of studies have shown that whether used alone or in combination, inhibition PI3Ks achieved promising effects in the PDAC treatment [92]. PX-866, which is a pan-PI3K inhibitor displayed good anti-tumor activity against PDAC cell line BxPC-3 *in vivo* model [93]. However, inhibition of the PI3K signaling pathway alone often leads to compensatory activation of the MAPK/MEK pathway, leading to inhibitor resistance [94]. In particular, the *KRAS* mutation, which is identified in 90% of PDAC patients, can activate the MAPK/MEK pathway, which may be the reason why PX-886 has only slight efficacy against *KRAS*-mutated PANC-1 and MIA PACA-2 cells [93]. Therefore, most PI3K inhibitors are often used in combination with other drugs or inhibitors in clinical trials to eliminate the resistance caused by single application [66].

1.2.4 Protein Kinase B (AKT)

Another key protein in the PI3K signaling pathway is protein kinase B (AKT). AKT is a serine/threonine kinase that mediates various biological functions [95]. There are three AKT isoforms in humans: AKT1, AKT2, and AKT3, which share a common structure and similar activation mechanisms [96]. AKT1 is primarily involved in the regulation of cell growth and division, AKT2 plays an important role in cellular energy and metabolism, and AKT3 is the least studied AKT isoform that has been found to be critical for brain development and viability of malignant glioma cells [97, 98]. The main factor for AKT activation is the binding of ligand to cell membrane receptor, these ligands include growth factors such as IGF-1 and PDGF, cytokines, hormones and mitogens [99, 100]. When PI3K is activated upon binding of growth factors to receptor tyrosine kinases (RTKs), PIP2 is converted to PIP3, phosphoinositide-dependent kinase 1 (PDK1) and AKT are recruited to the membrane and lead to downstream signaling through activation of AKT. Afterwards, it affects cell proliferation or survival through several downstream signaling pathways, such as activation of the nuclear factor kappa-light chain enhancer pathway of the activated B cell (NF-κB) pathway, inhibition of the p53 pathway [101]. Furthermore, AKT exerts its effects on cell cycle progression by phosphorylating and inhibiting the CDK inhibitors p21 and p27 [102]. Thus, AKT directly involved in cell quiescence, proliferation, malignancy and longevity. In PDAC, overexpression of AKT were observed in 30% - 40% of the patients, activated AKT (p-AKT) expression determined by immunohistochemistry is a new prognostic indicator [90, 103]. In particular, *AKT2*, an isoform of AKTs, whose overexpression not only represents a biological indicator of PDAC aggression, but also plays a critical role in the inhibitor resistance of PDAC [104]. Inhibition of AKT can also induce autophagy and caspase-mediated apoptosis [105]. Therefore, inhibition of AKT is a possible molecular target for the treatment of PDAC [90]. Currently, a variety of inhibitors against AKT have been developed and they are classified as ATP-competitive (e.g., AZD5363), allosteric (e.g., MK-2206) and AKT protein substrate binding site inhibitors (e.g., Perifosine) [92]. Among them, many have shown highly effective antitumor effects in the preclinical trials of PDAC. Moreover, the inhibitors for AKT have currently entered Phase I and II clinical trials for PDAC, and have achieved good efficacy [66].

1.2.5 Kirsten Rat Sarcoma Virus (KRAS)

Rat sarcoma (RAS) gene family, including Kirsten RAS (KRAS), Harvey RAS (HRAS), and neuroblastoma RAS (NRAS), often mutated in cancer [106]. Among them, *KRAS* is the most frequently mutated oncogene in PDAC, oncogenic *KRAS* mutations can be detected in approximately 92% of the PDAC genomes [20]. Point mutations in codon 12 are the most common mutations and are found in the majority of PDAC cases [24]. These mutations included 45% of G12D mutations, 35% of G12V mutations, 17% of G12R mutations, and a small number of G12A and G12C mutations [107]. As well as less common non-codon 12 mutations such as G13, Q61, K117, and A146 mutations. Activating *KRAS* mutations are considered a major driver of PDAC [24]. KRAS point mutations downregulate the GTPase activity of RAS and prevent GTPase from promoting the conversion of GTP to GDP, leading to permanent binding and activation of downstream signaling pathways such as PI3K/AKT/mTOR pathway or RAF/MEK/ERK pathway, which in turn leads to the initiation and development of PDAC [108]. Moreover, KRAS cooperate with other common oncogenes, such as *TP53*, *CDKN2A*, *BRCA3*, *SMAD4*, etc., to cause the initiation and development of PDAC [109-113]. Among these oncogenes or tumor suppressor genes, *KRAS* mutations were found in the earliest stages of PDAC development (PanIN-1), indication that it is the most important for tumorigenesis, while other genes are required for tumor progression [31]. *KRAS* mutation not only causes the initiation and development of PDAC, it also affects the treatment effect and long-term survival of patients [114-116]. *KRAS* is involved in the regulation of the tumor microenvironment and the recruitment of tumor-promoting cells leading to tumor invasion and metastasis [117, 118]. KRAS mutations are associated with low immune cell infiltration in PDAC, which correlates with poorer prognosis[119]. Therefore, a growing number of studies consider KRAS as a target for the treatment of PDAC. In a mouse model study, mice were injected with *KRAS* knockout PDAC cells and *KRAS* G12C PDAC cells. The *KRAS* knockout group rejected cells or grew tumors only after a longer latency period and were highly infiltrated by B and T lymphocytes, whereas cells in *KRAS* G12C group grew rapid and lack of B and T cell infiltration, which suggested a direct role for KRAS activation in the microenvironment that promotes immune evasion [120]. Immediately, a series of inhibitors targeting KRAS specific- or multiple- mutations were developed, such as Sotorasib (targeting KRAS G12C mutation), KX-58 (targeting KRAS G12D mutation) and BI-3406 (targeting KRAS G12, G13 mutations), etc. Moreover, good efficacy has been achieved in pre-clinical trials targeting PDAC [121-125]. In the CodebreaK100 clinical trial, 38 KRAS G12C-mutated PDAC patients were treated with Sotorasib, 21.1% (8/38) of the patients achieved partial response and 84.2% (32/38) of the patients had disease control [126]. Although studies on the inhibition of KRAS have achieved encouraging results, there are still limitations existing, especially for PDAC. At present, majority of the studies still focus on non-small cell lung cancer (NSCLS), while little attention has been paid to PDAC. In clinical trials targeting KRAS mutation inhibitors, PDAC patients are rarely enrolled. Therefore, therapies targeting KRAS mutations still require further studies.

1.3 Genetic Background and Outcomes of PDAC

Risk classification and medication guidance based on the genetic background are frequently used in clinical practice, and this strategy is frequently used in leukemia, NSCLC, ovarian cancer, and breast cancer *etc.* [127-130]. However, in pancreatic cancer, current common risk classification is based on tumor location, size, and metastasis, often ignoring the influence of genetic background on the tumor [131]. At present, an increasing number of the studies have revealed that changes in genetic background have important implications for the treatment response and prognosis of pancreatic cancer patients. The squamous subtype of PDAC rich in *TP53* mutations often shows a poor prognosis, but cell lines of this subtype are more sensitive to gemcitabine treatment [132]. In addition, the PDAC with higher *KRAS* mRNA expression was more sensitive to the epidermal growth factor receptor (EGFR) inhibitor Erlotinib [132]. In another retrospective study, patients with *BRCA1* or *BRCA2*-related PDAC showed an improvement in median overall survival with platinum-based therapy compared with non-platinum-based therapy [133]. The COMPASS study also demonstrated that advanced PDAC with different genetic backgrounds responded differently to chemotherapy [134]. Thus, genetic background is an important factor affecting chemotherapy, targeted therapy, and treatment response of PDAC. At the same time, studies have found that receiving precision treatment based on gene sequencing makes patients survive longer than those who received unmatched therapy [135]. Although surgery is currently still the main treatment for PDAC and the risk classification is mainly based on surgery-related indicators, with the development of drug therapy, it is increasingly important to understand the relationship between genetic background and therapy response.

2 Aim of the Study

Small molecular inhibitors play a critical role in the targeted therapy of PDAC, but have not yet become a routine regimen for clinical treatment of PDAC. Key proteins such as CK2, CDK, PI3K, AKT and KRAS are often considered as promising target molecules for therapeutic intervention strategies due to their important roles in the occurrence, development and prognosis of PDAC. The aim of this doctoral thesis was to explore the different effects of the above-mentioned key protein inhibitors on various PDAC cell lines, and to explore the effect of aberrations in the target genes of the inhibitors on the efficacy of the corresponding inhibitors by applying whole-exome sequencing (WES) and RNA sequencing (RNA-seq).

In addition, due to the high aberration rate of *TP53* in PDAC and its impact on the treatment and prognosis of PDAC patients a further purpose of this doctoral study was to explore the relationship between *TP53* status and the efficacy of small molecular inhibitors.

Furthermore, because of the central role that combination therapy plays in reducing drug side effects and avoiding drug resistance, *etc*. The goal of this study is also to explore the efficacy of KRAS-based inhibitors and combinations of KRAS-related pathway inhibitors in PDAC cell lines with different *KRAS* mutations. In addition, the aim also includes exploring the anti-tumor mechanism of these combinations in PDAC cell lines, in order to provide basic data for future *in vivo* testing and clinical evaluation.

3 Materials and Methods

Detailed information on the methodological process can be found in the attached three original publications. The most important methods for the work are briefly summarized in this part.

3.1 Characterization of Single Inhibitor-Induced Effects

3.1.1 Small Molecule Inhibitors

Kinase inhibitors, Silmitasertib (CK2 inhibitor), Dinaciclib (CDK1/2/5/9 inhibitor), Buparlisib (Pan-PI3K inhibitor), and MK-2206 (AKT1/2/3 inhibitor) were purchased from Selleck Chemicals. According to the manufacturer's instructions, all inhibitors were separately dissolved in dimethyl sulfoxide (DMSO) as a stock solution at a final concentration of 10 mM. The stock solutions were stored at -80°C and diluted into corresponding working concentrations before each experiment.

3.1.2 Cell Lines and Inhibitory Experiments

Ten PDAC cell lines AsPc-1, BxPc-3, Capan-1, Colo357, Panc-1, PaTu8902, PaTu8988T, PaTu8988S, SU.86.86, and T3M4 were used in single inhibitory experiments (Table 1). AsPc-1, BxPc-3, Colo357, Panc-1, SU.86.86, and T3M4 were cultured in RPMI1640 medium supplemented with 10% heat-inactivated fetal calf serum (FCS) and 1% Penicillin-Streptomycin (P/S) solution. PaTu8902, PaTu8988T, PaTu8988S were cultured in DMEM/F12 medium supplemented with 10% heated-inactivated FCS and 1% P/S solution. Capan-1 was cultured in RPMI1640 medium supplemented with 15% heat-inactivated FCS and 1% P/S solution. After verifying that all cell lines were not contaminated by mycoplasma, these PDAC cell lines were maintained in a 5% CO_2 humidified atmosphere at 37°C.

For all assays, the PDAC cell lines were seeded at a density of 3.3×10^4 cells per milliliter in 6-well plate, 24-well plate and 96-well plate. After 24 hours, the supernatant was discarded and media containing increasing concentrations of Silmitasertib (1 µM - 10 µM), Dinaciclib (0.001 µM – 1 µM), MK-2206 (1 µM - 10 µM), and Buparlisib (0.5 µM - 10 µM) or vehicle substance (DMSO, as control) were added to the corresponding PDAC cell lines. The treated cells were incubated for up to 72 hours at 37°C with 5% CO_2. At the indicated time points, cell proliferation, metabolic activities, cell biomass and apoptosis/necrosis were evaluated in at least three biologically independent replicates.

Table 1: PDAC cell lines

	AsPc-1	BxPc-3	Capan-1	Colo357	Panc-1	PaTu8902	PaTu8988S	PaTu8988T	SU.86.86	T3M4
Species	Homo sapiens	Homo sapiens	Homo sapiens	Homo sapiens	Homo sapiens	Homo sapiens	Homo sapiens	Homo sapiens	Homo sapiens	Homo sapiens
Disease	PDAC, (metastatic site: ascites)	PDAC	PDAC (metastatic site: liver)	PDAC	PDAC (metastatic site: epithelioid carcinoma)	PDAC	PDAC	PDAC	PDAC (metastatic site: liver)	PDAC (metastatic site: lymph node)
Gender	f	f	m	f	m	f	f	f	f	m
Age	62	61	40	77	56	44	64	64	57	64
Doubling time	38-40 hours	48-60 hours	50-100 hours	21 hours	42 hours	25-40 hours	40-60 hours	22-30 hours	48 hours	31 hours
Chr.	55	55	58	55	59	91	71	68	55	55

3.1.3 Cell Viability Assays

Cell proliferation was evaluated by absolute cell counting and trypan blue staining. After inhibitor exposure in 24-well plate, the cells were harvested and washed by phosphate-buffered saline (PBS). Following the cells were stained with trypan blue, the number of viable cells were determined by counting with a hemocytometer. Proliferation was expressed as the percentage of viable cells treated with the inhibitor compared to 100% DMSO control.
Metabolic activity was tested by Water Soluble Tetrazolium - 1 (WST-1). After exposure to the corresponding inhibitor, the cells were incubated with 15 µL WST-1 for up to 2 hours in 96-well plates. Absorbances at 450 nm and the reference wavelength 620 nm were measured by Promega GloMax®-Multi Microplate Multimode Reader. The metabolic activity was calculated as recommended by the manufacturer. Metabolic activity is expressed as a per-centage of the inhibitor-treated group to vehicle-treated controls (control=100%).
Biomass quantification was carried out by Crystal Violet (CV) staining. After exposure to the corresponding inhibitor in 96-well plates, the cells were washed once with PBS and stained with 50 µL 0.2 % CV solution on a shaker at room temperature for 10 minutes. Following the plates were washed twice with PBS. To elute bound CV, 100 µL 1% sodium dodecyl sulfate (SDS) was added to each well and incubated on a shaker at room temperature for 10 minutes. Finally, absorbances at 570 nm and reference wavelength at 620 nm were measured by Promega GloMax®-Multi Microplate Multimode Reader. For back-ground normalization, the absorbance of each group subtracted the absorbance of pure culture media. The amount of CV directly correlates to the cell biomass. The result is expressed as a percentage of the inhibitor-treated group to vehicle-treated controls (control=100%).

3.1.4 Apoptosis and Necrosis Analyses

Apoptosis and necrosis were evaluated by YO-PRO-1 and Propidium iodide (PI) double staining by flow cytometry. After exposure to the corresponding inhibitor, supernatants were collected and cells were harvested and washed twice with cold PBS. Following, cells were resuspended in 200 µL YO-PRO-1 (final concentration: 0.2 µM) solution. After incubating at room temperature for 20 minutes in the dark, cells were washed twice in cold PBS and resuspended in 400 µL cold PBS. Then cells were stained with PI (final concentration: 20 µg/ml) straightway before measurement. Unstained and single-stained cells were used as controls and measured in every single experiment. YO-PRO-1^-/PI^- cells are considered to be viable cells, YO-PRO-1^+/PI^- cells are considered to be apoptotic cells, and PI^+ cells are considered to be necrotic cells. Flow cytometry measurement was performed on FACSVerse, and all data were analyzed by BD FlowJo software.

3.1.5 Next Generation Sequencing

For WES, barcoded sequencing libraries were generated after enrichment with the SureSelect Human All Exon kit, pooled and sequenced on a HiSeq4000 instrument using 150 paired-end protocol to yield at least 20× coverage for >98% of the target region and an overall average

depth of coverage above 100×. An in-house bioinformatics pipeline, including read alignment to human genome reference hg19, variant calling (single nucleotide substitutions and small deletions/insertions), and variant annotation with publicly available database was used.
For RNA-seq, barcoded sequencing libraries were prepared with the TruSeq Stranded mRNA kit, pooled and sequenced on a NextSeq 500 System using the 75bp paired-end protocol. At least 30 million reads were obtained for each sample. The reads were aligned to reference genome GRCh37/Release38 with STAR V.2.7.6a using the two-pass mode [136]. Transcript abundance, transcript per million (TPM) estimates were calculated by counting the reads using featureCounts/subread V.2.0.1 [137].

3.1.6 Identification of IC50

IC50 values were calculated based on cell proliferation, metabolic activity, and biomass after 72 hours of inhibitor exposure. GraphPad Prism Version 8.0.2 (GraphPad Software Inc., San Diego, California, USA) was used to evaluate IC50. Briefly, after transforming concentrations and normalizing the results of the three vitality assays, nonlinear regression model (dose-response-inhibition vs. normalized response - variable slope) was used to evaluate the IC50 values. Calculate the IC50 corresponding to the three vitality assays, and apply these results to the response-based clustering analysis in order to evaluate the sensitivity of cell lines to inhibitors.

3.1.7 Response-Based Clustering Strategy

The cell sensitivity grouping is performed by the k-means++ clustering method based on an unsupervised machine learning algorithm. Briefly, after performing viability assays on all ten PDAC cell lines, we obtained the IC50 values. Then, these IC50 results were applied to the Sci-kit learn package using Python programming language to predict optimal clusters. The Silhouette score is used to detect the clustering density and the separation between clusters [138]. Set the ten cell lines to be divided into several clusters, and the cluster grouping iterated a maximum of 100 times to correct the wrong grouping. Finally, ten cell lines were divided into different clusters and identified as high, moderate, and low sensitivity groups based on their biological characteristics.

3.2 Characterization of Combined Inhibitor-Induced Effects

3.2.1 Small Molecule Inhibitors

Kinase inhibitors, BI-3406 (SOS1::KRAS inhibitor) was purchased from Chemietek. Sotorasib (KRAS G12C inhibitor), Buparlisib (pan-PI3K inhibitor), and Trametinib (MEK1/2 inhibitor) were purchased from Selleck Chemicals. According to the manufacturer's instructions, all inhibitors were separately dissolved in DMSO as a stock solution at a final concentration of 10mM. The stock solutions were stored at -80° C and diluted into corresponding working concentrations before each experiment.

3.2.2 Cell Lines and Inhibitory Experiments

PDAC cell lines AsPc-1, BxPc-3, Capan-1, and MIA PaCa-2 were used in combined inhibitory experiments. The culture methods of AsPc-1, BxPc-3, and Capan-1 have been described in section 3.1.2. MIA PaCa-2 was cultured in DMEM medium supplemented with 10% heated-inactivated FCS and 1% P/S solution.
BI-3406 or Sotorasib in combination with Buparlisib and Trametinib were used for combination therapy. Detailed combination therapies and corresponding concentrations of inhibitors can be found in the detailed information in the cited references and accompanying original publications.

3.2.3 Cell Viability Assays

Cell proliferation and biomass quantification have been described in section 3.1.3.

3.2.4 Apoptosis and Necrosis Analyses

Apoptosis and necrosis were evaluated by Annexin V FITC and PI double staining by flow cytometry. After 72 hours exposure to the vehicle control, single and combined inhibitors, cells were harvested and washed twice with cold PBS. After washing step, the cell pellet was resuspended in 100 µL Annexin V binding buffer (1×), and incubated with 5 µL of Annexin V FITC for 15 minutes at room temperature in the dark. Then cells were stained with PI (final concentration: 20 µg/ml) straightway before measurement. Unstained and single-stained cells are used to determine the negative and positive boundaries and measured in each experiment. Annexin V^-/PI^- cells are considered to be viable cells, Annexin V^+/PI^- cells are considered to be early apoptotic cells, and Annexin V^+/PI^+ cells are considered to be late apoptotic/necrotic cells. The method of flow cytometry measurement and data analysis have been described above.
Examination of PDAC cell lines morphology changes were carried out by pappenheim staining. After 72 hours exposure to vehicle control, single inhibitor or combined inhibitor, supernatants were collected and cells were harvested. After counting cells, resuspended cell pellet and adjusted the cell density of the control group and each experimental group to 5×10^4 cells/200 µL. Then 200 µL of cell suspension was fixed on a glass slide using Shandon Cytospin 3 centrifuge, and two cell slides were made for each group. After 24 hours air-drying, the slides were stained with May-Grünwald solution for 6 minutes, washed with phosphate buffer solution (pH=7.2) three times for 1 minute, then stained with Giemsa solution (1:10) for 20 minutes, and washed with phosphate buffer solution three times for 1 minute again. After the slides were air-dried for 24 hours, the morphology of cells was examined and visualized with Evos XL Core Imaging System, magnified 100 times. Each experiment was repeated 3 times to eliminate random errors.

3.2.5 Evaluation of Synergistic Effects Using the Bliss Independent Model

The interaction among inhibitors were evaluated by the Bliss independent model. The

interaction of the inhibitor combination is determined by the difference between the observed (E_O) and predicted (E_P) inhibition of the combination therapy.
In double inhibitors application, E_P was calculated with following equation:

$$E_P = E_A + E_B - E_A \times E_B,$$

where E_A and E_A are the relative inhibition of single-inhibitor A and B.
In triple inhibitors application, E_P was calculated with following equation:

$$E_P = E_A + E_B + E_C - E_A \times E_B - E_A \times E_C - E_B \times E_C - E_A \times E_B \times E_C,$$

where E_A, E_B, and E_C are the relative inhibition of single-inhibitor A, B and C.
$E_O > E_P$ indicated synergistic effect, $E_O = E_P$ indicated additional effect, $E_O < E_P$ indicated antagonistic effect. Bliss values for inhibitors combinations were calculated based on the results of proliferation and cell biomass of PDAC cell lines [139].

3.2.6 RNA Sequencing and DEG Analysis

1 µg of total RNA was used as input for an mRNA enrichment using poly-T oligo coated magnetic beads, and was chemically fragmented under elevated temperature. The fragmented RNA was then reverse-transcribed into the first- and second-strand cDNA using random hexamers and Superscript II reverse transcriptase. Double-stranded cDNA fragments were ligated with TruSeq RNA adapters with a unique DNA sequencing index and PCR-amplified. cDNA library concentration was quantified using a Qubit dsDNA HS Assay kit and normalized to 2 nM before multiplexing. The DNA libraries were sequenced at a final concentration of 13 pM for 125 bp single-end reads using the high-output mode on the HiSeq2500. The raw fastq reads were quality-checked using FastQC (version 0.11.5) and pre-processed by filtering out low quality reads with a mean Q-score <20 and trimming adapter-like sequences using TrimGalore version 0.6.5. High-quality reads were aligned to the reference genome GRCh38 (Ensembl release 106) using HISAT2 version 2.2 [140-142]. Uniquely mapped reads to each gene were extracted from the HISAT2 mapping results using HTSeq version 0.8.0 [143].
The resulting RNA-seq gene count data were further analyzed for DEGs using edgeR package. The Gene Ontology (GO) and Kyoto Encyclopedia of Genes and Genomes (KEGG) analysis were applied for the functional annotation and pathway analysis using the Gene Set Enrichment Analysis (GSEA) [144, 145]. A list including all sequenced genes was used as background.

3.3 Statistical Analysis

Each experiment was performed in at least three biologically independent experiments. Results of proliferation, metabolic activity, biomass quantification, and apoptosis/necrosis analysis were expressed as mean ± standard deviation (SD). Statistical significance was determined by one-way ANOVA (After proving the data within each group conformed to the Gaussian distribution) or Kruskal-Wallis-Test (The data within each group conformed to the non-Gaussian distribution) and displayed as *: $p < 0.033$, **: $p < 0.002$, ***: $p < 0.001$ versus the control group.

4 Results

The detailed results of the doctoral study are in the accompanying three original publications (in the appendix).

The key results are summarized below. In addition to the figures in the text, further figures can be found in the appendix (Section 8.2)

4.1 Work I

Inhibitory Response to CK II Inhibitor Silmitasertib and CDKs Inhibitor Dinaciclib Is Related to Genetic Differences in Pancreatic Ductal Adenocarcinoma Cell Lines

Ma, Y.; Sender, S.; Sekora, A.; Kong, W.; Bauer, P.; Ameziane, N.; Krake, S.; Radefeldt, M.; Al-Ali, R.; Weiss, F.U.; Lerch, M.M.; Parveen, A.; Zechner, D.; Junghanss, C.; Murua Escobar, H.
Int. J. Mol. Sci. **2022**, *23*, 4409. https://doi.org/10.3390/ijms23084409
Impact Factor 2022: 5.924

Own contribution to the work specified here:

- Drafting of the manuscript
- Editing the revision of the manuscript after peer review
- Involvement in study planning
- Carrying out majority of *in vitro* work (Cell viability determinations, apoptosis/necrosis measurement using flow cytometry, involvement in DNA and RNA extraction, gene variant and expression analysis, comprehensive analysis of genetic changes and cell response)
- Data evaluation, analysis, interpretation and graphical representations of all results

4.1.1 Effects of Silmitasertib and Dinaciclib on Cell Viability

The inhibitory effects of the CK2 inhibitor Silmitasertib and the CDKs inhibitor Dinaciclib were demonstrated in PDAC cell lines (Publication 1). However, in inducing cell death, Silmitasertib only increased the percentage of cell deaths in two out of ten PDAC cell lines, while Dinaciclib increased the percentage of cell deaths in 9 of 10 PDAC cell lines in all tested concentrations (Appendix 8.2.1).
Furthermore, based on the IC50 results, the k-means++ clustering method was applied to separate the 10 cell lines into 3 different sensitive groups. For Silmitasertib, ten PDAC cell lines were classified into low (PaTu8988S, Panc-1, PaTu8988T, PaTu8902, and Colo357), moderate (Capan-1, T3M4, and SU.86.86), and high (AsPc-1 and BxPc-3) sensitive group (Figure 3a). For Dinaciclib, ten PDAC cell lines were classified into low (Panc-1 and SU.86.86), moderate (BxPc-3, Capan-1 and PaTu8988S), and high (AsPc-1, Colo357, PaTu8902, PaTu8988T, and T3M4) sensitive group (Figure 3b).

Figure 3

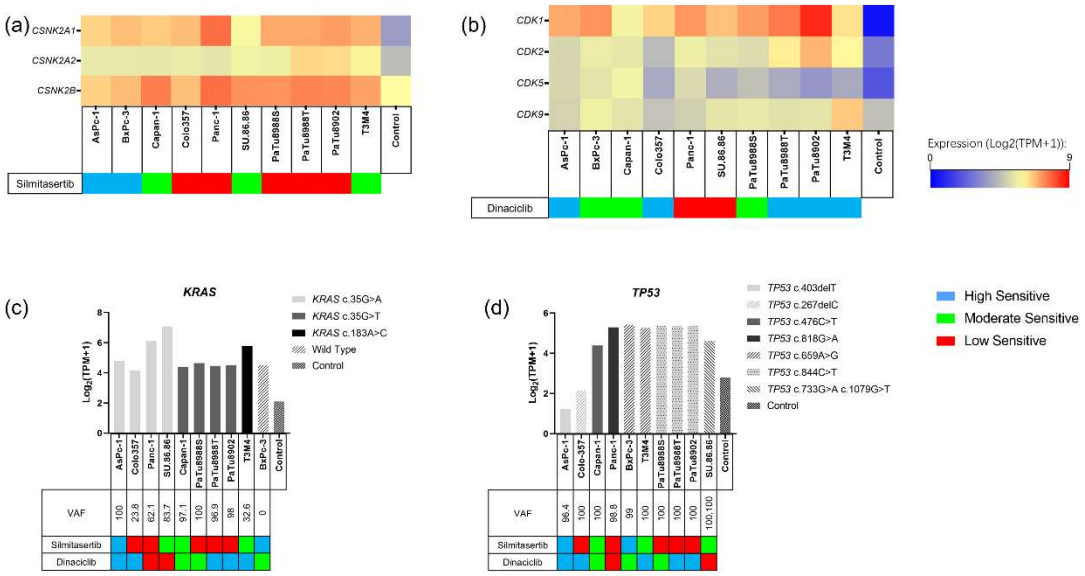

Figure 3: Silmitasertib (a) and Dinaciclib (b) target gene expression and sensitivity classification based on cell line biological response. According to the results of the cell viability assays, the 10 PDAC cell lines were classified into high, medium and low sensitivity groups using the k-means++ method. As well as *KRAS* (c) and *TP53* (d) gene variants, expression levels and allele frequencies.

4.1.2 Expression and Genetic Variants of Silmitasertib and Dinaciclib Target Genes

Although multiple variants of inhibitor target genes were identified in PDAC cell lines, none of the identified variants as potentially affecting the protein coding sequence in a form leading to aberrant protein function. In addition, RNA-seq results demonstrated that all inhibitor target genes had higher expression than non-neoplastic pancreatic tissue (as control) (Figure 3a, 3b).

4.1.3 KRAS and TP53 Gene Variants and the Relationship with Inhibitors Efficacy

Three missense *KRAS* variants were identified in nine of ten PDAC cell lines, KRAS c.35G>A (AsPc-1, Colo357, Panc-1, and SU.86.86), KRAS c.35G>T (Capan-1, PaTu8902, PaTu8988S, and PaTu8988T), and KRAS c.183A>C (T3M4). The expression level of *KRAS* in all PDAC cell lines (including wt cell line BxPc-3) were higher compared to non-neoplastic pancreas tissue. A comprehensive analysis of the cell viability and *KRAS* status, revealed that PDAC cell lines carrying the *KRAS* variants appeared to be less sensitive to Silmitasertib, the highly sensitive group contained only wild-type and one *KRAS* mutant cell line, while the rest of the *KRAS* mutant carrying cell lines were all classified into the moderate or low sensitivity group. In addition, *KRAS* c.35G point mutations have no major influence on the inhibitory effect of Dinaciclib, since cell lines containing the same *KRAS* c.35G mutation were classified into each of the three sensitivity groups, while wild-type (BxPc-3) is in the moderate sensitivity group.

Interestingly, the sensitivity of the *KRAS* c.183A>C mutant cell line (T3M4) is higher than BxPc-3. *KRAS* gene expression and VAF did not affect the efficacy of the two inhibitors (Figure 3c).

Eight *TP53* variants were identified in all PDAC cell lines. Frameshift variants, *TP53* c.403delT and *TP53* c.267delC, were identified in AsPc-1 and Colo357, respectively. Missense variants, *TP53* c.476C>T and *TP53* c.818G>A, were identified in Capan-1 and Panc-1, respectively. Missense variants including *TP53* c.733G>A and *TP53* c.1079G>T were both identified in SU.86.86. *TP53* c.659A>G was identified in BxPC-3 and T3M4. *TP53* c.844C>T was identified in PaTu8902, PaTu8988S, and PaTu8988T. The expressions of *TP53* with frameshift variants were lower than that of missense variants and control. A comprehensive analysis of cell viability and *TP53* status demonstrated that the two cell lines carrying frameshift variants (Colo357 and AsPc-1) were in the Dinaciclib highly sensitive group, while cell lines carrying point mutations were distributed in the three sensitive groups. However, this effect was not observed when treating the cells with Silmitasertib. In addition, cell lines carrying *TP53* c.844C>T, *TP53* c.818G>A, and *TP53* c.267delC variants were in the low sensitivity group. SU.86.86, which carry two *TP53* point mutations demonstrated no significant difference in sensitivity to Silmitasertib and Dinaciclib compared with other cell lines only carrying one variant. *TP53* gene expression and VAF did not affect the efficacy of the two inhibitors (Figure 3d).

4.2 Work II

The Inhibitory Response to PI3K/AKT Pathway Inhibitors MK-2206 and Buparlisib Is Related to Genetic Differences in Pancreatic Ductal Adenocarcinoma Cell Lines

Ma, Y.; Sender, S.; Sekora, A.; Kong, W.; Bauer, P.; Ameziane, N.; Al-Ali, R.; Krake, S.; Radefeldt, M.; Weiss, F.U.; Lerch, M.M.; Parveen, A.; Zechner, D.; Junghanss, C.; Murua Escobar, H.

Int. J. Mol. Sci. **2022**, *23*, 4295. https://doi.org/10.3390/ijms23084295

Impact Factor 2022: 5.924

Own contribution to the work specified here:

- Drafting of the manuscript
- Editing the revision of the manuscript after peer review
- Involvement in study planning
- Carrying out majority of *in vitro* work (Cell viability determinations, apoptosis/necrosis measurement using flow cytometry, involvement in DNA and RNA extraction, gene variant and expression analysis, comprehensive analysis of genetic changes and cell response)
- Data evaluation, analysis, interpretation and graphical representations of all results

4.2.1 Effects of MK-2206 and Buparlisib on Cell Viability

The inhibitory effects of the AKTs inhibitor MK-2206 and the pan-PI3K inhibitor Buparlisib were demonstrated in PDAC cell lines (Appendix 8.2.2). However, in inducing cell death, MK-2206 only increased the percentage of cell deaths in three out of ten PDAC cell lines, while Buparlisib increased the percentage of cell deaths in all PDAC cell lines (Appendix 8.2.2).

Furthermore, based on the IC50 results, the k-means++ clustering method was applied to separate the ten cell lines into 3 different sensitive groups. For MK-2206, ten PDAC cell lines were classified into low (Colo357 and SU.86.86), moderate (PaTu8988T, PaTu8902, Panc-1, Capan-1, AsPc-1, and T3M4), and high (PaTu8988S and BxPc-3) sensitivity group (Figure 4a). For Buparlisib, ten PDAC cell lines were classified into low (Panc-1 and SU.86.86), moderate (AsPc-1, Capan-1, PaTu8902, and PaTu8988S), and high (BxPc-3, Colo357, PaTu8988T, and T3M4) sensitivity group (Figure 4b).

4.2.2 Expression and Genetic Variants of MK-2206 and Buparlisib Target Genes

A total of nine MK-2206 target gene variants and seventeen Buparlisib target gene variants were identified in all ten PDAC cell lines. However, only two variants were confirmed to influence on primary structure of the respective proteins. The two variants, variant type and cell lines are *PIK3CG* c.2480C>G missense variant in Capan-1 and a *PIK3CA* c.1143C>G splice region variant in Colo357, respectively. Moreover, these two mutations were associated with increased expression level of the corresponding genes (Appendix 8.2.2).

4.2.3 KRAS and TP53 Gene Variants and the Relationship with Inhibitors Efficacy

The sequencing results of *KRAS* and *TP53* have been described in section 4.1.3.

A comprehensive analysis of the sensitivity and the *KRAS* status of all cell lines revealed that *KRAS* variants alone have no major influence on the inhibitory effect of Buparlisib, since cell lines harboring a *KRAS* mutation were classified into all sensitivity groups. Moreover, the four cell lines in the highly sensitive group contained all three *KRAS* mutant and wild-type cell lines. For MK-2206, the results were different. The highly sensitive group contained only wild-type and one *KRAS* mutant cell line, while the rest of the *KRAS*-mutant-carrying cell lines were

Figure 4

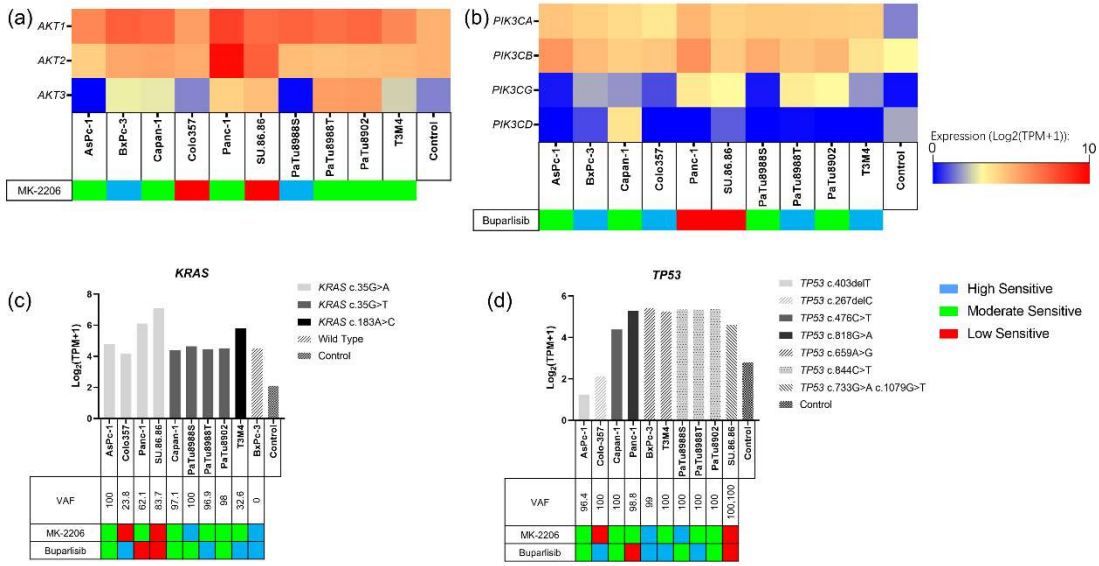

Figure 4: MK-2206 (a) and Buparlisib (b) target gene expression and sensitivity classification based on cell line biological response. According to the results of the cell viability assays, the 10 PDAC cell lines were classified into high, medium and low sensitivity groups using the k-means++ method. As well as *KRAS* (c) and *TP53* (d) gene variants, expression levels and allele frequencies.

distributed in the moderate or low sensitivity groups, indicating that PDAC cell lines carrying the *KRAS* variant were less sensitive to MK-2206. *KRAS* gene expression and VAF did not affect the efficacy of the two inhibitors (Figure 4c).

A comprehensive analysis of the sensitivity to both inhibitors and the *TP53* status of all cell lines revealed no obvious relationship between the status of this tumor suppressor gene and the efficacy of the inhibitors. Interestingly, SU.86.86, which carries two missense variants in *TP53*, was classified in the low-response group for both inhibitors. Further, *TP53* gene expression and VAF did not affect the efficacy of the two inhibitors (Figure 4d).

4.3 Work III

Inhibition of KRAS, MEK and PI3K Demonstrate Synergistic Anti-Tumor Effects in Pancreatic Ductal Adenocarcinoma Cell Lines

Ma, Y.; Schulz, B.; Trakooljul, N.; Al Ammar, M.; Sekora, A.; Sender, S.; Hadlich, F.; Zechner, D.; Weiss, F.U.; Lerch, M.M.; Jaster, R.; Junhanss, C.; Murua Escobar, H.
Cancers **2022**, *14*, 4467. https://doi.org/10.3390/cancers14184467
Impact Factor 2022: 6.575

Own contribution to the work specified here:

- Drafting of the manuscript
- Editing the revision of the manuscript after peer review
- Involvement in study planning
- Carrying out majority of *in vitro* work (Cell viability determinations, apoptosis/necrosis measurement using flow cytometry, morphological examinations according to pappenheim staining, RNA extraction, DEGs analysis, comprehensive analysis of genetic changes and cell response)
- Data evaluation, analysis, interpretation and graphical representations of all results

4.3.1 Effects of KRAS Inhibitors Single Application on PDAC Cell Lines

Compared with the DMSO control group, the SOS1::KRAS inhibitor BI-3406 demonstrated a weak inhibitory effect on PDAC cell lines carrying *KRAS* G12V (Capan-1 and PaTu8902). In addition, the inhibitory effect of BI-3406 on the cell proliferation and biomass of the *KRAS* wild-type cell line BxPc-3 is similar to that of *KRAS* G12V cell lines. Although BI-3406 demonstrated a relatively increased inhibitory effect on the cell lines carrying the other three *KRAS* mutations (AsPc-1 and Colo357, *KRAS* G12D; MIA PaCa-2, *KRAS* G12C; T3M4, *KRAS* Q61H), this effect is still weak (Figure 5a and Appendix 8.4.1).
The KRAS G12C inhibitor Sotorasib demonstrated the strongest inhibitory effect on MIA PaCa-2, which carry *KRAS* G12C variant. However, it has almost no inhibitory effect on the *KRAS* Q61H cell line T3M4. In addition, Sotorasib displayed similar inhibitory effects on wild-type and *KRAS* G12V cell lines. However, the inhibitory effects of Sotorasib on AsPc-1 and Colo357, which carry *KRAS* G12D varaint, are quite different, cell proliferation decreased by 50.14% and 37.22%, and biomass decreased by 41.94% and 27.30%, respectively (Figure 5b and Appendix 8.4.1).

4.3.2 Effects of KRAS Inhibitor Combined with PI3K and MEK1/2 Inhibitors on PDAC Cell Lines

In BI-3406-based combination inhibition, cell proliferation and biomass were significantly reduced in both double-inhibitor and triple-inhibitor combinations compared to the DMSO control group. Furthermore, Bliss-independent models demonstrated that BI-3406-based double or triple combined inhibition exhibited synergistic efficacy in all four PDAC cell lines (Figure 5c and Appendix 8.4.1).

Whereas, in Sortorasib-based combination inhibition, significant reductions in cell proliferation and biomass were also observed in both double-inhibitor and triple-inhibitor combinations when compared with the DMSO control group. However, the Bliss-independent model demonstrated that the synergistic effect of the double and triple inhibitor combinations could be observed only in MIA PaCa-2. In the non-KRAS G12C mutant cell lines, only additive effects were observed with the Sotorasib-based combination (Figure 5d and Appendix 8.4.1).

Figure 5

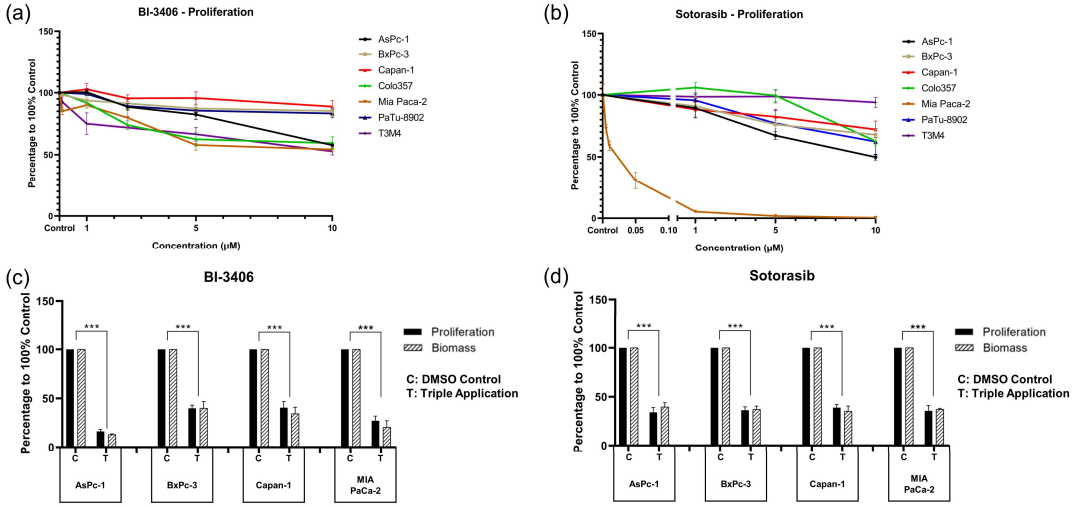

Figure 5: Proliferation changes of PDAC cell lines after exposure to different concentrations of BI-3406 (a) and Sotorasib (b). As well as proliferation and biomass changes of PDAC after exposure to DMSO control and BI-3406 (c) or Sotorasib (d) based triple inhibitor combination. Significance of a treatment effect compared to the DMSO control was determined by one-way ANOVA and displayed as ***: P<0.001 (n ≥ 3).

4.3.3 RNA-seq Revealed the Inhibitory Mechanism of the Two Inhibitor-Combinations

GO term function revealed that in the PDAC cell lines, DEGs were involved in regulating immune system, cell adhesion, cell migration, localization, locomotion, and response to stimulus in biological process, cell membrane and extracellular functions in cellular components, as well as cytokine binding in molecular functions. KEGG pathway enrichment analysis identified 8 overlapping pathways, which were involved in tumor, signal transduction, immune regulation and other functions. Moreover, RAS signaling was observed to be affected in AsPc-1, BxPc-3 and MIA PaCa-2, but not in Capan-1. (Appendix 8.4.1).

Comprehensive analysis of the GO term of MIA PaCa-2 in both inhibitor combinations Comparing the GO terms and KEGG pathway enrichment analysis of MIA PaCa-2 in the two inhibitor combinations did not reveal major differences. Both inhibitor combinations were involved in similar cellular functions. KEGG pathway analysis revealed that both inhibitor combinations were involved in immune regulation, signal transduction (especially PI3K/AKT, TNF, and JAK-STAT signaling pathways), metabolic activity and cancer pathways. The BI-3406 combination additionally participated in the MAPK pathway, however, this effect was not

observed in the Sotorasib combination (Appendix 8.4.1).

5 Discussion

Despite innovative therapeutic strategies, the current treatment of PDAC remains a major challenge [10]. In addition to standard surgery or chemotherapy, targeted and combination therapy approaches using small-molecule inhibitors have emerged as a treatment option for PDAC, but they are not yet widely used in clinical practice [146]. Due to the widespread existence of gene mutations such as *KRAS*, *TP53*, *SMAD4* in PDAC, these gene mutations also significantly affect the treatment effect and prognosis of patients [20, 27, 28]. Therefore, preclinical studies are urgently needed to elucidate the relationship between genetic background and inhibitor susceptibility to support further studies.

In PDAC, protein such as CK2, CDKs, AKTs, PI3Ks and KRAS affect tumor cell initiation, survival, metastasis, and drug resistance through different mechanisms. Furthermore, inhibiting or blocking these proteins plays a significant role in the treatment of PDAC. Therefore, targeting these proteins as therapeutic targets for PDAC and investigating the relationship between their efficacy and PDAC gene background will help to enhance our knowledge of PDAC and guide further research. In addition, through these studies, suitable inhibitor combinations are able to be selected for combined inhibition, and further explore the mechanism of combined inhibition.

5.1 Inhibition of CK2 Exhibits Antitumor Effect in PDAC Cell Lines, the Inhibitory Response is Related to Genetic Background

The current study demonstrated that the expression levels of Silmitasertib target genes (*CSNK2A1*, *CSNK2A2*, and *CSNK2B*) in all of the tested PDAC cell lines were higher than in non-neoplastic pancreatic tissue. This result suggests that these cell lines could be sensitive to Silmitasertib. Indeed, the inhibition of CK2 by Silmitasertib significantly affected cell proliferation of all cell lines except Panc-1, and significantly reduced the cell biomass in all PDAC cell lines. In addition, no correlation was seen when comparing the expression of CK2 genes in high-, moderate-, and low-sensitive cell lines. These results indicate that the genes directly targeted by Silmitasertib are not directly affected by aberrations modulating the observed antitumor effects of Silmitasertib on CK2. CK2 gene aberrations were detected in 2.9% (34/1228: *CSNK2A1*, 1%, *CSNK2A2*, 0.3%, *CDNK2B*, 1.6%) of PDAC patients, and only 0.2% (3/1228) involved protein structural changes, while the majority involved gene amplification [147]. Therefore, our study provides some reference value for the strategy of Silmitasertib in the treatment of PDAC.

PDAC patients with *KRAS* or *TP53* mutations had a poor prognosis [148-150], we also sought to explore whether these two genes are associated with inhibitor sensitivity.

Three different amino acid substitution variants of *KRAS* including *KRAS* G12D (c.35G>A), *KRAS* G12V (c.35G>T), and *KRAS* Q61H (c.183A>C) were identified in nine of ten PDAC cell lines. A comprehensive analysis of Silmitasertib efficacy and *KRAS* status suggests that carrying the *KRAS* variants reduced the PDAC sensitivity to Silmitasertib. Since AKT is an important effector kinase of CK2, inhibition of CK2 causes a reduced activation of AKT, whereas mutant KRAS directly activates the PI3K/AKT pathway [56, 108]. This antagonism results in reduced

sensitivity of *KRAS*-mutated cell lines to Silmitasertib. Overall, blocking CDKs with Dinaciclib in monotherapy may be beneficial to patients with the specific *KRAS* c.183A>C mutation, whereas Silmitasertib monotherapy in patients with *KRAS* point mutations may not be a good option.

All tested PDAC cell lines contained at least one *TP53* variant that causes amino acids to change. RNA-seq data revealed that the fs mutation was associated with low expression of TP53. Furthermore, studies have demonstrated that frameshift variants lead to a strong disruption of *TP53* function and that low *TP53* mRNA expression is associated with poor prognosis in patients with PDAC [149, 150]. A comprehensive analysis of *TP53* and cell response revealed that cell lines carrying specific *TP53* variants (c.267delC, c.818G>A, and c.844C>T) were less sensitive to Silmitasertib. These cell lines were all in the low (PaTu8988S, Panc-1, PaTu8988T, Pa-Tu8902, and Colo357) sensitivity group. It was reported that knockdown of CK2 causes the enhanced transactivation of p53, thereby increasing apoptosis [151]. However, due to the inactivation caused by mutations in TP53, inhibition of CK2 did not transactivate these proteins. This may be the reason for the reduced efficacy of Silmitasertib in cell lines with specific mutations in *TP53*. In addition, the expression level of *TP53* cannot fully explain the observed responses of all cell lines to Silmitasertib. These results suggest that *TP53* variants are indicators of PDAC responses to Silmitasertib inhibition, whereas *TP53* expression levels are not. Moreover, the results of the PDAC inhibitory assays indicate that patients with *TP53* mutations may benefit from a potential application of Silmitasertib.

In conclusion, the current study revealed the sensitivities of the PDAC cell lines when treated with Silmitasertib. Either the expression level of the inhibitor target genes or gene variants could not affect the sensitivity to Silmitasertib. The *KRAS* variants may reduce the sensitivity of PDAC cell lines to Silmitasertib. Specific *TP53* variants including c.267delC, c.818G>A, and c.844C>T, reduced the sensitivity of Silmitasertib to the PDAC cell lines. Thus, Silmitasertib displayed partially *in vitro* efficacy on PDAC cell lines, and further experiments are still needed to verify the *in vivo* efficacy and the effects of the target genes and hotspot genes on the efficacy of Silmitasertib.

5.2 Inhibition of CDK1/2/5/9 Exhibit Cytotoxic Effects on PDAC Cell Lines and the Cell Response is Associated with Genetic Background

Inhibition of CDK1/2/5/9 by Dinaciclib dramatically reduced cell proliferation, metabolic activities, and biomass in PDAC cell lines and this significant effect could be observed at nanomolar concentrations. RNA-Seq results demonstrated that expressions of *CDK1/2/5/9* were higher than the control in all tested PDAC cell lines, indicating the overexpression of *CDK1/2/5/9* in PDAC cell lines. Moreover, as the experimental results suggest that Dinaciclib inhibited cell viability at very low concentrations, the overexpression of target genes appeared to not affect the efficacy of dinaciclib in inhibiting the viability of PDAC cells. Therefore, Dinaciclib is an excellent candidate for PDACs with high expression of *CDK1/2/5/9*; on the other hand, due to the lack of data on the individuals with low *CDK1/2/5/9* expression, experiments are still needed to verify the feasibility of using Dinaciclib as a therapeutic candidate. Moreover, Dinaciclib target gene aberrations were present in 4.3% (46/1228: *CDK1*, 0.3%, *CDK2*, 1.1%,

CDK5, 2%, *CDK9*, 1%) of PDAC patients, and only 0.5% (6/1228) involved protein structural changes, while majority involved gene amplification [147]. Therefore, Dinaciclib appears to be a promising treatment option for the current PDAC patient with CDK abnormalities.

Significant differences in sensitivity to Dinaciclib could not be observed between cell lines harboring the *KRAS* c.35G point mutation and wild-type cell lines, indicating the inhibitory effect of Dinaciclib is not affected by the *KRAS* c.35G point mutation. Interestingly, T3M4 cells, which carry a *KRAS* c.183A>C variant are more sensitive to Dinaciclib than wild-type BxPc-3 cells, suggesting that Dinaciclib may improve the efficacy of patients with specific *KRAS* c.183A>C mutation, but due to the limited number of cell lines, further experiments are still needed to verify the relationship between this *KRAS* mutation and the efficacy of Dinaciclib.

A comprehensive analysis of *TP53* and cell response revealed that AsPc-1 and Colo357, which carry the frameshift variant, are both in the Dinaciclib high sensitivity group. This result suggested that Dinaciclib may be able to improve the prognosis of the *TP53* frameshift variants. While previous studies have shown that carriers of TP53 frameshift variants often have a very poor prognosis, the current results suggest that patients with *TP53* mutations, especially frameshift mutations, may benefit from the potential use of Dinaciclib [150, 152]. However, the expression level of *TP53* cannot fully explain the observed responses of all cell lines to Dinaciclib. These results indicate that *TP53* variants are an indicator of PDAC cells sensitivity to Dinaciclib, while the expression level of *TP53* is not.

Altogether, this study revealed the distinct sensitivities of the PDAC cell lines when treated with Dinaciclib. The high expression level of the inhibitor target genes could not affect the sensitivity of PDAC cells to Dinaciclib. The *KRAS* variants have no effect on the sensitivity of PDAC cell lines to Dinaciclib. Cell lines carrying *TP53* frameshift variants are highly sensitive to Dinaciclib compared to cell lines carrying *TP53* point mutations. Dinaciclib displayed excellent *in vitro* efficacy on PDAC cell lines, and further experiments are needed to verify the efficacy *in vivo* and clinical trials.

5.3 Inhibition of AKT1/2/3 Exhibits Inhibitory Effect on PDAC Cell Lines and the Cell Response is Associated with Genetic Background

This study confirmed that MK-2206 inhibited cell proliferation, metabolic activity, and biomass in a dose-dependent manner. However, the effects of apoptosis/necrosis induction were not distinct, and the percentage of dead cells was less than 20% at all tested concentrations in all cell lines. These results indicate that the efficacy of MK-2206 at inhibiting PDAC cell lines is not mainly caused by the induction of apoptosis/necrosis. In addition, we did not find any amino acid substitution of *AKT*s in tested PDAC cell lines. At the same time, transcriptomic analysis did not support the hypothesis that the expression level of *AKT*s affects the efficacy of MK-2206. However, *AKT2* expression seems to affect the efficacy of Buparlisib. Moreover, according to cBioPortal, although *AKT2* aberration occurred in only 3.99% (49/1228) of patients with PDAC, in 87.76% (43/49) of them, the overexpression of the genetic modulation of *AKT2* was observed [147]. An analysis of the functional relationship between AKT2 aberrations and Buparlisib efficacy remains to be completed.

Our experiments have also revealed that the anti-proliferative and cytotoxic effects of MK-

2206 are similar to, but nevertheless differ from, the observed metabolic effects, especially in Panc-1, PaTu8902, and PaTu8988T. It has been reported that some inhibitors induce cellular stress that alters cellular metabolic activity, and we observed similar properties with MK-2206[153, 154]. This result suggests that conclusions based on metabolic activity assays, such as WST-1 assays or CCK8 assays, need to be validated with other assays when MK-2206 is used.
A comprehensive analysis of MK-2206 and *KRAS* status demonstrated that carrying the *KRAS* variant appeared to cause a decrease in the sensitivity of PDAC cell lines to this inhibitor. Consistent with these data, one study demonstrated that, in cell lines of colorectal cancer, lung cancer, breast cancer, and melanoma, *KRAS* mutations were associated with significant resistance to AKT1/2 inhibition, this resistance is achieved through the activation of MEK/ERK by KRAS, which bypasses PI3K/AKT and directly activates eukaryotic translation initiation factor 4E-binding protein 1 (4E-BP1) [155]. Therefore, it might be important to consider *KRAS* status before treating patients with PDAC with MK-2206.
A comprehensive comparison of the sensitivity to MK-2206 and the expression level of TP53 showed that there was no obvious relationship between the two. However, SU.86.86, which carries two *TP53* missense variants, was classified to the hyposensitivity group, suggesting that two *TP53* missense variants are associated with reduced efficacy of AKT inhibitor. It was previously reported that advanced PDAC harboring a double mutation in *TP53* had an extremely poor response to epidermal growth factor receptor (EGFR)-inhibitor Erlotinib [156]. Our study indicated that *TP53* double mutation also reduces the efficacy of MK-2206. Therefore, when multiple TP53 mutations are identified in PDAC patients, switching inhibitors or multi-inhibitor combinations should be considered.
In conclusion, the present study revealed antitumor effects against PDAC cell lines when inhibiting AKTs. *KRAS* point mutations (c.35C > T, c.35C > A, and c.183A > C) appear to be related to the level of sensitivity to MK-2206. In addition, carrying two *TP53* missense variants appears to be associated with reduced sensitivity to MK-2206. Thus, our study suggests that inhibiting AKTs by MK-2206 is an optional strategy for the treatment of patients with PDAC but that it is still necessary to choose inhibitors based on genetic background.

5.4 Inhibition of PI3Ks Exhibit Distinct Antitumor Effect on PDAC Cell Lines and the Cell Response is Associated with Genetic Background

Our study demonstrated that the proliferation, metabolic activity, and cell biomass of all PDAC cell lines decreased in a dose-dependent manner after Buparlisib exposure. It has been reported that Buparlisib is a potent and highly specific oral pan-class I PI3K inhibitor in low concentrations [157]. Moreover, although at high concentrations (>5 μM), it may cause cell death by binding to tubulin, thereby inhibiting tubulin polymerization, in this study, significant inhibition mainly occurred below the concentration of 1 μM [158]. In addition, the IC50s of all cell viability assays were below 5 μM. These results suggest that Buparlisib can exert cytotoxic effects in PDAC cell lines by inhibiting PI3Ks.
A comprehensive analysis of WES and RNA-seq transcriptome analysis revealed that the *PIK3CG* c.2480C > G variant was correlated with gene overexpression in the corresponding cell line, whereas *PIK3CA* c.1143C > G was associated with a corresponding decrease in gene

expression in tumor cell lines, but at a level still higher than non-neoplastic controls. However, the sensitivity grouping demonstrated that the cell lines carrying these two gene aberrations did not display a specific response to the inhibitory effect of Buparlisib. Interestingly, two cell lines with high *AKT2* expression, Panc-1 and SU.86.86, have low sensitivity to Buparlisib. As reported, not only does the overexpression of *AKT2* represent a biological indicator of PDAC aggressiveness, but also *AKT2* plays a critical role in the inhibitor resistance of PDAC [90, 104, 159]. Our data indicate that high expression of *AKT2* is related to reducing the efficacy of Buparlisib. However, further functional experiments are still needed to verify the relationship between high *AKT2* expression and Buparlisib resistance.

The Buparlisib sensitivity groups and *KRAS* variants or expression level did not demonstrate any relationship. This is obvious, especially in the high sensitivity group, which included not only cell lines carrying *KRAS* variants but also a wild-type *KRAS*. These results suggest that the *KRAS* status alone does not influence the sensitivity to Buparlisib in PDAC cell lines.

We further analyzed the response of cell lines carrying *PI3K* and *KRAS* double mutations and a *KRAS* single mutation to Buparlisib. In four cell lines carrying the *KRAS* c.35G > A mutation (AsPc-1, Colo357, Panc-1, and SU.86.86), we identified that Colo357 also carries the *PIK3CA* c.1143C > G variant. Interestingly, Colo357 was highly sensitive to Buparlisib, while the other three cell lines were less sensitive. This might indicate that there are unknown interactions between the *PIK3CA* c.1143C > G variant and the *KRAS* c.35G > A variant. This *PIK3CA* variant could reduce the negative effects of *KRAS* on the sensitivity to Buparlisib. However, we did not observe any interaction when analyzing another PI3K mutation (*PIK3CG* c.2480C > G) in cell lines bearing the *KRAS* c35G > T variant (Capan-1, PaTu8902, PaTu8988S, and PaTu8988T) when using either inhibitor.

In our study, a comprehensive analysis of the cell viability assays and the number of *TP53* variants revealed that SU.86.86 is in the low-sensitivity group when treated with Buparlisib, suggesting that two *TP53* mutations are related to reducing the efficacy of PI3K inhibition by Buparlisib. Therefore, when multiple *TP53* mutations are identified in PDAC patients, the combination of inhibitors and drugs should be considered.

Altogether, the present study revealed distinct antitumor effects against PDAC cell lines when inhibiting the PI3K by Buparlisib. Exploring the inhibitor response and the corresponding target gene aberrations shows that neither *PIK3CA* nor *PIK3CG* aberration alone affect the inhibitor response of PDAC cell lines to Buparlisib. Moreover, in the relationship between the observed inhibitor response and aberrations of *KRAS* and *TP53*, *KRAS* point mutations (c.35C > T, c.35C > A, and c.183A > C) alone are not able to determine the level of sensitivity to Buparlisib. Cell line carrying a specific *PIK3CA* variant is associated with enhanced Buparlisib inhibition in *KRAS*-mutated cell lines. In addition, carrying two *TP53* missense variants appears to be related to reduced sensitivity to Buparlisib. Thus, our study suggests that inhibiting PI3K by Buparlisib is an optional strategy for the treatment of patients with PDAC but still need to choose inhibitors based on genetic background.

5.5 Efficacy and Mechanism of KRAS inhibitors Alone or in Combination with Downstream Inhibitors in PDAC Cell Lines

KRAS mutations are the most common mutations in PDAC patients and are characterized by poor prognosis and resistance to general therapy [25, 114]. In our study, Sotorasib targeting the KRAS G12C mutation exhibited the expected inhibitory efficacy in MIA Paca-2 and already significantly inhibited cell proliferation and biomass at very low concentrations (0.005 µM). Meanwhile, Sotorasib at the concentration of 10 µM also demonstrated partial inhibition of other tested PDAC cell lines except T3M4 (KRAS Q61H). The cell proliferation and biomass decreased by 32% - 50% and 24% - 41%, respectively. However, in T3M4, little inhibition of cell proliferation and biomass was observed at all concentrations tested. This may be due to the fact that the Q61H mutation has the lowest intrinsic GTPase activity and requires less upstream signaling to maintain in a GTP-bound status [160]. The results of this study demonstrate that Sotorasib has inhibitory effects on KRAS G12D, G12V and wild-type PDAC cell lines at a concentration of 10 µM, a plasma concentration achievable in clinical trials [121]. It has been reported that Sotorasib only targets KRAS G12C, and all current clinical trials are also targeting KRAS G12C-mutated tumors, including PDAC, but since Sotorasib has inhibitory effect on cells with other KRAS G12 mutation at high concentrations, this suggests that Sotorasib may have the potential to target proteins other than KRAS G12C. Since the mutations of PDAC are mainly KRAS G12D (45%) and KRAS G12V (35%), this result is more meaningful for the treatment of PDAC [105].

As for the multi-KRAS mutation inhibitor BI-3406, our results were comparable to those previously reported in 2D cultures [125]. The biological responses of cell lines carrying the KRAS G12V mutation (Capan-1 and PaTu8902) were similar to the wild-type cell line BxPc-3, with only about 15% decrease at 10 µM. Although BI-3406 has previously been reported to achieve good inhibitory effects on KRAS G12V-mutated NSCLC cell lines, this antitumor effect appears to be poor for PDAC cell lines [125]. In cell lines harboring KRAS G12C and G12D mutations, the 10 µM concentration inhibited cell proliferation and biomass by more than 30%. Although BI-3406 as a single inhibitor showed little inhibitory effect on PDAC cell lines, it demonstrated a dramatically synergistic effect in combined inhibition with downstream pathway inhibitors, especially the MEK1/2 inhibitor Trametinib. The combination of BI-3406 and Trametinib demonstrated synergistic effect in both *KRAS*-mutated and wild-type PDAC cell lines. This is probably because BI-3406 combined with Trametinib can block the negative feedback regulatory mechanism by reducing phospho (p)-MEK and p-ERK levels, resulting in a strong synergistic effect [125]. Since this regulatory mechanism exists both in *KRAS*-mutated and wild-type cell lines, therefore, this double-inhibitor combination was also effective against BxPc-3. For the combination of BI-3406 and Buparlisib, although the Bliss independent model assessment indicated a synergistic effect in this combination, the comparison with the single-application efficacy of Buparlisib found that this combination was only significantly different in MIA PaCa-2, while significant differences were not observed in the other cell lines. This suggests that the combination of BI-3406 with Buparlisib demonstrated only additive effects in AsPc-1, BxPc-3 and Capan-1. Since Buparlisib does not reduce p-MEK and p-ERK levels, it is highly likely fails to activate the negative feedback loop, resulting in little synergistic effect

[125]. Moreover, the triple inhibitor combination of BI-3406 also demonstrated significant synergistic effect, and the inhibitory efficacy was increased compared with the double inhibitor combination. These results suggested that the BI-3406-based inhibitor combination is a potential therapeutic approach for *KRAS* G12 mutant or wild-type PDAC.

The double-inhibitor combination based on Sotorasib also displayed synergistic effect, but only in MIA PaCa-2. Since RAS directly forms a complex with PI3K to further activate the PI3K signaling pathway, inhibition of these two proteins greatly reduces the activation of this pathway and might explain the synergistic effect of these two inhibitors [161-164]. Additive effects were observed in AsPc-1, BxPc-3 and Capan-1, indicating that the unknown target protein of Sotorasib in non-*KRAS* G12C mutant cells does not overlap with the RAS/RAF/MEK/ERK pathway or the PI3K/AKT pathway. Furthermore, in MIA PaCa-2, when compared with the BI-3406-based combination, the inhibitory effect of Sotorasib and Trametinib was weak. This possibly because RAS directly forms a complex with PI3K to further activate the PI3K signaling pathway, direct inhibition of the two proteins greatly reduces the activation of the PI3K protein and increase the synergistic effect of two inhibitors. In addition, the triple inhibitor combination based on Sotorasib displayed synergistic effect only in MIA PaCa-2, further explaining that the unknown target protein of Sotorasib does not interact with the RAS downstream pathway. These results suggest that Sotorasib-based inhibitor combinations are only suitable for the treatment of KRAS G12C-mutated PDAC.

The BI-3406 triple inhibitor combination modulated immunity, cell adhesion and migration, and targeted cancer pathways in all four cell lines. This indicates that this inhibitor combination can directly influence the pathophysiology of tumor cells, but might also indirectly inhibit the growth of PDAC cells by modulating the immune system as well as cell-to-cell interactions. Furthermore, we observed that in all four cell lines both triple inhibitor combinations regulated DEGs, which are involved in response to hypoxia. These genes (*ALDOA*, *IL6*, *IL6R*, *EGF*, *VEFG*, *PDK-1*, *ENO1*, *etc.*) were all associated to the hypoxia inducible factor-1 (HIF-1) pathway, suggesting that both combinations can act on the HIF-1 pathway. Several studies have shown that HIF-1 is associated with tumor growth in a variety of cancers including PDAC [165]. Inhibition of mTOR block the translation of HIF-1 mRNA, and inhibition of ERK can also lead to inhibition of HIF-1 [166, 167]. The combination of the two inhibitors in this experiment affected both mTOR and ERK, leading to changes in the downstream HIF-1 pathway, which seems to be another mechanism of this inhibitor combination.

Altogether, our current study demonstrates the antiproliferative effects of KRAS inhibitors alone or in combination with downstream inhibitors in PDAC cell lines *in vitro*. Moreover, the dose of each inhibitor was greatly reduced when used in combination, thereby reducing the side effects of the inhibitor. The KRAS::SOS1 inhibitor BI-3406 was able to enhance the anti-proliferative effect of downstream inhibitors in KRAS wild-type, KRAS G12C and KRAS G12D mutant cell lines, but not for KRAS G12V mutant cell lines. The KRAS G12C inhibitor Sotorasib mainly enhanced the anti-proliferative effect of downstream inhibitors in KRAS G12C mutant cell lines.

5.6 Summary

In conclusion, this study confirmed the antitumor potential of inhibiting CK2, CDKs, PI3K, AKT

and KRAS in different PDAC cell lines. The target gene of Silmitasertib (*CSNK2A1*, *CSNK2A2*, and *CSNK2B*) and Dinaciclib (*CDK1*, *CDK2*, *CDK5*, and *CDK9*) did not affect drug sensitivity in terms of aberrations and expression levels, while aberrations or expression levels of MK-220 target genes (*AKT1*, *AKT2*, and *AKT3*), Buparlisib target genes (*PIK3CA*, *PIK3CB*, *PIK3CG*, and *PIK3CD*) and PDAC hotspot genes (*KRAS* and *TP53*) were associated with differences in inhibitor sensitivity. Both KRAS inhibitors and KRAS inhibitor-based combinations showed antitumor potential in different PDAC cell lines, but the synergistic potential was not the same due to the different mechanisms of inhibition. At the same time, the synergistic potential of these inhibitor combinations varied for different KRAS mutant cell lines. Our current study demonstrates the antitumor properties of these novel specific pathway inhibitors in PDAC cell lines and the influence of some univariate genetic background differences on the efficacy of these inhibitors has also been initially proposed.

6 Conclusion and Outlook

Currently, PDAC remains a huge burden worldwide with an unsatisfying survival rate, especially for patients with advanced disease. Although the use of novel inhibitors has significantly improved patients' survival, there are still differences in inhibitor sensitivity due to the influence of different genetic backgrounds. Therefore, individualized selection of treatment regimens based on a patient's genetic background has become a research hotspot. This study focused on the sensitivity of PDAC cell lines of different genetic backgrounds to several novel pathway inhibitors. Furthermore, the effects of the aberrations of the target genes of these inhibitors and the common hot spot gene aberrations of PDAC on the efficacy of these inhibitors were comprehensively analyzed, and the background genes that had potential impact on the therapeutic effect were evaluated to provide the basis for clinical personalized treatment.

The antitumor potential of the novel inhibitors was confirmed on different PDAC cell lines. Furthermore, cells were grouped for sensitivity based on the results of these cell viability assays. Combined with the sequencing results of WES and RNA-seq, the effect of univariate genetic variation on drug sensitivity was preliminarily analyzed. Our study revealed that aberrations or expression levels of *AKT1*, *AKT2*, *AKT3*, *PIK3CA*, *PIK3CB*, *PIK3CG*, *PIK3CD*, *KRAS*, and *TP53* genes were associated with differences in inhibitor sensitivity. The *CSNK2A1*, *CSNK2A2*, *CSNK2B*, *CDK1*, *CDK2*, *CDK5*, and *CDK9* genes did not affect the inhibitor sensitivity in terms of their aberrations and expression levels. However, due to the interaction between different genetic aberrations, effects on downstream signaling, and dysregulation of expression, they can also have a major impact on drug sensitivity. We will focus on analyzing the effects of multivariate genetic variation on drug sensitivity in future studies.

Due to the important role of *KRAS* in PDAC. We also analyzed the antitumor and synergistic potential of KRAS inhibitors combined with downstream pathway inhibitors in PDAC cell lines. Both combinations based on different *KRAS* inhibitors showed antitumor potential in different PDAC cell lines, however, the synergistic potential of BI-3406 and Sotorasib was not the same due to the difference in the mechanism of inhibition by BI-3406 and Sotorasib. At the same time, the synergistic potential of these drug combinations is also different for different *KRAS* mutant cell lines. The underlying mechanisms leading to these differences are currently being analyzed.

In conclusion, our current study demonstrates the antitumor properties of these novel specific pathway inhibitors in PDAC cell lines. At the same time, the effect of some univariate genetic background differences on the efficacy of these inhibitors was also tentatively proposed. It provides good support for follow-up studies and clinical research.

7 References

1. Pishvaian MJ, Brody JR: **Therapeutic Implications of Molecular Subtyping for Pancreatic Cancer**. *Oncology (Williston Park)* 2017, **31**(3):159-166, 168.
2. McGuire S: **World Cancer Report 2014. Geneva, Switzerland: World Health Organization, International Agency for Research on Cancer, WHO Press, 2015**. *Adv Nutr* 2016, **7**(2):418-419.
3. **GCO** [https://gco.iarc.fr/]
4. Malvezzi M, Bertuccio P, Levi F *et al*: **European cancer mortality predictions for the year 2014**. *Ann Oncol* 2014, **25**(8):1650-1656.
5. Tempero MA: **NCCN Guidelines Updates: Pancreatic Cancer**. *J Natl Compr Canc Netw* 2019, **17**(5.5):603-605.
6. Klompmaker S, de Rooij T, Korteweg JJ *et al*: **Systematic review of outcomes after distal pancreatectomy with coeliac axis resection for locally advanced pancreatic cancer**. *Br J Surg* 2016, **103**(8):941-949.
7. Kyriazanos ID, Tsoukalos GG, Papageorgiou G *et al*: **Local recurrence of pancreatic cancer after primary surgical intervention: how to deal with this devastating scenario?** *Surg Oncol* 2011, **20**(4):e133-142.
8. Xu XD, Zhao Y, Zhang M *et al*: **Inhibition of Autophagy by Deguelin Sensitizes Pancreatic Cancer Cells to Doxorubicin**. *Int J Mol Sci* 2017, **18**(2).
9. Lovecek M, Skalicky P, Chudacek J *et al*: **Different clinical presentations of metachronous pulmonary metastases after resection of pancreatic ductal adenocarcinoma: Retrospective study and review of the literature**. *World J Gastroenterol* 2017, **23**(35):6420-6428.
10. Ryan DP, Hong TS, Bardeesy N: **Pancreatic adenocarcinoma**. *N Engl J Med* 2014, **371**(11):1039-1049.
11. McMenamin UC, McCain S, Kunzmann AT: **Do smoking and alcohol behaviours influence GI cancer survival?** *Best Pract Res Clin Gastroenterol* 2017, **31**(5):569-577.
12. Masoudi S, Momayez Sanat Z, Mahmud Saleh A *et al*: **Menstrual and Reproductive Factors and Risk of Pancreatic Cancer in Women**. *Middle East J Dig Dis* 2017, **9**(3):146-149.
13. Wolpin BM, Chan AT, Hartge P *et al*: **ABO blood group and the risk of pancreatic cancer**. *J Natl Cancer Inst* 2009, **101**(6):424-431.
14. Wolpin BM, Kraft P, Gross M *et al*: **Pancreatic cancer risk and ABO blood group alleles: results from the pancreatic cancer cohort consortium**. *Cancer Res* 2010, **70**(3):1015-1023.
15. Stevens RJ, Roddam AW, Beral V: **Pancreatic cancer in type 1 and young-onset diabetes: systematic review and meta-analysis**. *Br J Cancer* 2007, **96**(3):507-509.
16. Huxley R, Ansary-Moghaddam A, Berrington de Gonzalez A *et al*: **Type-II diabetes and pancreatic cancer: a meta-analysis of 36 studies**. *Br J Cancer* 2005, **92**(11):2076-2083.
17. Maisonneuve P, Lowenfels AB: **Epidemiology of pancreatic cancer: an update**. *Dig Dis* 2010, **28**(4-5):645-656.
18. Hruban RH, Canto MI, Goggins M *et al*: **Update on familial pancreatic cancer**. *Adv Surg* 2010, **44**:293-311.

19. Klein AP, Brune KA, Petersen GM *et al*: **Prospective risk of pancreatic cancer in familial pancreatic cancer kindreds**. *Cancer Res* 2004, **64**(7):2634-2638.
20. Jones S, Zhang X, Parsons DW *et al*: **Core signaling pathways in human pancreatic cancers revealed by global genomic analyses**. *Science* 2008, **321**(5897):1801-1806.
21. Campbell PJ, Yachida S, Mudie LJ *et al*: **The patterns and dynamics of genomic instability in metastatic pancreatic cancer**. *Nature* 2010, **467**(7319):1109-1113.
22. Biankin AV, Waddell N, Kassahn KS *et al*: **Pancreatic cancer genomes reveal aberrations in axon guidance pathway genes**. *Nature* 2012, **491**(7424):399-405.
23. Waddell N, Pajic M, Patch AM *et al*: **Whole genomes redefine the mutational landscape of pancreatic cancer**. *Nature* 2015, **518**(7540):495-501.
24. Witkiewicz AK, McMillan EA, Balaji U *et al*: **Whole-exome sequencing of pancreatic cancer defines genetic diversity and therapeutic targets**. *Nat Commun* 2015, **6**:6744.
25. Bailey P, Chang DK, Nones K *et al*: **Genomic analyses identify molecular subtypes of pancreatic cancer**. *Nature* 2016, **531**(7592):47-52.
26. Vogelstein B, Kinzler KW: **Cancer genes and the pathways they control**. *Nat Med* 2004, **10**(8):789-799.
27. Hwang RF, Gordon EM, Anderson WF *et al*: **Gene therapy for primary and metastatic pancreatic cancer with intraperitoneal retroviral vector bearing the wild-type p53 gene**. *Surgery* 1998, **124**(2):143-150; discussion 150-141.
28. Hahn SA, Schutte M, Hoque AT *et al*: **DPC4, a candidate tumor suppressor gene at human chromosome 18q21.1**. *Science* 1996, **271**(5247):350-353.
29. Puri S, Folias AE, Hebrok M: **Plasticity and dedifferentiation within the pancreas: development, homeostasis, and disease**. *Cell Stem Cell* 2015, **16**(1):18-31.
30. Kopp JL, von Figura G, Mayes E *et al*: **Identification of Sox9-dependent acinar-to-ductal reprogramming as the principal mechanism for initiation of pancreatic ductal adenocarcinoma**. *Cancer Cell* 2012, **22**(6):737-750.
31. Kanda M, Matthaei H, Wu J *et al*: **Presence of somatic mutations in most early-stage pancreatic intraepithelial neoplasia**. *Gastroenterology* 2012, **142**(4):730-733 e739.
32. Hruban RH, Takaori K, Klimstra DS *et al*: **An illustrated consensus on the classification of pancreatic intraepithelial neoplasia and intraductal papillary mucinous neoplasms**. *Am J Surg Pathol* 2004, **28**(8):977-987.
33. Wu J, Matthaei H, Maitra A *et al*: **Recurrent GNAS mutations define an unexpected pathway for pancreatic cyst development**. *Sci Transl Med* 2011, **3**(92):92ra66.
34. Hruban RH, Goggins M, Parsons J *et al*: **Progression model for pancreatic cancer**. *Clin Cancer Res* 2000, **6**(8):2969-2972.
35. Hruban RH, Wilentz RE, Kern SE: **Genetic progression in the pancreatic ducts**. *Am J Pathol* 2000, **156**(6):1821-1825.
36. Kinzler KW, Vogelstein B: **Cancer-susceptibility genes. Gatekeepers and caretakers**. *Nature* 1997, **386**(6627):761, 763.
37. Yamano M, Fujii H, Takagaki T *et al*: **Genetic progression and divergence in pancreatic carcinoma**. *Am J Pathol* 2000, **156**(6):2123-2133.
38. Wilentz RE, Geradts J, Maynard R *et al*: **Inactivation of the p16 (INK4A) tumor-suppressor gene in pancreatic duct lesions: loss of intranuclear expression**. *Cancer Res* 1998, **58**(20):4740-4744.

39. DiGiuseppe JA, Hruban RH, Goodman SN *et al*: **Overexpression of p53 protein in adenocarcinoma of the pancreas**. *Am J Clin Pathol* 1994, **101**(6):684-688.
40. Goggins M, Hruban RH, Kern SE: **BRCA2 is inactivated late in the development of pancreatic intraepithelial neoplasia: evidence and implications**. *Am J Pathol* 2000, **156**(5):1767-1771.
41. Wilentz RE, Iacobuzio-Donahue CA, Argani P *et al*: **Loss of expression of Dpc4 in pancreatic intraepithelial neoplasia: evidence that DPC4 inactivation occurs late in neoplastic progression**. *Cancer Res* 2000, **60**(7):2002-2006.
42. Gruber R, van Haarlem LJ, Warnaar SO *et al*: **The human antimouse immunoglobulin response and the anti-idiotypic network have no influence on clinical outcome in patients with minimal residual colorectal cancer treated with monoclonal antibody CO17-1A**. *Cancer Res* 2000, **60**(7):1921-1926.
43. Giovinazzo F, Turri G, Zanini S *et al*: **Clinical implications of biological markers in Pancreatic Ductal Adenocarcinoma**. *Surg Oncol* 2012, **21**(4):e171-182.
44. **Proteinatlas** [https://www.proteinatlas.org/humanproteome/pathology/pancreatic+cancer]
45. Smit VT, Boot AJ, Smits AM *et al*: **KRAS codon 12 mutations occur very frequently in pancreatic adenocarcinomas**. *Nucleic Acids Res* 1988, **16**(16):7773-7782.
46. Caldas C, Hahn SA, da Costa LT *et al*: **Frequent somatic mutations and homozygous deletions of the p16 (MTS1) gene in pancreatic adenocarcinoma**. *Nat Genet* 1994, **8**(1):27-32.
47. Redston MS, Caldas C, Seymour AB *et al*: **p53 mutations in pancreatic carcinoma and evidence of common involvement of homocopolymer tracts in DNA microdeletions**. *Cancer Res* 1994, **54**(11):3025-3033.
48. Maurice D, Pierreux CE, Howell M *et al*: **Loss of Smad4 function in pancreatic tumors: C-terminal truncation leads to decreased stability**. *J Biol Chem* 2001, **276**(46):43175-43181.
49. Bond-Smith G, Banga N, Hammond TM *et al*: **Pancreatic adenocarcinoma**. *BMJ* 2012, **344**:e2476.
50. Burnett G, Kennedy EP: **The enzymatic phosphorylation of proteins**. *J Biol Chem* 1954, **211**(2):969-980.
51. UniProt C: **UniProt: a worldwide hub of protein knowledge**. *Nucleic Acids Res* 2019, **47**(D1):D506-D515.
52. Qaiser F, Trembley JH, Kren BT *et al*: **Protein kinase CK2 inhibition induces cell death via early impact on mitochondrial function**. *J Cell Biochem* 2014, **115**(12):2103-2115.
53. Faust M, Jung M, Gunther J *et al*: **Localization of individual subunits of protein kinase CK2 to the endoplasmic reticulum and to the Golgi apparatus**. *Mol Cell Biochem* 2001, **227**(1-2):73-80.
54. Rodriguez FA, Contreras C, Bolanos-Garcia V *et al*: **Protein kinase CK2 as an ectokinase: the role of the regulatory CK2beta subunit**. *Proc Natl Acad Sci U S A* 2008, **105**(15):5693-5698.
55. Litchfield DW: **Protein kinase CK2: structure, regulation and role in cellular decisions of life and death**. *Biochem J* 2003, **369**(Pt 1):1-15.
56. Ruzzene M, Bertacchini J, Toker A *et al*: **Cross-talk between the CK2 and AKT signaling**

pathways in cancer. *Adv Biol Regul* 2017, **64**:1-8.
57. Di Maira G, Salvi M, Arrigoni G *et al*: **Protein kinase CK2 phosphorylates and upregulates Akt/PKB**. *Cell Death & Differentiation* 2005, **12**(6):668-677.
58. Vazquez F, Grossman SR, Takahashi Y *et al*: **Phosphorylation of the PTEN tail acts as an inhibitory switch by preventing its recruitment into a protein complex**. *J Biol Chem* 2001, **276**(52):48627-48630.
59. Hanahan D, Weinberg RA: **Hallmarks of cancer: the next generation**. *Cell* 2011, **144**(5):646-674.
60. Zheng Y, Qin H, Frank SJ *et al*: **A CK2-dependent mechanism for activation of the JAK-STAT signaling pathway**. *Blood* 2011, **118**(1):156-166.
61. Schevzov G, Kee AJ, Wang B *et al*: **Regulation of cell proliferation by ERK and signal-dependent nuclear translocation of ERK is dependent on Tm5NM1-containing actin filaments**. *Mol Biol Cell* 2015, **26**(13):2475-2490.
62. Kreutzer JN, Ruzzene M, Guerra B: **Enhancing chemosensitivity to gemcitabine via RNA interference targeting the catalytic subunits of protein kinase CK2 in human pancreatic cancer cells**. *BMC Cancer* 2010, **10**:440.
63. Giroux V, Iovanna J, Dagorn JC: **Probing the human kinome for kinases involved in pancreatic cancer cell survival and gemcitabine resistance**. *FASEB J* 2006, **20**(12):1982-1991.
64. Siddiqui-Jain A, Drygin D, Streiner N *et al*: **CX-4945, an orally bioavailable selective inhibitor of protein kinase CK2, inhibits prosurvival and angiogenic signaling and exhibits antitumor efficacy**. *Cancer Res* 2010, **70**(24):10288-10298.
65. Hamacher R, Saur D, Fritsch R *et al*: **Casein kinase II inhibition induces apoptosis in pancreatic cancer cells**. *Oncol Rep* 2007, **18**(3):695-701.
66. **ClinicalTrials.gov** [https://www.clinicaltrials.gov/]
67. Malumbres M, Barbacid M: **Cell cycle, CDKs and cancer: a changing paradigm**. *Nat Rev Cancer* 2009, **9**(3):153-166.
68. Hunter T, Pines J: **Cyclins and cancer. II: Cyclin D and CDK inhibitors come of age**. *Cell* 1994, **79**(4):573-582.
69. Bregman DB, Pestell RG, Kidd VJ: **Cell cycle regulation and RNA polymerase II**. *Front Biosci* 2000, **5**:D244-257.
70. Sharma S, Sicinski P: **A kinase of many talents: non-neuronal functions of CDK5 in development and disease**. *Open Biol* 2020, **10**(1):190287.
71. Chen X, Niu H, Chung WH *et al*: **Cell cycle regulation of DNA double-strand break end resection by Cdk1-dependent Dna2 phosphorylation**. *Nat Struct Mol Biol* 2011, **18**(9):1015-1019.
72. Yu DS, Zhao R, Hsu EL *et al*: **Cyclin-dependent kinase 9-cyclin K functions in the replication stress response**. *EMBO Rep* 2010, **11**(11):876-882.
73. Roskoski R, Jr.: **Cyclin-dependent protein kinase inhibitors including palbociclib as anticancer drugs**. *Pharmacol Res* 2016, **107**:249-275.
74. Eggers JP, Grandgenett PM, Collisson EC *et al*: **Cyclin-dependent kinase 5 is amplified and overexpressed in pancreatic cancer and activated by mutant K-Ras**. *Clin Cancer Res* 2011, **17**(19):6140-6150.
75. Feldmann G, Mishra A, Bisht S *et al*: **Cyclin-dependent kinase inhibitor Dinaciclib**

(SCH727965) inhibits pancreatic cancer growth and progression in murine xenograft models. *Cancer Biol Ther* 2011, **12**(7):598-609.

76. Cai D, Latham VM, Jr., Zhang X *et al*: **Correction: Combined Depletion of Cell Cycle and Transcriptional Cyclin-Dependent Kinase Activities Induces Apoptosis in Cancer Cells**. *Cancer Res* 2020, **80**(2):361.
77. Gojo I, Zhang B, Fenton RG: **The cyclin-dependent kinase inhibitor flavopiridol induces apoptosis in multiple myeloma cells through transcriptional repression and down-regulation of Mcl-1**. *Clin Cancer Res* 2002, **8**(11):3527-3538.
78. Le Tourneau C, Faivre S, Laurence V *et al*: **Phase I evaluation of seliciclib (R-roscovitine), a novel oral cyclin-dependent kinase inhibitor, in patients with advanced malignancies**. *Eur J Cancer* 2010, **46**(18):3243-3250.
79. Mita MM, Mita AC, Moseley JL *et al*: **Phase 1 safety, pharmacokinetic and pharmacodynamic study of the cyclin-dependent kinase inhibitor dinaciclib administered every three weeks in patients with advanced malignancies**. *Br J Cancer* 2017, **117**(9):1258-1268.
80. Kazi A, Chen L, Xiang S *et al*: **Global Phosphoproteomics Reveal CDK Suppression as a Vulnerability to KRas Addiction in Pancreatic Cancer**. *Clin Cancer Res* 2021, **27**(14):4012-4024.
81. Donahue TR, Tran LM, Hill R *et al*: **Integrative survival-based molecular profiling of human pancreatic cancer**. *Clin Cancer Res* 2012, **18**(5):1352-1363.
82. Engelman JA, Luo J, Cantley LC: **The evolution of phosphatidylinositol 3-kinases as regulators of growth and metabolism**. *Nat Rev Genet* 2006, **7**(8):606-619.
83. Yuan TL, Cantley LC: **PI3K pathway alterations in cancer: variations on a theme**. *Oncogene* 2008, **27**(41):5497-5510.
84. Alessi DR, James SR, Downes CP *et al*: **Characterization of a 3-phosphoinositide-dependent protein kinase which phosphorylates and activates protein kinase Balpha**. *Curr Biol* 1997, **7**(4):261-269.
85. Guo H, German P, Bai S *et al*: **The PI3K/AKT Pathway and Renal Cell Carcinoma**. *J Genet Genomics* 2015, **42**(7):343-353.
86. Stemke-Hale K, Gonzalez-Angulo AM, Lluch A *et al*: **An integrative genomic and proteomic analysis of PIK3CA, PTEN, and AKT mutations in breast cancer**. *Cancer Res* 2008, **68**(15):6084-6091.
87. Aziz SA, Davies M, Pick E *et al*: **Phosphatidylinositol-3-kinase as a therapeutic target in melanoma**. *Clin Cancer Res* 2009, **15**(9):3029-3036.
88. Zhou BP, Hu MC, Miller SA *et al*: **HER-2/neu blocks tumor necrosis factor-induced apoptosis via the Akt/NF-kappaB pathway**. *J Biol Chem* 2000, **275**(11):8027-8031.
89. Eser S, Reiff N, Messer M *et al*: **Selective requirement of PI3K/PDK1 signaling for Kras oncogene-driven pancreatic cell plasticity and cancer**. *Cancer Cell* 2013, **23**(3):406-420.
90. Yamamoto S, Tomita Y, Hoshida Y *et al*: **Prognostic significance of activated Akt expression in pancreatic ductal adenocarcinoma**. *Clin Cancer Res* 2004, **10**(8):2846-2850.
91. Schlieman MG, Fahy BN, Ramsamooj R *et al*: **Incidence, mechanism and prognostic value of activated AKT in pancreas cancer**. *Br J Cancer* 2003, **89**(11):2110-2115.

92. Murthy D, Attri KS, Singh PK: **Phosphoinositide 3-Kinase Signaling Pathway in Pancreatic Ductal Adenocarcinoma Progression, Pathogenesis, and Therapeutics**. *Front Physiol* 2018, **9**:335.
93. Ihle NT, Lemos R, Jr., Wipf P *et al*: **Mutations in the phosphatidylinositol-3-kinase pathway predict for antitumor activity of the inhibitor PX-866 whereas oncogenic Ras is a dominant predictor for resistance**. *Cancer Res* 2009, **69**(1):143-150.
94. Van Dort ME, Galban S, Wang H *et al*: **Dual inhibition of allosteric mitogen-activated protein kinase (MEK) and phosphatidylinositol 3-kinase (PI3K) oncogenic targets with a bifunctional inhibitor**. *Bioorg Med Chem* 2015, **23**(7):1386-1394.
95. Manning BD, Toker A: **AKT/PKB Signaling: Navigating the Network**. *Cell* 2017, **169**(3):381-405.
96. Wang J, Zhao W, Guo H *et al*: **AKT isoform-specific expression and activation across cancer lineages**. *BMC Cancer* 2018, **18**(1):742.
97. Zhou GL, Tucker DF, Bae SS *et al*: **Opposing roles for Akt1 and Akt2 in Rac/Pak signaling and cell migration**. *J Biol Chem* 2006, **281**(47):36443-36453.
98. Easton RM, Cho H, Roovers K *et al*: **Role for Akt3/protein kinase Bgamma in attainment of normal brain size**. *Mol Cell Biol* 2005, **25**(5):1869-1878.
99. Liao Y, Hung MC: **Physiological regulation of Akt activity and stability**. *Am J Transl Res* 2010, **2**(1):19-42.
100. Scheid MP, Woodgett JR: **Unravelling the activation mechanisms of protein kinase B/Akt**. *FEBS Lett* 2003, **546**(1):108-112.
101. Wang Y, Kuramitsu Y, Baron B *et al*: **PI3K inhibitor LY294002, as opposed to wortmannin, enhances AKT phosphorylation in gemcitabine-resistant pancreatic cancer cells**. *Int J Oncol* 2017, **50**(2):606-612.
102. Jacinto E, Facchinetti V, Liu D *et al*: **SIN1/MIP1 maintains rictor-mTOR complex integrity and regulates Akt phosphorylation and substrate specificity**. *Cell* 2006, **127**(1):125-137.
103. Cheng JQ, Lindsley CW, Cheng GZ *et al*: **The Akt/PKB pathway: molecular target for cancer drug discovery**. *Oncogene* 2005, **24**(50):7482-7492.
104. Altomare DA, Tanno S, De Rienzo A *et al*: **Frequent activation of AKT2 kinase in human pancreatic carcinomas**. *J Cell Biochem* 2002, **87**(4):470-476.
105. Mann KM, Ying H, Juan J *et al*: **KRAS-related proteins in pancreatic cancer**. *Pharmacol Ther* 2016, **168**:29-42.
106. Prior IA, Lewis PD, Mattos C: **A comprehensive survey of Ras mutations in cancer**. *Cancer Res* 2012, **72**(10):2457-2467.
107. Moore AR, Rosenberg SC, McCormick F *et al*: **RAS-targeted therapies: is the undruggable drugged?** *Nat Rev Drug Discov* 2020, **19**(8):533-552.
108. di Magliano MP, Logsdon CD: **Roles for KRAS in pancreatic tumor development and progression**. *Gastroenterology* 2013, **144**(6):1220-1229.
109. Hingorani SR, Wang L, Multani AS *et al*: **Trp53R172H and KrasG12D cooperate to promote chromosomal instability and widely metastatic pancreatic ductal adenocarcinoma in mice**. *Cancer Cell* 2005, **7**(5):469-483.
110. Bardeesy N, Cheng KH, Berger JH *et al*: **Smad4 is dispensable for normal pancreas development yet critical in progression and tumor biology of pancreas cancer**. *Genes*

Dev 2006, **20**(22):3130-3146.

111. Bardeesy N, Aguirre AJ, Chu GC *et al*: **Both p16(Ink4a) and the p19(Arf)-p53 pathway constrain progression of pancreatic adenocarcinoma in the mouse**. *Proc Natl Acad Sci U S A* 2006, **103**(15):5947-5952.
112. Aguirre AJ, Bardeesy N, Sinha M *et al*: **Activated Kras and Ink4a/Arf deficiency cooperate to produce metastatic pancreatic ductal adenocarcinoma**. *Genes Dev* 2003, **17**(24):3112-3126.
113. Guerra C, Barbacid M: **Genetically engineered mouse models of pancreatic adenocarcinoma**. *Mol Oncol* 2013, **7**(2):232-247.
114. Bournet B, Buscail C, Muscari F *et al*: **Targeting KRAS for diagnosis, prognosis, and treatment of pancreatic cancer: Hopes and realities**. *Eur J Cancer* 2016, **54**:75-83.
115. Zhao H, Wu S, Li H *et al*: **ROS/KRAS/AMPK Signaling Contributes to Gemcitabine-Induced Stem-like Cell Properties in Pancreatic Cancer**. *Mol Ther Oncolytics* 2019, **14**:299-312.
116. Kawesha A, Ghaneh P, Andren-Sandberg A *et al*: **K-ras oncogene subtype mutations are associated with survival but not expression of p53, p16(INK4A), p21(WAF-1), cyclin D1, erbB-2 and erbB-3 in resected pancreatic ductal adenocarcinoma**. *Int J Cancer* 2000, **89**(6):469-474.
117. Hamarsheh S, Gross O, Brummer T *et al*: **Immune modulatory effects of oncogenic KRAS in cancer**. *Nat Commun* 2020, **11**(1):5439.
118. Dias Carvalho P, Guimaraes CF, Cardoso AP *et al*: **KRAS Oncogenic Signaling Extends beyond Cancer Cells to Orchestrate the Microenvironment**. *Cancer Res* 2018, **78**(1):7-14.
119. Pu N, Chen Q, Gao S *et al*: **Genetic landscape of prognostic value in pancreatic ductal adenocarcinoma microenvironment**. *Ann Transl Med* 2019, **7**(22):645.
120. Ischenko I, D'Amico S, Rao M *et al*: **KRAS drives immune evasion in a genetic model of pancreatic cancer**. *Nat Commun* 2021, **12**(1):1482.
121. Hong DS, Fakih MG, Strickler JH *et al*: **KRAS(G12C) Inhibition with Sotorasib in Advanced Solid Tumors**. *N Engl J Med* 2020, **383**(13):1207-1217.
122. Janes MR, Zhang J, Li LS *et al*: **Targeting KRAS Mutant Cancers with a Covalent G12C-Specific Inhibitor**. *Cell* 2018, **172**(3):578-589 e517.
123. Hallin J, Engstrom LD, Hargis L *et al*: **The KRAS(G12C) Inhibitor MRTX849 Provides Insight toward Therapeutic Susceptibility of KRAS-Mutant Cancers in Mouse Models and Patients**. *Cancer Discov* 2020, **10**(1):54-71.
124. Nagasaka M, Li Y, Sukari A *et al*: **KRAS G12C Game of Thrones, which direct KRAS inhibitor will claim the iron throne?** *Cancer Treat Rev* 2020, **84**:101974.
125. Hofmann MH, Gmachl M, Ramharter J *et al*: **BI-3406, a Potent and Selective SOS1-KRAS Interaction Inhibitor, Is Effective in KRAS-Driven Cancers through Combined MEK Inhibition**. *Cancer Discov* 2021, **11**(1):142-157.
126. Strickler JH, Satake H, Hollebecque A *et al*: **First data for sotorasib in patients with pancreatic cancer with KRAS p.G12C mutation: A phase I/II study evaluating efficacy and safety**. *Journal of Clinical Oncology* 2022, **40**(36_suppl):360490-360490.
127. Bullinger L, Dohner K, Dohner H: **Genomics of Acute Myeloid Leukemia Diagnosis and Pathways**. *J Clin Oncol* 2017, **35**(9):934-946.

128. Litton JK, Burstein HJ, Turner NC: **Molecular Testing in Breast Cancer**. *Am Soc Clin Oncol Educ Book* 2019, **39**:e1-e7.
129. Imyanitov EN, Iyevleva AG, Levchenko EV: **Molecular testing and targeted therapy for non-small cell lung cancer: Current status and perspectives**. *Crit Rev Oncol Hematol* 2021, **157**:103194.
130. Walker-Smith TL, Peck J: **Genetic and Genomic Advances in Breast Cancer Diagnosis and Treatment**. *Nurs Womens Health* 2019, **23**(6):518-525.
131. Allen PJ, Kuk D, Castillo CF *et al*: **Multi-institutional Validation Study of the American Joint Commission on Cancer (8th Edition) Changes for T and N Staging in Patients With Pancreatic Adenocarcinoma**. *Ann Surg* 2017, **265**(1):185-191.
132. Collisson EA, Sadanandam A, Olson P *et al*: **Subtypes of pancreatic ductal adenocarcinoma and their differing responses to therapy**. *Nat Med* 2011, **17**(4):500-503.
133. Golan T, Sella T, O'Reilly EM *et al*: **Overall survival and clinical characteristics of BRCA mutation carriers with stage I/II pancreatic cancer**. *Br J Cancer* 2017, **116**(6):697-702.
134. Aung KL, Fischer SE, Denroche RE *et al*: **Genomics-Driven Precision Medicine for Advanced Pancreatic Cancer: Early Results from the COMPASS Trial**. *Clin Cancer Res* 2018, **24**(6):1344-1354.
135. Lowery MA, Jordan EJ, Basturk O *et al*: **Real-Time Genomic Profiling of Pancreatic Ductal Adenocarcinoma: Potential Actionability and Correlation with Clinical Phenotype**. *Clin Cancer Res* 2017, **23**(20):6094-6100.
136. Liao Y, Smyth GK, Shi W: **featureCounts: an efficient general purpose program for assigning sequence reads to genomic features**. *Bioinformatics* 2014, **30**(7):923-930.
137. Dobin A, Davis CA, Schlesinger F *et al*: **STAR: ultrafast universal RNA-seq aligner**. *Bioinformatics* 2013, **29**(1):15-21.
138. **SKlearn** [https://scikit-learn.org/stable/index.html (accessed on 25 November 2021)]
139. Goldoni M, Johansson C: **A mathematical approach to study combined effects of toxicants in vitro: evaluation of the Bliss independence criterion and the Loewe additivity model**. *Toxicol In Vitro* 2007, **21**(5):759-769.
140. **Babraham Bioinformatics** [http://www.bioinformatics.babraham.ac.uk/]
141. Kim D, Langmead B, Salzberg SL: **HISAT: a fast spliced aligner with low memory requirements**. *Nat Methods* 2015, **12**(4):357-360.
142. Pertea M, Kim D, Pertea GM *et al*: **Transcript-level expression analysis of RNA-seq experiments with HISAT, StringTie and Ballgown**. *Nat Protoc* 2016, **11**(9):1650-1667.
143. Anders S, Pyl PT, Huber W: **HTSeq--a Python framework to work with high-throughput sequencing data**. *Bioinformatics* 2015, **31**(2):166-169.
144. Subramanian A, Tamayo P, Mootha VK *et al*: **Gene set enrichment analysis: a knowledge-based approach for interpreting genome-wide expression profiles**. *Proc Natl Acad Sci U S A* 2005, **102**(43):15545-15550.
145. Clark NR, Hu KS, Feldmann AS *et al*: **The characteristic direction: a geometrical approach to identify differentially expressed genes**. *BMC Bioinformatics* 2014, **15**:79.
146. [The NCCN clinical practice guidelines in oncology Pancreatic Adenocarcinoma (version 1.2022). https://www.nccn.org/guidelines/guidelines-detail?category=1&id=1455]

147. Gao J, Aksoy BA, Dogrusoz U *et al*: **Integrative analysis of complex cancer genomics and clinical profiles using the cBioPortal**. *Sci Signal* 2013, **6**(269):pl1.
148. Boeck S, Jung A, Laubender RP *et al*: **KRAS mutation status is not predictive for objective response to anti-EGFR treatment with erlotinib in patients with advanced pancreatic cancer**. *J Gastroenterol* 2013, **48**(4):544-548.
149. Kotler E, Shani O, Goldfeld G *et al*: **A Systematic p53 Mutation Library Links Differential Functional Impact to Cancer Mutation Pattern and Evolutionary Conservation**. *Mol Cell* 2018, **71**(5):873.
150. Grochola LF, Taubert H, Greither T *et al*: **Elevated transcript levels from the MDM2 P1 promoter and low p53 transcript levels are associated with poor prognosis in human pancreatic ductal adenocarcinoma**. *Pancreas* 2011, **40**(2):265-270.
151. Brown MS, Diallo OT, Hu M *et al*: **CK2 modulation of NF-kappaB, TP53, and the malignant phenotype in head and neck cancer by anti-CK2 oligonucleotides in vitro or in vivo via sub-50-nm nanocapsules**. *Clin Cancer Res* 2010, **16**(8):2295-2307.
152. Kotler E, Shani O, Goldfeld G *et al*: **A Systematic p53 Mutation Library Links Differential Functional Impact to Cancer Mutation Pattern and Evolutionary Conservation**. *Mol Cell* 2018, **71**(1):178-190 e178.
153. Welch WJ: **How cells respond to stress**. *Sci Am* 1993, **268**(5):56-64.
154. Berridge MV, Herst PM, Tan AS: **Tetrazolium dyes as tools in cell biology: new insights into their cellular reduction**. *Biotechnol Annu Rev* 2005, **11**:127-152.
155. She QB, Halilovic E, Ye Q *et al*: **4E-BP1 is a key effector of the oncogenic activation of the AKT and ERK signaling pathways that integrates their function in tumors**. *Cancer Cell* 2010, **18**(1):39-51.
156. Ormanns S, Siveke JT, Heinemann V *et al*: **pERK, pAKT and p53 as tissue biomarkers in erlotinib-treated patients with advanced pancreatic cancer: a translational subgroup analysis from AIO-PK0104**. *BMC Cancer* 2014, **14**:624.
157. Burger MT, Pecchi S, Wagman A *et al*: **Identification of NVP-BKM120 as a Potent, Selective, Orally Bioavailable Class I PI3 Kinase Inhibitor for Treating Cancer**. *ACS Med Chem Lett* 2011, **2**(10):774-779.
158. Criscitiello C, Viale G, Curigliano G *et al*: **Profile of buparlisib and its potential in the treatment of breast cancer: evidence to date**. *Breast Cancer (Dove Med Press)* 2018, **10**:23-29.
159. Banno E, Togashi Y, de Velasco MA *et al*: **Clinical significance of Akt2 in advanced pancreatic cancer treated with erlotinib**. *Int J Oncol* 2017, **50**(6):2049-2058.
160. Hunter JC, Manandhar A, Carrasco MA *et al*: **Biochemical and Structural Analysis of Common Cancer-Associated KRAS Mutations**. *Mol Cancer Res* 2015, **13**(9):1325-1335.
161. Rodriguez-Viciana P, Warne PH, Dhand R *et al*: **Phosphatidylinositol-3-OH kinase as a direct target of Ras**. *Nature* 1994, **370**(6490):527-532.
162. Rodriguez-Viciana P, Warne PH, Vanhaesebroeck B *et al*: **Activation of phosphoinositide 3-kinase by interaction with Ras and by point mutation**. *EMBO J* 1996, **15**(10):2442-2451.
163. Rubio I, Rodriguez-Viciana P, Downward J *et al*: **Interaction of Ras with phosphoinositide 3-kinase gamma**. *Biochem J* 1997, **326 (Pt 3)**:891-895.
164. Vanhaesebroeck B, Welham MJ, Kotani K *et al*: **P110delta, a novel phosphoinositide**

3-kinase in leukocytes. *Proc Natl Acad Sci U S A* 1997, **94**(9):4330-4335.

165. Semenza GL: **Defining the role of hypoxia-inducible factor 1 in cancer biology and therapeutics**. *Oncogene* 2010, **29**(5):625-634.

166. Laughner E, Taghavi P, Chiles K *et al*: **HER2 (neu) signaling increases the rate of hypoxia-inducible factor 1alpha (HIF-1alpha) synthesis: novel mechanism for HIF-1-mediated vascular endothelial growth factor expression**. *Mol Cell Biol* 2001, **21**(12):3995-4004.

167. Pages G, Pouyssegur J: **Transcriptional regulation of the Vascular Endothelial Growth Factor gene--a concert of activating factors**. *Cardiovasc Res* 2005, **65**(3):564-573.

8 Appendix

8.1 Abbreviations

Abbreviation	Meaning
4E-BP1	Eukaryotic Translation Initiation Factor 4E-Binding Protein 1
AKT, *AKT*	Protein Kinase B
BRCA2	Breast Cancer Gene 2
CA19-9	Carbohydrate Antigen 19-9
CDK	Cyclin-Dependent Protein Kinase
CDKN2A	Cyclin Dependent Kinase Inhibitor 2A
CEA	Carcinoembryonic Antigen
CK2	Casein Kinase II
CV	Crystal Violet
DEG	Differentially Expressed Gene
DMSO	Dimethyl Sulfoxide
DRB	5,6-Dichloro-1-ß-D-Ribofuranosylbenzimidazole
EGFR	Epidermal Growth Factor Receptor
ERK	Extracellular-Signal Regulated Kinase
FCS	Fetal Calf Serum
GDP	Guanosine Diphosphate
GNAS	Guanine Nucleotide Binding Protein, Alpha Stimulating Complex Locus
GO	Gene Ontology
GSEA	Gene Set Enrichment Analysis
GTP	Guanosine Triphosphate
HER2/neu	Human Epidermal Growth Factor Receptor 2
IC50	Half-Maximal Inhibitory Concentration
JAK	Janus Kinase
JNK	C-Jun N-terminal Kinase
KEGG	Kyoto Encyclopedia of Genes and Genomes
KRAS, *KRAS*	Kirsten Rat Sarcoma Virus
MAPK	Mitogen-Activated Protein Kinase
MEK	Mitogen-Activated Protein Kinase Kinase
MKK4	Mitogen-Activated Protein Kinase Kinase 4
mTOR	Mammalian Target of Rapamycin
NF-κB	Nuclear Factor Kappa-Light Chain Enhancer Pathway of the Activated B Cell
NSCLC	Non-Small Cell Lung Cancer
P/S	Penicillin-Streptomycin
PanIN	Pancreatic Intraepithelial Neoplasia
PBS	Phosphate-Buffered Saline
PDAC	Pancreatic Ductal Adenocarcinoma
PDK1	Phosphoinositide-Dependent Kinase 1
PI	Propidium Iodide
PI3K	Phosphoinositide 3-Kinase

PIP2	Phosphatidylinositol 4,5-Bisphosphate
PIP3	Phosphatidylinositol 3,4,5-Bisphosphate
Rb	Retinoblastoma
RNA-seq	RNA Sequencing
SD	Standard Deviation
SDS	Sodium Dodecyl Sulfate
SMAD4	Mothers Against Decapentaplegic Homolog 4
SOS1	Son of Sevenless Homolog 1
STAT	Signal Transducer and Activator of Transcription
TP53	Tumor Protein P53
WES	Whole-Exome Sequencing
WST-1	Water Soluble Tetrazolium - 1

8.2 Original Publications

1. **Ma, Y.**; Sender, S.; Sekora, A.; Kong, W.; Bauer, P.; Ameziane, N.; Krake, S.; Radefeldt, M.; Al-Ali, R.; Weiss, F.U.; Lerch, M.M.; Parveen, A.; Zechner, D.; Junghanss, C.; Murua Escobar, H.. Inhibitory Response to CK II Inhibitor Silmitasertib and CDKs Inhibitor Dinaciclib Is Related to Genetic Differences in Pancreatic Ductal Adenocarcinoma Cell Lines. *Int. J. Mol. Sci.* **2022**, *23*, 4409.
2. **Ma, Y.**; Sender, S.; Sekora, A.; Kong, W.; Bauer, P.; Ameziane, N.; Al-Ali, R.; Krake, S.; Radefeldt, M.; Weiss, F.U.; Lerch, M.M.; Parveen, A.; Zechner, D.; Junghanss, C.; Murua Escobar, H.. The Inhibitory Response to PI3K/AKT Pathway Inhibitors MK-2206 and Buparlisib Is Related to Genetic Differences in Pancreatic Ductal Adenocarcinoma Cell Lines. *Int. J. Mol. Sci.* **2022**, *23*, 4295.
3. **Ma, Y.**; Schulz, B.; Trakooljul, N.; Al Ammar, M.; Sekora, A.; Sender, S.; Hadlich, F.; Zechner, D.; Weiss, F.U.; Lerch, M.M.; Jaster, R.; Junhanss, C.; Murua Escobar, H.. Inhibition of KRAS, MEK and PI3K Demonstrate Synergistic Anti-Tumor Effects in Pancreatic Ductal Adenocarcinoma Cell Lines. *Cancers* **2022**, *14*, 4467.

8.2.1 Inhibitory Response to CK II Inhibitor Silmitasertib and CDKs Inhibitor Dinaciclib Is Related to Genetic Differences in Pancreatic Ductal Adenocarcinoma Cell Line

International Journal of
Molecular Sciences

MDPI

Article

Inhibitory Response to CK II Inhibitor Silmitasertib and CDKs Inhibitor Dinaciclib Is Related to Genetic Differences in Pancreatic Ductal Adenocarcinoma Cell Lines

Yixuan Ma [1], Sina Sender [1], Anett Sekora [1], Weibo Kong [1,2], Peter Bauer [1,3], Najim Ameziane [3,4], Susann Krake [3], Mandy Radefeldt [3], Ruslan Al-Ali [3], Frank Ulrich Weiss [5], Markus M. Lerch [5,6], Alisha Parveen [7], Dietmar Zechner [7], Christian Junghanss [1] and Hugo Murua Escobar [1,*]

1 Department of Medicine Clinic III, Hematology, Oncology and Palliative Medicine, Rostock University Medical Center, 18057 Rostock, Germany; yixuan.ma@med.uni-rostock.de (Y.M.); sina.sender@med.uni-rostock.de (S.S.); anett.sekora@med.uni-rostock.de (A.S.); kong@fbn-dummerstorf.de (W.K.); peter.bauer@centogene.com (P.B.); christian.junghanss@med.uni-rostock.de (C.J.)
2 Institute of Muscle Biology and Growth, Research Institute for Farm Animal Biology (FBN), 18196 Dummerstorf, Germany
3 CENTOGENE GmbH, 18057 Rostock, Germany; najim.ameziane@arcensus-diagnostics.com (N.A.); susann.krake@centogene.com (S.K.); mandy.radefeldt@centogene.com (M.R.); ruslan.al-ali@centogene.com (R.A.-A.)
4 Arcensus GmbH, 18055 Rostock, Germany
5 Department of Medicine A, University Medicine, University of Greifswald, 17475 Greifswald, Germany; ulrich.weiss@med.uni-greifswald.de (F.U.W.); markus.lerch@med.uni-muenchen.de (M.M.L.)
6 LMU Munich University Hospital, 81377 Munich, Germany
7 Institute for Experimental Surgery, University of Rostock, 18057 Rostock, Germany; alisha.parveen@med.uni-rostock.de (A.P.); dietmar.zechner@uni-rostock.de (D.Z.)
* Correspondence: hugo.murua.escobar@med.uni-rostock.de; Tel.: +49-381494-7519 or +49-381494-7639; Fax: +49-381494-45803

Abstract: Casein kinase II (CK2) and cyclin-dependent kinases (CDKs) frequently interact within multiple pathways in pancreatic ductal adenocarcinoma (PDAC). Application of CK2- and CDK-inhibitors have been considered as a therapeutic option, but are currently not part of routine chemotherapy regimens. We investigated ten PDAC cell lines exposed to increasing concentrations of silmitasertib and dinaciclib. Cell proliferation, metabolic activity, biomass, and apoptosis/necrosis were evaluated, and bioinformatic clustering was used to classify cell lines into sensitive groups based on their response to inhibitors. Furthermore, whole exome sequencing (WES) and RNA sequencing (RNA-Seq) was conducted to assess recurrent mutations and the expression profile of inhibitor targets and genes frequently mutated in PDAC, respectively. Dinaciclib and silmitasertib demonstrated pronounced and limited cell line specific effects in cell death induction, respectively. WES revealed no genomic variants causing changes in the primary structure of the corresponding inhibitor target proteins. RNA-Seq demonstrated that the expression of all inhibitor target genes was higher in the PDAC cell lines compared to non-neoplastic pancreatic tissue. The observed differences in PDAC cell line sensitivity to silmitasertib or dinaciclib did not depend on target gene expression or the identified gene variants. For the PDAC hotspot genes kirsten rat sarcoma virus (*KRAS*) and tumor protein p53 (*TP53*), three and eight variants were identified, respectively. In conclusion, both inhibitors demonstrated in vitro efficacy on the PDAC cell lines. However, aberrations and expression of inhibitor target genes did not appear to affect the efficacy of the corresponding inhibitors. In addition, specific aberrations in *TP53* and *KRAS* affected the efficacy of both inhibitors.

Keywords: casein kinase II; cyclin dependent kinase; pancreatic ductal adenocarcinoma; *KRAS*; *TP53*

check for updates

Citation: Ma, Y.; Sender, S.; Sekora, A.; Kong, W.; Bauer, P.; Ameziane, N.; Krake, S.; Radefeldt, M.; Al-Ali, R.; Weiss, F.U.; et al. Inhibitory Response to CK II Inhibitor Silmitasertib and CDKs Inhibitor Dinaciclib Is Related to Genetic Differences in Pancreatic Ductal Adenocarcinoma Cell Lines. *Int. J. Mol. Sci.* **2022**, *23*, 4409. https://doi.org/10.3390/ijms23084409

Academic Editor: Marco Falasca

Received: 18 March 2022
Accepted: 15 April 2022
Published: 16 April 2022

1. Introduction

Pancreatic ductal adenocarcinoma (PDAC) is one of the most common malignancies and ranks fourth among all cancer-related deaths in both men and women [1]. Due to the lack of effective therapy, tumor metastasis, and chemo resistance, the prognosis of PDAC is poor [2–5]. Furthermore, the "cure rate" for PDAC is only 9%, and without treatment, the median survival of patients with metastatic disease is only three months [6]. Although extensive research has been carried out in recent years, there were only slight improvements to disease prognosis, median survival is still less than 12 months, and recently, the overall 5-year survival rate only increased to 10% [1].

Casein kinase II (CK2) is a highly conserved serine/threonine kinase, which is constitutively active and ubiquitously expressed in mammalian cells. CK2 has a wide range of candidate physiological targets and is involved in a series of complex cellular functions [7]. For example, CK2 activates protein kinase B (AKT) by direct phosphorylation or indirect regulation [8]. The activated phosphoinositide 3-kinase (PI3K)/AKT pathway influences proliferation and survival [9]. In addition, CK2 upregulates the JAK/STAT and RAS/MEK/ERK signaling pathways and provides survival advantage and proliferative capacity to cancer cells [10,11]. Furthermore, CK2 is able to cooperate with the MKK4/JNK pathway and promotes the survival of PDAC cells [12]. The downregulation of CK2 via RNA interference enhances chemosensitivity to gemcitabine in PDAC cell lines [12–14]. Both cell assays and animal models revealed the anti-tumor activity of silmitasertib, a CK2 inhibitor, in BxPc-3 cells [15]. Other CK2 specific-inhibitors also induce the apoptosis of the MIA Paca-2 and Dan-G cell lines [14]. However, in these experiments, different cell lines showed different responses to CK2 inhibitors. Therefore, studying the influence of genetic background on the efficacy of silmitasertib is of considerable interest. In addition, although silmitasertib has entered multiple clinical trials, clinical trials related to pancreatic cancer have not been reported [16].

CK2 is not the only protein kinase that plays a critical role in PDAC. Cyclin-dependent protein kinases (CDKs) are critical regulators of cell cycle progression. This dysregulation of the cell cycle is the fundamental process of cancer growth and spread [17]. Within the CDK family, CDK1 and CDK2 regulate cell cycle progression by contributing to the phosphorylation and inactivation of the retinoblastoma (Rb) tumor suppressor gene product throughout late G1, S, and G2-M phases [18]. Another family member, CDK9, is involved in the regulation of RNA polymerase II and the control of cellular transcription [19]. CDK5 has been well characterized for its role in the central nervous system rather than the cell cycle [20]. Several CDK family members are highly expressed in different cancer types including PDACs [21]. Moreover, some studies have indicated that CDKs play critical roles in cancer proliferation, migration, invasion, and metastasis [22,23]. In addition, inhibition or knockdown of CDKs demonstrated satisfactory inhibition of cancer cells. Inhibition of CDK1, CDK2, and CDK9 caused cell cycle arrest [24–26]. Activated CDKs induce resistance to cisplatin in cervical cancer and are involved in radiation resistance in lung cancer [27,28]. In PDAC cell lines, inhibition of CDKs' kinase activity significantly decreased the migration and invasion of cancer cells in vitro [22]. In addition, CDK5 inhibition promotes the chemosensitivity of PDAC cell lines to gemcitabine in vivo [22]. A combination of CDKs and AKT inhibitors has been shown to dramatically block PDAC tumor growth and metastasis in vivo [23]. Although the inhibition of CDKs by dinaciclib has been shown to inhibit the viability of PDAC in both cellular and animal models, the observed effect is highly variable, depending on different cell lines and CDK inhibitors, respectively. So far, the reasons for these differences are still not fully understood [23,29,30]. However, based on the significant effects of CDK inhibitors, several inhibitors alcociclib (flavopiridol), dinaciclib, ibociclib, and AT7519 have entered several clinical trials against PDAC [21,31,32].

Different genetic aberrations affecting direct drug target genes, downstream pathways, or key oncogenic regulators also have an impact on drug efficacy. *KRAS* and *TP53* are two of the hotspot genes frequently mutated in PDAC. It has been reported that *KRAS*

and *TP53* mutations can be found in approximately 92% and 70% of PDAC patients, respectively [33,34]. Moreover, patients with *KRAS* mutations showed a bad response to first-line gemcitabine-based therapy and represented a poor prognosis [35]. PDAC patients with regular *TP53* expression were reported to show a significant improvement in progression-free survival when compared to complete loss. Interestingly, cases showing as many as two *TP53* somatic variants are reported to have a better prognosis than when compared to cases exceeding accumulation of more than three somatic variants [36,37]. Therefore, due to the impact of *KRAS* and *TP53* on the prognosis and drug efficacy of PDAC, we explored the influence of the somatic variants of these two genes on the response of PDAC cell lines to CK2 and CDK inhibitors.

Akin to the above-mentioned studies, several other publications have demonstrated the influence of CK2 and CDKs on the pathophysiology of PDAC. However, for these drug target genes, it is still poorly understood if and which somatic variants affect sensitivity to the respective inhibitors [14,23]. In general, CK2 and CDK gene expression does not vary significantly in most mammalian tissues and species [38]. We therefore investigated the effects of the CK2 inhibitor (silmitasertib) and CDK1/2/5/9 inhibitor (dinaciclib) in ten PDAC cell lines (AsPc-1, BxPc-3, Capan-1, Panc-1, PaTu8902, PaTu8988T, PaTu8988S, SU.86.86, T3M4, and Colo357). In order to evaluate gene expression and gene variants in these cell lines, whole transcriptome and whole exome sequencing (WES) were performed with the aim to explore the relationship between the sensitivity of these inhibitors and the gene expression of inhibitor targets and mutations in *KRAS* oncogene and *TP53* tumor suppressor genes.

2. Results

2.1. Effects of Silmitasertib and Dinaciclib on Cell Proliferation, Biomass, and Metabolic Activity

The CK2 inhibitor silmitasertib significantly inhibited cell proliferation of PDAC cell lines starting from 1 µM for the most sensitive cell line BxPc-3. Meanwhile, significant inhibition of biomass was observed with silmitasertib in all cell lines tested, with AsPc-1 and BxPc-3 significantly inhibited from 1 µM. Moreover, silmitasertib significantly reduced the metabolic activity of cells, with the majority of PDAC cell lines (eight out of ten) initiated significant reductions at 5 µM (Supplementary Figure S1 and Table S1). The IC_{50} values for proliferation and biomass showed a range from 2.131 µM to 16.20 µM for proliferation and a matching range from 1.691 µM to 14.32 µM for biomass (Figure 1a, Supplementary Figure S2 and Table S2).

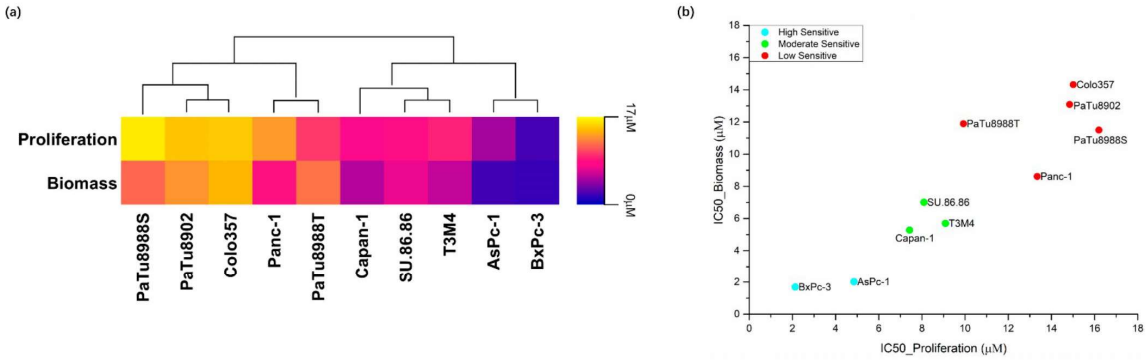

Figure 1. IC_{50} values when assessing proliferation and cell biomass after 72 h to silmitasertib exposure in ten PDAC cell lines (**a**) as well as the classification of these cell lines by k-means++ (unsupervised machine learning algorithm) to a low (red), moderate (green), and high (blue) sensitivity group (**b**).

IC_{50} values of cell proliferation and biomass were applied in the following bioinformatic clustering (k-means++ clustering method, Materials and Methods 4.10) for sensitivity classification of cell lines. Ten PDAC cell lines were separated into three groups with low

(PaTu8988S, Panc-1, PaTu8988T, PaTu8902, and Colo357), moderate (Capan-1, T3M4, and SU.86.86), and high sensitivity (AsPc-1 and BxPc-3) (Figure 1b and Supplementary Figure S2).

The CDK1/2/5/9 inhibitor dinaciclib significantly inhibits the cell proliferation, metabolic activities, and biomass of all PDAC cell lines starting from the lowest tested concentration (0.001 µM), but responses varied between cell lines (Supplementary Figure S3 and Table S3). At the lowest tested concentration, Colo357, PaTu8988T, and T3M4 observed significant inhibition in cell proliferation assays; Colo357, PaTu8988S, and T3M4 observed significant inhibition in metabolic activity assays; and Capan-1, Colo357, and PaTu8988T observed significant inhibition in biomass assays. The IC_{50} values ranged from 0.001253 µM to 0.01111 µM (proliferation) and 0.002146 µM to 0.01390 µM (biomass) (Figure 2a, Supplementary Figure S4 and Table S4).

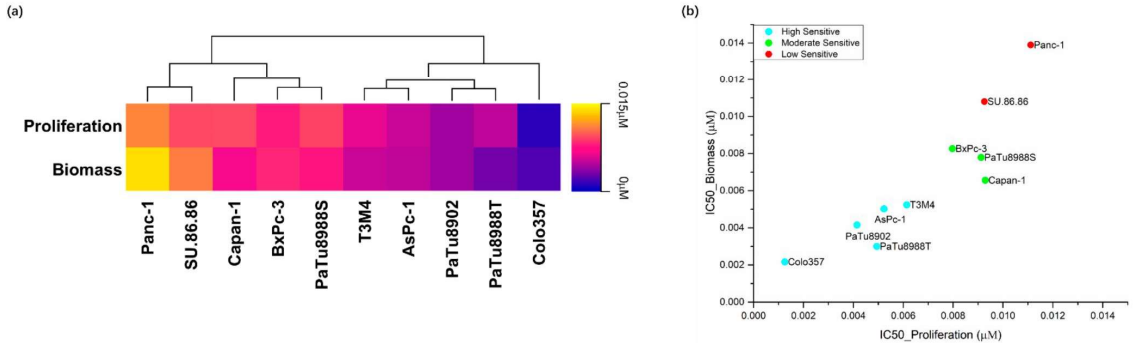

Figure 2. IC_{50} values when assessing proliferation and cell biomass after 72 h dinaciclib exposure in ten PDAC cell lines (**a**) as well as the classification of these cell lines by k-means++ (unsupervised machine learning algorithm) to a low (red), moderate (green), and high (blue) sensitivity group (**b**).

IC_{50} values of cell proliferation and biomass were applied in bioinformatics clustering (k-means++ clustering method, Materials and Methods 4.10) for sensitivity classification of the cell lines. Ten PDAC cell lines were separated into three groups with low (Panc-1 and SU.86.86), moderate (BxPc-3, Capan-1 and PaTu8988S), and high (AsPc-1, Colo357, PaTu8902, PaTu8988T, and T3M4) sensitivity (Figure 2b and Supplementary Figure S4). Both herein used compounds were reported to be well tolerated in vivo [15,39]. The ranges of inhibitor concentrations were below the maximum plasma concentration.

2.2. Silmitasertib and Dinaciclib Induced Cell Deaths in PDAC Cell Lines

Silmitasertib only increased the percentage of cell deaths in two out of ten PDAC cell lines after 72 h. Significant increases in apoptotic/necrotic cells were only observed in AsPc-1 and T3M4 at a concentration of 10 µM (Supplementary Figures S5 and S7 and Table S5). The percentages of apoptotic/necrotic cells in AsPc-1 and T3M4 at 10 µM were 23.13% and 29.33%, respectively. However, significant increases in apoptotic/necrotic cells were not observed in other PDAC cell lines. At the same time, we observed that silmitasertib even significantly reduced cell death in Colo357 when compared to the DMSO control, but due to the low percentages of cell death; this reduction is more like a mathematical artifact.

Dinaciclib strongly induced apoptosis/necrosis in nine of ten PDAC cell lines in a dose-dependent manner. Only the apoptotic/necrotic induction of PaTu8988T was not significant at the tested concentrations (0.003 µM, 0.005 µM, 0.006 µM, and 0.01 µM). Significant increases in apoptotic/necrotic cells were observed starting at a concentration of 0.0075 µM (Supplementary Figures S6 and S8 and Table S6). Interestingly, in comparison to the DMSO control, decreasing percentages of apoptotic/necrotic cells were observed in PaTu8988S at all tested concentrations (0.005 µM, 0.0075 µM, 0.01 µM, and 0.05 µM).

2.3. Expression and Genetic Variants of Silmitasertib or Dinaciclib Target Genes

The expression of target genes for each inhibitor (for silmitasertib: *CSNK2A1*, *CSNK2A2*, and *CSNK2B*; for dinaciclib: *CDK1*, *CDK2*, *CDK5*, and *CDK9*) was evaluated in all cell lines by RNA-Seq. The expression level was estimated as Log_2 (transcripts per kilobase million (TPM) + 1) and compared to the expression data of non-neoplastic pancreatic tissue, which was chosen as a control. All target genes were expressed higher in the PDAC cell lines than in normal pancreatic tissue. The inhibitor target gene expression in PDAC compared with the control are as follows (PDAC Minimum–Maximum vs. control): *CSNK2A1* (5.83–7.69 vs. 3.63), *CSNK2A2* (5.41–6.47 vs. 4.43), *CSNK2B* (6.53–7.52 vs. 6.00), *CDK1* (5.73–8.51 vs. 0.41), *CDK2* (4.37–6.95 vs. 2.83), *CDK5* (3.51–5.32 vs. 1.98), and *CDK9* (4.57–6.63 vs. 4.50) (Figure 3a,b and Supplementary Table S7).

The target genes for silmitasertib (*CSNK2A1*, *CSNK2A2*, *CSNK2B*) and dinaciclib (*CDK1*, *CDK2*, *CDK5*, *CDK9*) were selected to analyze transcript variants by WES.

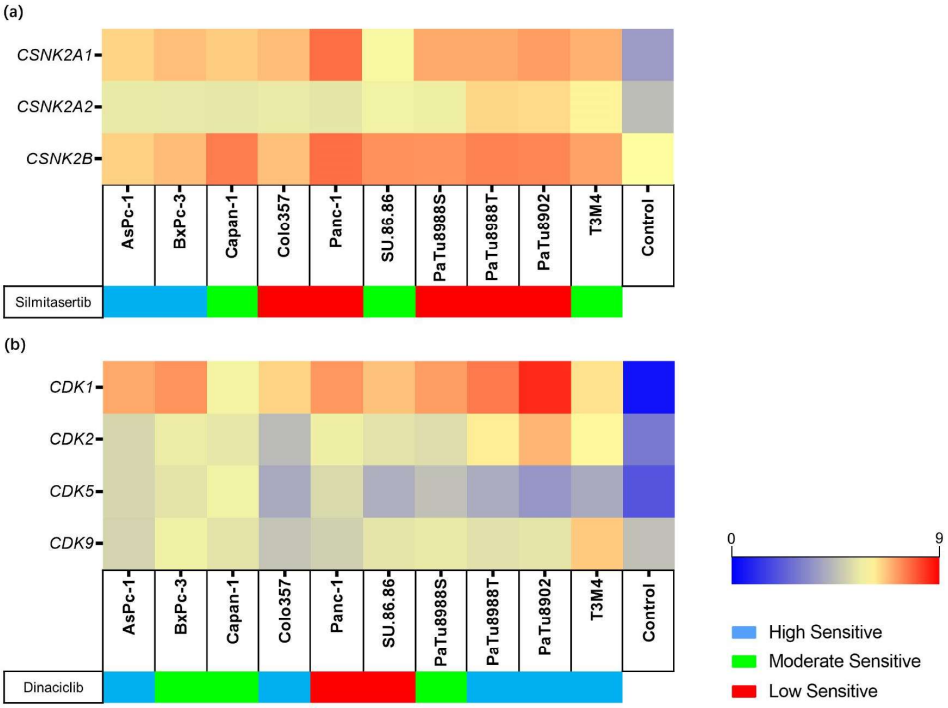

Figure 3. Gene expression levels of inhibitor target genes in the cell lines and control. The different sensitivity to silmitasertib (**a**) and dinaciclib (**b**) is indicated for each cell line. Gene expression levels are displayed as Log2 (TPM+1).

Focusing on silmitasertib target genes, initially, a total of twenty-four variants including fourteen *CSNK2A1* variants, eight *CSNK2A2* variants, and two *CSNK2B* variants were identified in ten PDAC cell lines in all types of variants (Supplementary Table S8). The initial twenty-four candidate variants were identified in eight cell lines: no variants were identified in Colo357 and SU.86.86; one variant was identified in AsPc-1 and PaTu8902; two variants were identified in Capan-1 and PaTu8988S; three variants were identified in Panc-1; and five variants were identified in BxPc-3, PaTu8988T, and T3M4. Variant filtering according to the Method 4.8 classified none of the identified variants as potentially affecting the protein coding sequence, and as such, presumably leading to aberrant protein function.

When focusing on dinaciclib target genes, a total of fifteen variants including nine *CDK1* variants, four *CDK2* variants, one *CDK5*, and one *CDK9* variant were identified

in ten PDAC cell lines (Supplementary Table S9). The initial fifteen candidate variants were identified in eight cell lines: no variants were identified in AsPc-1 and Colo357; one variant was identified in Capan-1, PaTu8902, PaTu8988T, PaTu8988S, and SU.86.86; two variants were identified in BxPc-3 and Panc-1; and six variants were identified in Colo357. Variant filtering according to Method 4.8 classified none of the identified variants as potentially affecting the protein coding sequence in such, presumably leading to aberrant protein function.

2.4. KRAS and TP53 Gene Variants Were Observed in PDAC Cell Lines

2.4.1. KRAS Variants and Expression in PDAC Cell Lines

WES identified *KRAS* variants in nine of the ten tested PDAC cell lines (Figure 4 and Supplementary Table S10). Three different *KRAS* variants were identified, *KRAS* c.35G>A (p.Gly12Asp), *KRAS* c.35G>T (p.Gly12Val), and *KRAS* c.183A>C (p.Gln61His), all of them were missense variants. *KRAS* c.35G>A were observed in AsPc-1 (variant allele frequency (VAF): 100), Colo357 (VAF: 23.8), Panc-1 (VAF: 62.1), and SU.86.86 (VAF: 83.7). *KRAS* c.35G>T were identified in Capan-1 (VAF: 97.1), PaTu8902 (VAF: 100), PaTu8988S (VAF: 96.9), and PaTu8988T (VAF: 98). *KRAS* c.183A>C was identified in T3M4 (VAF: 32.6).

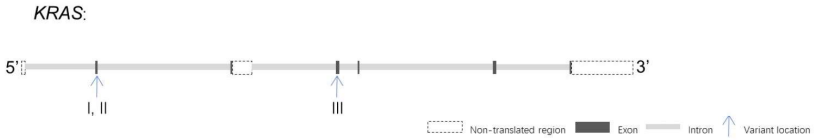

KRAS: GRCh37, <reverse strand.
Chromosome 12: 25,357,723-25,403,870
I. Missense variant: chr 12, 25398284-25398284; c.35G>A; Sample with variant: AsPc-1, Colo357, Panc-1, SU.86.86.
II. Missense variant: chr 12, 25398284-25398284; c.35G>T; Sample with variant: Capan-1, PaTu8902, PaTu8988S, PaTu8988T.
III. Missense variant: chr 12, 25380275-25380275; c.183A>C; Sample with variant: T3M4

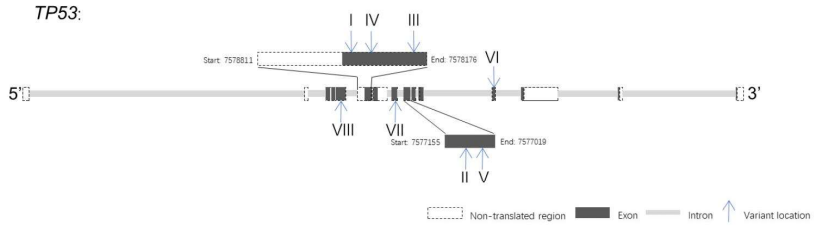

TP53: GRCh37, <reverse strand.
Chromosome 17: 7,565,097-7,590,856
I. Frameshift variant: chr 17, 7578526-7578530; c.403delT; Sample with variant: AsPc-1.
II. Missense variant: chr 17, 7577120-7577120; c.818G>A; Sample with variant: Panc-1.
III. Missense variant: chr 17, 7578190-7578190; c.659A>G; Sample with variant: BxPc-3, T3M4.
IV. Missense variant: chr 17, 7578454-7578454; c.476C>T; Sample with variant: Capan-1.
V. Missense variant: chr 17, 7577094-7577094; c.844C>T; Sample with variant: PaTu8902, PaTu8988S, PaTu8988T
VI. Missense variant: chr 17, 7573948-7573948; c.1079G>T; Sample with variant: SU.86.86.
VII. Missense variant: chr 17, 7577548-7577548; c.733G>A; Sample with variant: SU.86.86.
VIII. Frameshift variant: chr 17, 7579419-7579424; c.267delC; Sample with variant: Colo357.

Figure 4. Gene maps indicating the variant sites of *KRAS* and *TP53* in different PDAC cell lines. GRCh37: Genome Reference Consortium Human Build 37, Chr: chromosome.

The expressions of *KRAS* in all PDAC cell lines were higher than those compared to non-neoplastic pancreas tissue (4.16–7.09 vs. 2.14) (Figure 5 and Supplementary Table S12). Both the lowest and highest *KRAS* expressions were observed in the *KRAS* c.35G>A variant, which were identified in Colo357 (4.61) and SU.86.86 (7.09), respectively. The expressions

of all *KRAS* c.35G>T variants, which were identified in Capan-1, PaTu8988S, PaTu8988T, and PaTu8902 were similar to wild type BxPc-3 (4.40, 4.65, 4.46, 4.51 vs. 4.53, respectively), the expression of *KRAS* c.183A>C in T3M4 and *KRAS* c.35G>A in AsPc-1, and Panc-1 and SU.86.86 were higher than wild type BxPc-3 (4.79–7.09 vs. 4.53).

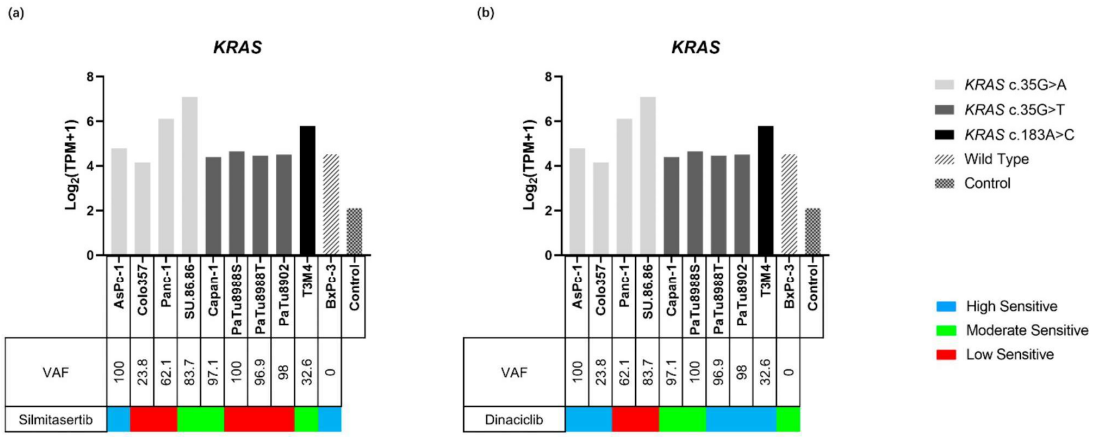

Figure 5. Gene expression of *KRAS* in ten PDAC cell lines and the control. The sensitivity to silmitasertib (**a**) and dinaciclib (**b**) as well as the variants of *KRAS* are indicated for each cell lines. Gene expression levels are displayed as Log_2 (TPM+1).

2.4.2. KRAS and Inhibitor Response

A comprehensive analysis of the cell viability assays and *KRAS* status revealed that PDAC cell lines carrying the *KRAS* variant appeared to be less sensitive to silmitasertib and the high sensitive group contained only the wild-type and one *KRAS* mutant cell line, while the rest of the *KRAS* mutant carrying cell lines were all classified into the moderate or low sensitivity groups (Figure 5a). In addition, *KRAS* c.35G single nucleotide variants had no major influence on the inhibitory effect of dinaciclib, since cell lines containing the same *KRAS* c.35G position variant (*KRAS* c.35G>A, *KRAS* c.35G>T) were classified into each of the three sensitivity groups, while wild-type (BxPc-3) was in the moderate sensitivity group. Interestingly, the sensitivity of the *KRAS* c.183A>C mutant cell line (T3M4) was higher than BxPc-3 (Figure 5b). *KRAS* gene expression and VAF did not affect the efficacy of the two inhibitors (Figure 5).

2.4.3. TP53 Variants and Expression in PDAC Cell Lines

Two different types of variants including frameshift (fs) variant and missense variant of *TP53* were identified in the PDAC cell lines (Figure 4 and Supplementary Table S11). Fs variants, *TP53* c.403delT (p.Cys135fs) and *TP53* c.267delC (p.Ser90fs), were identified in AsPc-1 (variant allele frequency (VAF): 96.4) and Colo357 (VAF: 100), respectively. Missense variants, *TP53* c.476C>T (p.Ala159Val) and *TP53* c.818G>A (p.Arg273His), were identified in Capan-1 (VAF: 100) and Panc-1 (VAF: 98.8), respectively. Double missense mutation including *TP53* c.733G>A (p.Gly245Ser) and *TP53* c.1079G>T (p.Gly360Val) were identified in SU.86.86 (VAF: 100, 100, respectively). *TP53* c.659A>G (p.Tyr220Cys) was identified in BxPC-3 (VAF: 99) and T3M4 (VAF: 100). *TP53* c.844C>T (p.Arg282Trp) was identified in PaTu8902 (VAF: 100), PaTu8988S (VAF: 100), and PaTu8988T (VAF: 100). The expressions of *TP53* with frameshift variants were lower than that of the missense variants (1.24–2.13 vs. 4.39–5.42) and control (2.83) (Figure 6 and Supplementary Table S13).

2.4.4. TP53 and Inhibitor Response

A comprehensive analysis of cell viability assays and *TP53* status demonstrated that the two cell lines carrying fs variants (Colo357 and AsPc-1) were in the dinaciclib high

sensitive group, while cell lines carrying point mutations were distributed in the three sensitivity groups (Figure 6b). However, this effect was not observed when treating the cells with silmitasertib (Figure 6a). In addition, cell lines carrying *TP53* c.844C>T, *TP53* c.818G>A, and *TP53* c.267delC variants were in the low sensitivity group. SU.86.86, which carries two *TP53* missense variants, demonstrated no significant difference in sensitivity to silmitasertib and dinaciclib compared with other cell lines only carrying one variant. *TP53* gene expression and VAF did not affect the efficacy of the two inhibitors (Figure 6).

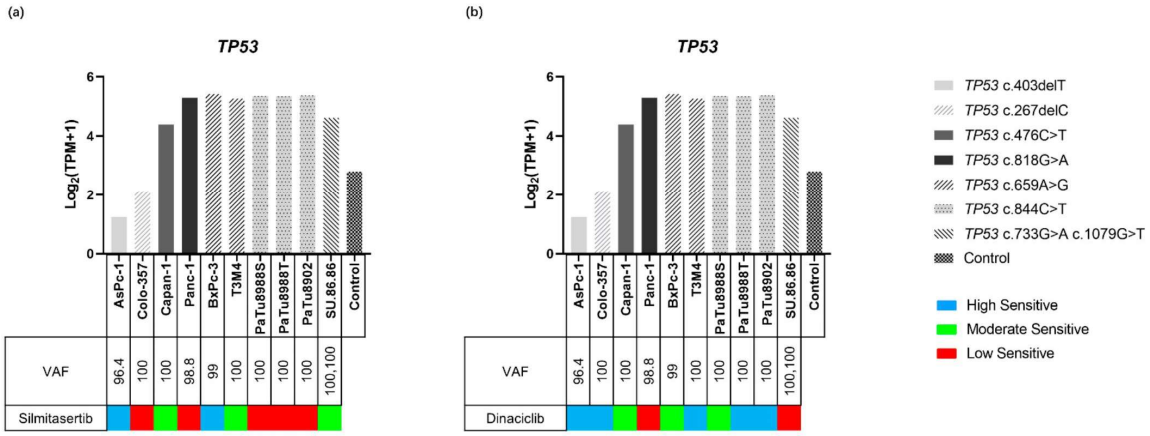

Figure 6. Gene expression of *TP53* in ten PDAC cell lines and the control. The sensitivity to silmitasertib (**a**) and dinaciclib (**b**) as well as the variants of *TP53* are indicated for each cell lines. Gene expression levels are displayed as Log_2 (TPM+1). Missense variants were associated with gene higher expression while frameshift variants were related to low gene expression.

3. Discussion

This study demonstrated that the expression levels of silmitasertib target genes (*CSNK2A1, CSNK2A2,* and *CSNK2B)* in all of the tested PDAC cell lines were higher than in non-neoplastic pancreatic tissue. This result suggests that these cell lines could be sensitive to silmitasertib. Indeed, the inhibition of CK2 by silmitasertib significantly affected cell proliferation of all cell lines except Panc-1, and significantly reduced the cell biomass in all PDAC cell lines. However, silmitasertib did not perform well in reducing the metabolic activity of the PDAC cell lines, and the effects of silmitasertib in inducing apoptosis were also very weak, with significant effects only observed in AsPc-1 and T3M4, which indicates that silmitasertib may inhibit the proliferation of PDAC cells by inducing cell-cycle arrest or cell autophagy rather than apoptosis [40]. Moreover, the cell responses to silmitasertib presented an obvious difference among PDAC cell lines. PDAC cell lines including PaTu8988T, Panc-1, PaTu8902, Colo357, and PaTu8988S represented low responses to silmitasertib inhibition. Although twenty-four variants of CK2 genes in PDAC cell lines were identified, after the filtering step, all variants were excluded for further analysis. In addition, no correlation was seen when comparing the expression of CK2 genes in high-, moderate-, and low-sensitive cell lines. These results indicate that the genes directly targeted by silmitasertib are not directly affected by aberrations modulating the observed antitumor effects of silmitasertib on CK2.

Inhibition of CDKs by dinaciclib dramatically reduced cell proliferation, metabolic activities, and biomass in PDAC cell lines and this significant effect could be observed at nanomolar concentrations. These results are similar to previous reports that suggested that dinaciclib could be a candidate for novel treatment options in PDAC [23,41]. Furthermore, compared with the DMSO control group, dinaciclib was able to increase the percentage of apoptotic/necrotic cells in PDAC cell lines except in PaTu8988S. This suggests that in addition to inducing apoptosis, dinaciclib may inhibit cell proliferation by other mecha-

nisms, but further experiments are still needed for this to be proven [42]. RNA-Seq results demonstrated that expressions of *CDK1/2/5/9* were higher than the control in all tested PDAC cell lines, indicating overexpression of *CDK1/2/5/9* in PDAC cell lines. Moreover, as the experimental results suggest that dinaciclib inhibited cell viability at very low concentrations, the overexpression of target genes appeared to not affect the efficacy of dinaciclib in inhibiting the viability of PDAC cells. Therefore, dinaciclib is an excellent candidate for PDACs with high expression of *CDK1/2/5/9*; on the other hand, due to the lack of data on the individuals with low *CDK1/2/5/9* expression, experiments are still needed to verify the feasibility of using dinaciclib as a therapeutic candidate.

CK2 gene aberrations were detected in 2.9% (34/1228: *CSNK2A1*, 1%, *CSNK2A2*, 0.3%, *CDNK2B*, 1.6%) of PDAC patients, and only 0.2% (3/1228) involved protein structural changes, while the majority involved gene amplification [43]. Similar to silmitasertib target genes, dinaciclib target gene aberrations were present in 4.3% (46/1228: *CDK1*, 0.3%, *CDK2*, 1.1%, *CDK5*, 2%, *CDK9*, 1%) of PDAC patients, and only 0.5% (6/1228) involved protein structural changes, while the majority involved gene amplification [43]. Therefore, our study provides some reference value for the strategy of silmitasertib and dinaciclib in the treatment of PDAC.

We identified three different amino acid substitution variants of *KRAS* in nine of ten PDAC cell lines including *KRAS* p.Gly12Asp (c.35G>A), *KRAS* p.Gly12Val (c.35G>T), and *KRAS* p.Gln61His (c.183A>C). It was reported that patients with *KRAS* mutations showed a weak response to first-line gemcitabine-based therapy and had a poor prognosis [35]. In our study, significant differences in sensitivity to dinaciclib could not be observed between cell lines harboring the *KRAS* c.35G point mutation and wild-type cell lines, suggesting the inhibitory effect of dinaciclib is not affected by the *KRAS* c.35G point mutation. Interestingly, T3M4 cells, which carry a *KRAS* c.183A>C variant are more sensitive to dinaciclib than wild-type BxPc-3 cells, suggesting that dinaciclib may improve the efficacy of patients with specific *KRAS* c.183A>C mutation, but due to the limited number of cell lines, further experiments are still needed to verify the relationship between this *KRAS* mutation and the efficacy of dinaciclib. However, a comprehensive analysis of silmitasertib efficacy and *KRAS* mutations suggests that carrying the *KRAS* variants reduced the PDAC sensitivity to silmitasertib. Since AKT is an important effector kinase of CK2, inhibition of CK2 causes a reduced activation of AKT, whereas mutant KRAS directly activates the PI3K/AKT pathway [8,44]. This antagonism results in reduced sensitivity of *KRAS*-mutated cell lines to ssilmitasertib. Overall, blocking CDKs with dinaciclib in monotherapy may be beneficial to patients with the specific *KRAS* c.183A>C mutation, whereas silmitasertib monotherapy in patients with *KRAS* point mutations may not be a good option.

We identified that all tested PDAC cell lines contained at least one *TP53* mutation that causes amino acids to change. Our sequencing data revealed that the expression of *TP53* with fs mutations were lower than those of *TP53* with point mutations. Fs variants resulted in a strong disruption of *TP53* function, and low *TP53* mRNA expression was associated with a poor prognosis in PDAC patients [45,46]. On the other hand, the expressions of all missense variants of *TP53* in PDAC cell lines was higher than in the control, and it has been reported that some specific point mutations inactivate *TP53* (p.Arg175, p.Gly245, p. Arg248, p.Arg249, p.Arg273, and p.Arg282) and confer an advantage in tumor growth [47,48]. The same mechanism possibly also exists in the *TP53* p.Ala159Val, p.Tyr220Cys, and p.Gly360Val variants, which demonstrated similar expression properties. In addition, combined with the results of the PDAC inhibitory assays, cell lines carrying specific *TP53* variants (c.267delC, c.818G>A, and c.844C>T) were less sensitive to silmitasertib. These cell lines were all in the low (PaTu8988S, Panc-1, PaTu8988T, PaTu8902, and Colo357) sensitivity group. Knockdown of CK2 causes the enhanced transactivation of p53, thereby increasing apoptosis [49]. However, due to the inactivation caused by mutations in *TP53*, inhibition of CK2 did not transactivate these proteins. This may be the reason for the reduced efficacy of silmitasertib in cell lines with specific mutations in *TP53*. AsPc-1 and Colo357, which carry the fs variant, are both in the dinaciclib high sensitivity group, suggesting that

dinaciclib may be able to improve the poor prognosis of the *TP53* fs mutation. However, the expression level of *TP53* cannot fully explain the observed responses of all cell lines to silmitasertib or dinaciclib. These results indicate that *TP53* variants are an indicator of an inhibitory response, while the expression level of *TP53* is not. Furthermore, the results of the PDAC inhibitory assays indicate that patients with *TP53* mutations may benefit from a potential application of dinaciclib and silmitasertib.

Our study focused on univariate genetic variants and did not evaluate the potential effect of complex variant landscapes. Thus, our conclusions are limited to direct genetic variants observed in the respective target genes of the evaluated inhibitors. Interactions between different gene aberrations, influence on downstream signaling as well as expression deregulations can also have significant influence. Accordingly, a bioinformatical complex analysis allowing drug target, target downstream signaling as well as bioinformatical modeling is needed. Furthermore, the complex validation of predicted mechanistic targets on cell biological level should be performed in the future to further evaluate factors influencing drug response.

4. Materials and Methods

4.1. Kinase Inhibitors

Kinase inhibitors, silmitasertib (CK2 inhibitor) and dinaciclib (CDK1/2/5/9 inhibitor) were purchased from Selleck Chemicals (Absource Diagnostics GmbH, Munich, Germany). According to the manufacturer's instructions, silmitasertib and dinaciclib were separately dissolved in dimethyl sulfoxide (DMSO) (Sigma Aldrich Chemie GmbH, Steinheim, Germany) as a stock solution at a final concentration of 10 mM. The stock solutions were stored at −80 °C and diluted into corresponding working concentrations before each experiment.

4.2. Cell Lines and Cell Culture

PDAC cell lines AsPc-1, BxPc-3, Capan-1, Colo357, Panc-1, PaTu8902, PaTu8988T, PaTu8988S, SU.86.86, and T3M4 were kindly provided by the University of Greifswald. AsPc-1, BxPc-3, Colo357, Panc-1, SU.86.86, and T3M4 were cultured in RPMI1640 medium (PAN-Biotech, Aidenbach, Germany) supplemented with 10% heat-inactivated fetal calf serum (FCS) (PAN-Biotech) and 1% penicillin-streptomycin solution (10,000 U/mL Penicillin, 10 mg/mL Streptomycin) (PAN-Biotech). PaTu8902, PaTu8988T, PaTu8988S were cultured in DMEM/F12 medium (PAN-Biotech) supplemented with 10% heated-inactivated FCS and 1% penicillin-streptomycin solution. Capan-1 was cultured in RPMI1640 medium supplemented with 15% heat-inactivated FCS and 1% penicillin-streptomycin solution. After verifying that all cell lines were not contaminated by mycoplasma, these PDAC cell lines were maintained in a 5% CO_2 incubator at 37 °C with a humidified atmosphere.

For all assays, the PDAC cell lines were seeded at the density of 3.3×10^4 cells per milliliter in a 6-well plate (totally 4.5 mL per well), 24-well plate (totally 1.5 mL per well), or 96-well plate (totally 150 µL per well). For viability assays, after 24 h, the supernatant was discarded and media containing increasing concentrations (range from 1–10 µM for silmitasertib and 0.001–1 µM for dinaciclib) of inhibitors or vehicle (DMSO, as the control) were added to the corresponding PDAC cell lines. For the apoptosis/necrosis analysis, the inhibitor concentrations were selected according to the results of the cell viability assays. The inhibitor concentrations were adjusted according to the response observed in the viability assays for further analysis of the induced apoptotic and necrotic events. The treated cells were incubated for 72 h at 37 °C with 5% CO_2. At the indicated time points, cell proliferation, metabolic activity, cell biomass, or apoptosis/necrosis was evaluated in at least three biologically independent replicates.

4.3. Cell Viability Assays

4.3.1. Proliferation

Cell proliferation was evaluated by absolute counting and Trypan blue (Sigma-Aldrich Chemie GmbH, Steinheim, Germany) staining. After drug exposure in 24-well plates, the cells were harvested and washed by 1× PBS (PAN-Biotech). Following the cells being stained with Trypan blue, the number of viable cells was determined by counting with a hemocytometer. Proliferation was expressed as a percentage of viable cells treated with the inhibitor to the vehicle-treated control (control = 100%).

4.3.2. Metabolic Activity

Metabolic activity was tested by using the Water Soluble Tetrazolium—1 (WST-1) assay (TaKaRa Bio Inc., Kusatsu, Japan). After exposure to the corresponding inhibitor, the cells were incubated with 15 µL WST-1 for 2 h in 96-well plates. Absorbances at 450 nm and the reference wavelength of 620 nm were measured by Promega GloMax®-Multi Microplate Multimode Reader (Promega, Madison, WI, USA) and the metabolic activity was calculated as recommended by the manufacturer. Metabolic activity was expressed as a percentage of the inhibitor-treated group to the vehicle-treated controls (control = 100%).

4.3.3. Biomass Quantification

Biomass quantification was carried out by Crystal Violet (CV) (Sigma-Aldrich Chemie GmbH) staining. After exposure to the corresponding inhibitors in 96-well plates, the cells were washed once with PBS and stained with 50 µL 0.2% CV solution on a shaker at room temperature for 10 min. Following this, the plates were washed twice with PBS. To elute bound CV, 100 µL 1% sodium dodecyl sulfate (SDS) (SERVA Electrophoresis GmbH, Heidelberg, Germany) was added to each well and incubated on a shaker at room temperature for 10 min. Finally, absorbances at 570 nm and reference wavelength at 620 nm were measured by a Promega GloMax®-Multi Microplate Multimode Reader for background normalization. CV cell biomass estimation result was expressed as a percentage of the inhibitor-treated group to vehicle-treated controls (control = 100%).

4.4. Identification of IC_{50}

IC_{50} values were calculated based on cell proliferation, metabolic activity, and biomass after 72 h of inhibitor exposure. GraphPad Prism Version 8.0.2 (GraphPad Software Inc., San Diego, CA, USA) was used to evaluate IC_{50}. Briefly, after transforming concentrations and normalizing the results of the three vitality assays, nonlinear regression model (dose-response-inhibition vs. normalized response–variable slope) was used to evaluate the IC_{50} values. Calculate the IC_{50} corresponding to the three vitality assays, and apply these results to the response-based clustering analysis in order to evaluate the sensitivity of cell lines to inhibitors.

4.5. Apoptosis and Necrosis Analyses

Apoptosis and necrosis were evaluated by YO-PRO-1 (Invitrogen, Darmstadt, Germany) and propidium iodide (PI) (Sigma-Aldrich Chemie GmbH) double staining by flow cytometry. After exposure to the corresponding inhibitor, supernatants were collected and cells were harvested and washed twice with cold PBS. Following this, cells were resuspended in 200 µL YO-PRO-1 (final concentration: 0.2 µM) solution. After incubating at room temperature for 20 min in the dark, cells were washed twice in cold PBS and resuspended in 400 µL cold PBS. Then, cells were stained with PI (final concentration: 20 µg/mL) straightway before measurement. Unstained and single-stained cells were used as controls and measured in every single experiment. YO-PRO-1^-/PI^- cells are considered to be viable cells, YO-PRO-1^+/PI^- cells are considered to be apoptotic cells, and PI^+ cells are considered to be necrotic cells. Flow cytometry measurement was performed on FACSverse (Becton, Dickinson and Company (BD), Heidelberg, Germany) and all data were analyzed by BD FlowJo software (BD).

4.6. Nucleic Acid Extraction

Genomic DNA was extracted by the NucleoSpin® Tissue Kit (MACHEREY-NAGEL GmbH, Dueren, Germany) according to the manufacturers' instructions. In brief, 5×10^6 cells were harvested from each continuous cultural cell line and washed twice with cold sterile PBS. Cell pellets were lysed, then the lysis that contained genomic DNA were extracted and purified by a silica membrane of the NucleoSpin column. Finally, genomic DNA was eluted by 30 µL of nuclease-free water.

Total RNAs were extracted by miRNeasy Mini Kit (QIAGEN GmbH, Hilden, Germany) according to the manufacturers' instructions. In brief, 5×10^6 cells were harvested from each continuous cultural cell line and washed twice with cold sterile PBS. Cell pellets were resuspended in 700 µL QIAzol Lysis Reagent (QIAGEN GmbH), then the aqueous phase that contained the total RNA of the lysed cells were extracted and purified by a silica membrane of RNeasy Mini spin columns. Finally, total RNA was eluted by 30 µL of nuclease-free water.

After extraction, nucleic acid concentrations as well as OD 260/280 and OD 260/230 ratios were measured with a NanoDrop 1000 Spectrophotometer (Thermo Fisher Scientific Inc., Waltham, MA, USA).

4.7. Whole Exome Sequencing

Barcoded sequencing libraries were generated after enrichment with the SureSelect Human All Exon Kit (Agilent, Santa Clara, CA, USA), pooled and sequenced on a HiSeq4000 (Illumina Inc., San Diego, CA, USA) instrument using 150 paired-end protocol to yield at least 20× coverage for >98% of the target region and an overall average depth of coverage above 100×. An in-house bioinformatics pipeline including read alignment to human genome reference hg 19, variant calling (single nucleotide substitutions and small deletions/insertions), and variant annotation with publicly available data based was used.

4.8. Variant Calling Filtering Strategy

After WES, the sequencing data from ten PDAC cell lines were obtained and filtered in order to select variants with the expected highest impact on gene function. Briefly, variants were filtered based on quality (qual), VAF, depth of coverage (DP), and variant type. In order to exclude false positive variants, only variants with qual > 100, VAF > 20, and DP > 9 were included in our analysis. Germline mutations were excluded through a comparison with the COSMIC and dbSNP databases. Then, variant types were excluded that were not able to cause amino acid substitution, RNA structure change, or base insertions/deletions (indels). These variant types include synonymous variants, intronic variants, upstream or downstream variants, 3 prime or 5 prime UTR variants. After this filtering procedure, missense variants, splice region variants, inframe indels, frameshift variants, gene fusion, start/stop gain, or lost were kept for further analysis (Figure 7).

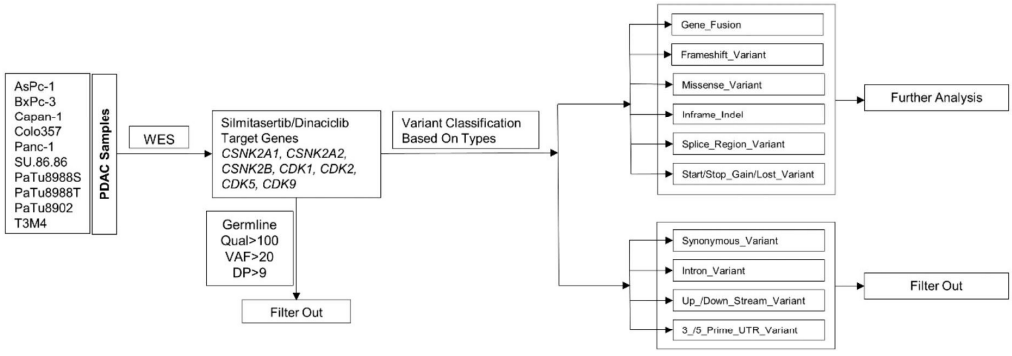

Figure 7. Filtering strategy of inhibitor target genes.

4.9. Gene Expression Analyses

Barcoded sequencing libraries were prepared with the TruSeq Stranded mRNA Kit (Illumina), pooled, and sequenced on a NextSeq 500 System (Illumina) using the 75 bp paired-end protocol. At least 30 million reads were obtained for each sample. The reads were aligned to reference genome GRCh37/Release 38 with STAR V.2.7.6a using the two-pass mode [50]. Transcript abundance estimates were calculated by counting the reads using featureCounts/subread V.2.0.1 [51].

The expression data of non-neoplastic pancreatic tissue from The Genotype-Tissue Expression (GTEx) and The Cancer Genome Atlas Program (TCGA) were chosen as the control. Non-inhibitor target genes were analyzed to exclude the tumor-induced upregulation of all genes.

4.10. Response-Based Clustering Strategy

The cell sensitivity grouping was performed by the k-means++ clustering method based on an unsupervised machine learning algorithm. Briefly, after performing viability assays on all ten PDAC cell lines, we obtained the IC_{50} values of cell proliferation and biomass. Then, these IC_{50} results were applied to the Sci-kit learn package using Python programming language to predict optimal clusters. The Silhouette score was used to detect the clustering density and the separation between clusters [52]. Ten cell lines were set to be divided into several clusters, and the cluster grouping was iterated a maximum of 100 times to test for the robustness of the classification. Finally, the ten cell lines were divided into different clusters, and identified as high, moderate, and low sensitivity groups based on their biological characteristics.

4.11. Statistical Analyses

Data were replicated with at least three biologically independent experiments. Results of proliferation, metabolic activity, biomass quantification, and apoptosis/necrosis analysis were expressed as mean ± standard deviation (SD). Statistical significance was determined by one-way ANOVA (after proving the data within each group conformed to the Gaussian distribution) or Kruskal–Wallis test (the data within each group conformed to non-Gaussian distribution) and displayed as * $p < 0.033$, ** $p < 0.002$, *** $p < 0.001$ versus the control group.

5. Conclusions

Our present study revealed distinct sensitivities of the PDAC cell lines when treated with dinaciclib or silmitasertib. Neither the expression level of the inhibitor target genes nor gene variants could affect the differences in the observed sensitivity to these drugs. For PDAC hotspot genes, the *KRAS* variants may reduce the sensitivity of PDAC cell lines to silmitasertib. Specific *TP53* variants including c.267delC, c.818G>A, and c.844C>T, reduced the sensitivity of silmitasertib to the PDAC cell lines. Interestingly, cell lines carrying *TP53* frameshift variants are highly sensitive to dinaciclib compared to cell lines carrying *TP53* point mutations. Thus, both inhibitors displayed excellent in vitro efficacy on PDAC cell lines, and further experiments are still needed to verify the in vivo efficacy and the effects of the target genes and hotspot genes on the efficacy of the inhibitors.

Supplementary Materials: The following supporting information can be downloaded at: https://www.mdpi.com/article/10.3390/ijms23084409/s1.

Author Contributions: Conceptualization, H.M.E.; Methodology, Y.M., S.S., A.S., N.A. and A.P.; Software, Y.M., M.R. and A.P.; Validation, Y.M., S.S. and H.M.E.; Formal analysis, Y.M., S.S., N.A., R.A.-A. and A.P.; Investigation, Y.M., S.S., A.S., P.B., N.A., S.K., R.A.-A. and M.R.; Resources, F.U.W. and M.M.L.; Data curation, Y.M.; Writing—original draft preparation, Y.M.; Writing—review and editing, W.K., S.S., N.A., D.Z., A.P. and H.M.E.; Visualization, Y.M.; Supervision, C.J. and H.M.E. All authors have read and agreed to the published version of the manuscript.

Funding: This research was funded by the PiCoP project (Funded by European Community, Europäischer Fonds für regionale Entwicklung (EFRE), grant TBI-V-1-241-VBW-084/State Mecklenburg-Western-Pomerania, Germany).

Institutional Review Board Statement: Not applicable.

Informed Consent Statement: Not applicable.

Data Availability Statement: The data supporting the reported results can be found on the website in detail in the article.

Acknowledgments: The authors gratefully thank the PiCoP project (Funded by European Community, Europäischer Fonds für regionale Entwicklung (EFRE), grant TBI-V-1-241-VBW-084/State Mecklenburg–Western Pomerania, Germany) for supporting this research. We would like to thank Patrick Brennan (Department of Medicine Clinic III, Hematology, Oncology and Palliative Medicine, Rostock University Medical Center, Germany) for his contribution to the improvement in the English language and style.

Conflicts of Interest: The authors declare no conflict of interest.

Abbreviations

AKT, *AKT*	Protein kinase B
Ala	Alanine
Arg	Arginine
Asp	Aspartate
CDK, *CDK*	Cyclin-dependent kinase
CK2, *CSNK2*	Casein kinase II
CV	Crystal violet
Cys	Cysteine
DMSO	Dimethyl sulfoxide
DP	Depth of coverage
DRB	5,6-Dichloro-1-ß-D-ribofuranosylbenzimidazole
ERK	Extracellular regulated kinase
FCS	Fetal calf serum
Fs	Frameshift
Gln	Glutamine
Gly	Glycine
GTEx	The genotype-tissue expression
His	Histidine
IC50	Half maximal inhibitory concentration
Indel	Insertion/deletion
JAK	Janus kinase
JNK	C-Jun N-terminal kinase
KRAS, *KRAS*	Kirsten's rat sarcoma viral oncogene homolog
MEK	Mitogen-activated protein kinase kinase
MKK4	Dual-specificity mitogen-activated protein kinase kinase 4
OD	Optical density
PBS	Phosphate buffer saline
PDAC	Pancreatic ductal adenocarcinoma
PI	Propidium iodide
PI3K	Phosphoinositide 3-kinase
PIP3	Phosphatidylinositol 3,4,5-trisphosphate
PTEN	Phosphatase and tensin homolog
qual	Variant confidence
Rb	Retinoblastoma
RNA-seq	RNA sequencing
Ser	Serine
STAT	Signal transducer and activator of transcription
TCGA	The Cancer Genome Atlas Program

Thr	Threonine
P53, *TP53*	Tumor protein p53
TPM	Transcripts per kilobase million
UTR	Untranslated region
VAF	Variant allele frequency
Val	Valine
WES	Whole exome sequencing
WST-1	Water soluble tetrazolium-1

References

1. Siegel, R.L.; Miller, K.D.; Fuchs, H.E.; Jemal, A. Cancer Statistics, 2021. *CA Cancer J. Clin.* **2021**, *71*, 7–33. [CrossRef] [PubMed]
2. Klompmaker, S.; de Rooij, T.; Korteweg, J.J.; van Dieren, S.; van Lienden, K.P.; van Gulik, T.M.; Busch, O.R.; Besselink, M.G. Systematic review of outcomes after distal pancreatectomy with coeliac axis resection for locally advanced pancreatic cancer. *Br. J. Surg.* **2016**, *103*, 941–949. [CrossRef] [PubMed]
3. Kyriazanos, I.D.; Tsoukalos, G.G.; Papageorgiou, G.; Verigos, K.E.; Miliadis, L.; Stoidis, C.N. Local recurrence of pancreatic cancer after primary surgical intervention: How to deal with this devastating scenario? *Surg. Oncol.* **2011**, *20*, e133–e142. [CrossRef] [PubMed]
4. Xu, X.D.; Zhao, Y.; Zhang, M.; He, R.Z.; Shi, X.H.; Guo, X.J.; Shi, C.J.; Peng, F.; Wang, M.; Shen, M.; et al. Inhibition of Autophagy by Deguelin Sensitizes Pancreatic Cancer Cells to Doxorubicin. *Int. J. Mol. Sci.* **2017**, *18*, 370. [CrossRef]
5. Lovecek, M.; Skalicky, P.; Chudacek, J.; Szkorupa, M.; Svebisova, H.; Lemstrova, R.; Ehrmann, J.; Melichar, B.; Yogeswara, T.; Klos, D.; et al. Different clinical presentations of metachronous pulmonary metastases after resection of pancreatic ductal adenocarcinoma: Retrospective study and review of the literature. *World J. Gastroenterol.* **2017**, *23*, 6420–6428. [CrossRef] [PubMed]
6. Tempero, M.A. NCCN Guidelines Updates: Pancreatic Cancer. *J. Natl. Compr. Cancer Netw.* **2019**, *17*, 603–605. [CrossRef]
7. Litchfield, D.W. Protein kinase CK2: Structure, regulation and role in cellular decisions of life and death. *Biochem. J.* **2003**, *369*, 1–15. [CrossRef]
8. Ruzzene, M.; Bertacchini, J.; Toker, A.; Marmiroli, S. Cross-talk between the CK2 and AKT signaling pathways in cancer. *Adv. Biol. Regul.* **2017**, *64*, 1–8. [CrossRef]
9. Hanahan, D.; Weinberg, R.A. Hallmarks of cancer: The next generation. *Cell* **2011**, *144*, 646–674. [CrossRef]
10. Zheng, Y.; Qin, H.; Frank, S.J.; Deng, L.; Litchfield, D.W.; Tefferi, A.; Pardanani, A.; Lin, F.T.; Li, J.; Sha, B.; et al. A CK2-dependent mechanism for activation of the JAK-STAT signaling pathway. *Blood* **2011**, *118*, 156–166. [CrossRef]
11. Schevzov, G.; Kee, A.J.; Wang, B.; Sequeira, V.B.; Hook, J.; Coombes, J.D.; Lucas, C.A.; Stehn, J.R.; Musgrove, E.A.; Cretu, A.; et al. Regulation of cell proliferation by ERK and signal-dependent nuclear translocation of ERK is dependent on Tm5NM1-containing actin filaments. *Mol. Biol. Cell* **2015**, *26*, 2475–2490. [CrossRef] [PubMed]
12. Kreutzer, J.N.; Ruzzene, M.; Guerra, B. Enhancing chemosensitivity to gemcitabine via RNA interference targeting the catalytic subunits of protein kinase CK2 in human pancreatic cancer cells. *BMC Cancer* **2010**, *10*, 440. [CrossRef] [PubMed]
13. Giroux, V.; Iovanna, J.; Dagorn, J.C. Probing the human kinome for kinases involved in pancreatic cancer cell survival and gemcitabine resistance. *FASEB J.* **2006**, *20*, 1982–1991. [CrossRef] [PubMed]
14. Hamacher, R.; Saur, D.; Fritsch, R.; Reichert, M.; Schmid, R.M.; Schneider, G. Casein kinase II inhibition induces apoptosis in pancreatic cancer cells. *Oncol. Rep.* **2007**, *18*, 695–701. [CrossRef] [PubMed]
15. Siddiqui-Jain, A.; Drygin, D.; Streiner, N.; Chua, P.; Pierre, F.; O'Brien, S.E.; Bliesath, J.; Omori, M.; Huser, N.; Ho, C.; et al. CX-4945, an orally bioavailable selective inhibitor of protein kinase CK2, inhibits prosurvival and angiogenic signaling and exhibits antitumor efficacy. *Cancer Res.* **2010**, *70*, 10288–10298. [CrossRef]
16. Clinicaltrials. Available online: https://www.clinicaltrials.gov/ (accessed on 1 October 2021).
17. Malumbres, M.; Barbacid, M. Cell cycle, CDKs and cancer: A changing paradigm. *Nat. Rev. Cancer* **2009**, *9*, 153–166. [CrossRef]
18. Hunter, T.; Pines, J. Cyclins and cancer. II: Cyclin D and CDK inhibitors come of age. *Cell* **1994**, *79*, 573–582. [CrossRef]
19. Bregman, D.B.; Pestell, R.G.; Kidd, V.J. Cell cycle regulation and RNA polymerase II. *Front. Biosci.* **2000**, *5*, D244–D257. [CrossRef]
20. Sharma, S.; Sicinski, P. A kinase of many talents: Non-neuronal functions of CDK5 in development and disease. *Open Biol.* **2020**, *10*, 190287. [CrossRef]
21. Roskoski, R., Jr. Cyclin-dependent protein kinase inhibitors including palbociclib as anticancer drugs. *Pharmacol. Res.* **2016**, *107*, 249–275. [CrossRef]
22. Eggers, J.P.; Grandgenett, P.M.; Collisson, E.C.; Lewallen, M.E.; Tremayne, J.; Singh, P.K.; Swanson, B.J.; Andersen, J.M.; Caffrey, T.C.; High, R.R.; et al. Cyclin-dependent kinase 5 is amplified and overexpressed in pancreatic cancer and activated by mutant K-Ras. *Clin. Cancer Res.* **2011**, *17*, 6140–6150. [CrossRef] [PubMed]
23. Feldmann, G.; Mishra, A.; Bisht, S.; Karikari, C.; Garrido-Laguna, I.; Rasheed, Z.; Ottenhof, N.A.; Dadon, T.; Alvarez, H.; Fendrich, V.; et al. Cyclin-dependent kinase inhibitor Dinaciclib (SCH727965) inhibits pancreatic cancer growth and progression in murine xenograft models. *Cancer Biol. Ther.* **2011**, *12*, 598–609. [CrossRef] [PubMed]
24. Cai, D.; Latham, V.M., Jr.; Zhang, X.; Shapiro, G.I. Correction: Combined Depletion of Cell Cycle and Transcriptional Cyclin-Dependent Kinase Activities Induces Apoptosis in Cancer Cells. *Cancer Res.* **2020**, *80*, 361. [CrossRef] [PubMed]

25. Gojo, I.; Zhang, B.; Fenton, R.G. The cyclin-dependent kinase inhibitor flavopiridol induces apoptosis in multiple myeloma cells through transcriptional repression and down-regulation of Mcl-1. *Clin. Cancer Res.* **2002**, *8*, 3527–3538. [PubMed]
26. Chen, R.; Keating, M.J.; Gandhi, V.; Plunkett, W. Transcription inhibition by flavopiridol: Mechanism of chronic lymphocytic leukemia cell death. *Blood* **2005**, *106*, 2513–2519. [CrossRef] [PubMed]
27. Li, R.; Liu, G.Z.; Luo, S.Y.; Chen, R.; Zhang, J.X. Cyclin I promotes cisplatin resistance via Cdk5 activation in cervical cancer. *Eur. Rev. Med. Pharmacol. Sci.* **2015**, *19*, 4533–4541.
28. Zeng, Y.; Liu, Q.; Wang, Y.; Tian, C.; Yang, Q.; Zhao, Y.; Liu, L.; Wu, G.; Xu, S. CDK5 Activates Hippo Signaling to Confer Resistance to Radiation Therapy Via Upregulating TAZ in Lung Cancer. *Int. J. Radiat. Oncol. Biol. Phys.* **2020**, *108*, 758–769. [CrossRef]
29. Kazi, A.; Chen, L.; Xiang, S.; Vangipurapu, R.; Yang, H.; Beato, F.; Fang, B.; Williams, T.M.; Husain, K.; Underwood, P.; et al. Global Phosphoproteomics Reveal CDK Suppression as a Vulnerability to KRas Addiction in Pancreatic Cancer. *Clin. Cancer Res.* **2021**, *27*, 4012–4024. [CrossRef]
30. Vassilev, L.T. Cell cycle synchronization at the G2/M phase border by reversible inhibition of CDK1. *Cell Cycle* **2006**, *5*, 2555–2556. [CrossRef]
31. Le Tourneau, C.; Faivre, S.; Laurence, V.; Delbaldo, C.; Vera, K.; Girre, V.; Chiao, J.; Armour, S.; Frame, S.; Green, S.R.; et al. Phase I evaluation of seliciclib (R-roscovitine), a novel oral cyclin-dependent kinase inhibitor, in patients with advanced malignancies. *Eur. J. Cancer* **2010**, *46*, 3243–3250. [CrossRef]
32. Mita, M.M.; Mita, A.C.; Moseley, J.L.; Poon, J.; Small, K.A.; Jou, Y.M.; Kirschmeier, P.; Zhang, D.; Zhu, Y.; Statkevich, P.; et al. Phase 1 safety, pharmacokinetic and pharmacodynamic study of the cyclin-dependent kinase inhibitor dinaciclib administered every three weeks in patients with advanced malignancies. *Br. J. Cancer* **2017**, *117*, 1258–1268. [CrossRef] [PubMed]
33. Cicenas, J.; Kvederaviciute, K.; Meskinyte, I.; Meskinyte-Kausiliene, E.; Skeberdyte, A.; Cicenas, J. KRAS, TP53, CDKN2A, SMAD4, BRCA1, and BRCA2 Mutations in Pancreatic Cancer. *Cancers* **2017**, *9*, 42. [CrossRef] [PubMed]
34. Hwang, R.F.; Gordon, E.M.; Anderson, W.F.; Parekh, D. Gene therapy for primary and metastatic pancreatic cancer with intraperitoneal retroviral vector bearing the wild-type p53 gene. *Surgery* **1998**, *124*, 143–150; discussion 150–151. [CrossRef]
35. Boeck, S.; Jung, A.; Laubender, R.P.; Neumann, J.; Egg, R.; Goritschan, C.; Ormanns, S.; Haas, M.; Modest, D.P.; Kirchner, T.; et al. KRAS mutation status is not predictive for objective response to anti-EGFR treatment with erlotinib in patients with advanced pancreatic cancer. *J. Gastroenterol.* **2013**, *48*, 544–548. [CrossRef] [PubMed]
36. Ormanns, S.; Siveke, J.T.; Heinemann, V.; Haas, M.; Sipos, B.; Schlitter, A.M.; Esposito, I.; Jung, A.; Laubender, R.P.; Kruger, S.; et al. pERK, pAKT and p53 as tissue biomarkers in erlotinib-treated patients with advanced pancreatic cancer: A translational subgroup analysis from AIO-PK0104. *BMC Cancer* **2014**, *14*, 624. [CrossRef] [PubMed]
37. Hayashi, H.; Kohno, T.; Ueno, H.; Hiraoka, N.; Kondo, S.; Saito, M.; Shimada, Y.; Ichikawa, H.; Kato, M.; Shibata, T.; et al. Utility of Assessing the Number of Mutated KRAS, CDKN2A, TP53, and SMAD4 Genes Using a Targeted Deep Sequencing Assay as a Prognostic Biomarker for Pancreatic Cancer. *Pancreas* **2017**, *46*, 335–340. [CrossRef] [PubMed]
38. EBML. Available online: https://www.ebi.ac.uk/gxa/home (accessed on 10 April 2022).
39. Gojo, I.; Sadowska, M.; Walker, A.; Feldman, E.J.; Iyer, S.P.; Baer, M.R.; Sausville, E.A.; Lapidus, R.G.; Zhang, D.; Zhu, Y.; et al. Clinical and laboratory studies of the novel cyclin-dependent kinase inhibitor dinaciclib (SCH 727965) in acute leukemias. *Cancer Chemother. Pharmacol.* **2013**, *72*, 897–908. [CrossRef]
40. Hwang, D.W.; So, K.S.; Kim, S.C.; Park, K.M.; Lee, Y.J.; Kim, S.W.; Choi, C.M.; Rho, J.K.; Choi, Y.J.; Lee, J.C. Autophagy Induced by CX-4945, a Casein Kinase 2 Inhibitor, Enhances Apoptosis in Pancreatic Cancer Cell Lines. *Pancreas* **2017**, *46*, 575–581. [CrossRef]
41. Subramaniam, D.; Periyasamy, G.; Ponnurangam, S.; Chakrabarti, D.; Sugumar, A.; Padigaru, M.; Weir, S.J.; Balakrishnan, A.; Sharma, S.; Anant, S. CDK-4 inhibitor P276 sensitizes pancreatic cancer cells to gemcitabine-induced apoptosis. *Mol. Cancer Ther.* **2012**, *11*, 1598–1608. [CrossRef]
42. Criscitiello, C.; Viale, G.; Esposito, A.; Curigliano, G. Dinaciclib for the treatment of breast cancer. *Expert Opin. Investig. Drugs* **2014**, *23*, 1305–1312. [CrossRef]
43. Gao, J.; Aksoy, B.A.; Dogrusoz, U.; Dresdner, G.; Gross, B.; Sumer, S.O.; Sun, Y.; Jacobsen, A.; Sinha, R.; Larsson, E.; et al. Integrative analysis of complex cancer genomics and clinical profiles using the cBioPortal. *Sci. Signal.* **2013**, *6*, pl1. [CrossRef] [PubMed]
44. di Magliano, M.P.; Logsdon, C.D. Roles for KRAS in pancreatic tumor development and progression. *Gastroenterology* **2013**, *144*, 1220–1229. [CrossRef] [PubMed]
45. Grochola, L.F.; Taubert, H.; Greither, T.; Bhanot, U.; Udelnow, A.; Wurl, P. Elevated transcript levels from the MDM2 P1 promoter and low p53 transcript levels are associated with poor prognosis in human pancreatic ductal adenocarcinoma. *Pancreas* **2011**, *40*, 265–270. [CrossRef] [PubMed]
46. Kotler, E.; Shani, O.; Goldfeld, G.; Lotan-Pompan, M.; Tarcic, O.; Gershoni, A.; Hopf, T.A.; Marks, D.S.; Oren, M.; Segal, E. A Systematic p53 Mutation Library Links Differential Functional Impact to Cancer Mutation Pattern and Evolutionary Conservation. *Mol. Cell* **2018**, *71*, 178–190. [CrossRef] [PubMed]
47. Petitjean, A.; Mathe, E.; Kato, S.; Ishioka, C.; Tavtigian, S.V.; Hainaut, P.; Olivier, M. Impact of mutant p53 functional properties on TP53 mutation patterns and tumor phenotype: Lessons from recent developments in the IARC TP53 database. *Hum. Mutat.* **2007**, *28*, 622–629. [CrossRef]

48. Brosh, R.; Rotter, V. When mutants gain new powers: News from the mutant p53 field. *Nat. Rev. Cancer* **2009**, *9*, 701–713. [CrossRef]
49. Brown, M.S.; Diallo, O.T.; Hu, M.; Ehsanian, R.; Yang, X.; Arun, P.; Lu, H.; Korman, V.; Unger, G.; Ahmed, K.; et al. CK2 modulation of NF-kappaB, TP53, and the malignant phenotype in head and neck cancer by anti-CK2 oligonucleotides in vitro or in vivo via sub-50-nm nanocapsules. *Clin. Cancer Res.* **2010**, *16*, 2295–2307. [CrossRef]
50. Dobin, A.; Davis, C.A.; Schlesinger, F.; Drenkow, J.; Zaleski, C.; Jha, S.; Batut, P.; Chaisson, M.; Gingeras, T.R. STAR: Ultrafast universal RNA-seq aligner. *Bioinformatics* **2013**, *29*, 15–21. [CrossRef]
51. Liao, Y.; Smyth, G.K.; Shi, W. featureCounts: An efficient general purpose program for assigning sequence reads to genomic features. *Bioinformatics* **2014**, *30*, 923–930. [CrossRef]
52. SKlearn. Available online: https://scikit-learn.org/stable/index.html (accessed on 25 November 2021).

8.2.2 The Inhibitory Response to PI3K/AKT Pathway Inhibitors MK-2206 and Buparlisib Is Related to Genetic Differences in Pancreatic Ductal Adenocarcinoma Cell Line

International Journal of
Molecular Sciences

MDPI

Article

The Inhibitory Response to PI3K/AKT Pathway Inhibitors MK-2206 and Buparlisib Is Related to Genetic Differences in Pancreatic Ductal Adenocarcinoma Cell Lines

Yixuan Ma [1], Sina Sender [1], Anett Sekora [1], Weibo Kong [1,2], Peter Bauer [1,3], Najim Ameziane [3,4], Ruslan Al-Ali [3], Susann Krake [3], Mandy Radefeldt [3], Frank Ulrich Weiss [5], Markus M. Lerch [5,6], Alisha Parveen [7], Dietmar Zechner [7], Christian Junghanss [1] and Hugo Murua Escobar [1,*,†]

1 Department of Medicine Clinic III, Hematology, Oncology and Palliative Medicine, Rostock University Medical Center, 18057 Rostock, Germany; yixuan.ma@med.uni-rostock.de (Y.M.); sina.sender@med.uni-rostock.de (S.S.); anett.sekora@med.uni-rostock.de (A.S.); kong@fbn-dummerstorf.de (W.K.); peter.bauer@centogene.com (P.B.); christian.junghanss@med.uni-rostock.de (C.J.)
2 Institute of Muscle Biology and Growth, Research Institute for Farm Animal Biology (FBN), 18196 Dummerstorf, Germany
3 CENTOGENE GmbH, 18057 Rostock, Germany; najim.ameziane@arcensus-diagnostics.com (N.A.); ruslan.al-ali@centogene.com (R.A.-A.); susann.krake@centogene.com (S.K.); mandy.radefeldt@centogene.com (M.R.)
4 Arcensus GmbH, 18055 Rostock, Germany
5 Department of Medicine A, University Medicine, University of Greifswald, 17475 Greifswald, Germany; ulrich.weiss@med.uni-greifswald.de (F.U.W.); markus.lerch@med.uni-muenchen.de (M.M.L.)
6 LMU Munich University Hospital, 81377 Munich, Germany
7 Institute for Experimental Surgery, University of Rostock, 18057 Rostock, Germany; alisha.parveen@med.uni-rostock.de (A.P.); dietmar.zechner@uni-rostock.de (D.Z.)
* Correspondence: hugo.murua.escobar@med.uni-rostock.de; Tel.: +49-381494-7519 or +49-381494-7639; Fax: +49-381494-45803
† Current address: Department of Medicine Clinic III, Hematology, Oncology and Palliative Medicine, Rostock University Medical Center, Ernst-Heydemann-Str. 6, 18057 Rostock, Germany.

check for updates

Citation: Ma, Y.; Sender, S.; Sekora, A.; Kong, W.; Bauer, P.; Ameziane, N.; Al-Ali, R.; Krake, S.; Radefeldt, M.; Weiss, F.U.; et al. The Inhibitory Response to PI3K/AKT Pathway Inhibitors MK-2206 and Buparlisib Is Related to Genetic Differences in Pancreatic Ductal Adenocarcinoma Cell Lines. *Int. J. Mol. Sci.* **2022**, *23*, 4295. https://doi.org/10.3390/ijms23084295

Academic Editor: Xiaoqun Dong

Received: 21 March 2022
Accepted: 11 April 2022
Published: 13 April 2022

Publisher's Note: MDPI stays neutral with regard to jurisdictional claims in published maps and institutional affiliations.

Abstract: The aberrant activation of the phosphoinositide 3-kinase (PI3K)/ protein kinase B (AKT) pathway is common in pancreatic ductal adenocarcinomas (PDAC). The application of inhibitors against PI3K and AKT has been considered as a therapeutic option. We investigated PDAC cell lines exposed to increasing concentrations of MK-2206 (an AKT1/2/3 inhibitor) and Buparlisib (a pan-PI3K inhibitor). Cell proliferation, metabolic activity, biomass, and apoptosis/necrosis were evaluated. Further, whole-exome sequencing (WES) and RNA sequencing (RNA-seq) were performed to analyze the recurrent aberrations and expression profiles of the inhibitor target genes and the genes frequently mutated in PDAC (Kirsten rat sarcoma virus (*KRAS*), Tumor protein p53 (*TP53*)). MK-2206 and Buparlisib demonstrated pronounced cytotoxic effects and limited cell-line-specific effects in cell death induction. WES revealed two sequence variants within the direct target genes (*PIK3CA* c.1143C > G in Colo357 and *PIK3CD* c.2480C > G in Capan-1), but a direct link to the Buparlisib response was not observed. RNA-seq demonstrated that the expression level of the inhibitor target genes did not affect the efficacy of the corresponding inhibitors. Moreover, increased resistance to MK-2206 was observed in the analyzed cell lines carrying a *KRAS* variant. Further, increased resistance to both inhibitors was observed in SU.86.86 carrying two *TP53* missense variants. Additionally, the presence of the *PIK3CA* c.1143C > G in *KRAS*-variant-carrying cell lines was observed to correlate with increased sensitivity to Buparlisib. In conclusion, the present study reveals the distinct antitumor effects of PI3K/AKT pathway inhibitors against PDAC cell lines. Aberrations in specific target genes, as well as *KRAS* and *TP53*, individually or together, affect the efficacy of the two PI3K/AKT pathway inhibitors.

Keywords: PI3K/AKT pathway; pancreatic ductal adenocarcinoma; *KRAS*; *TP53*

1. Introduction

Pancreatic ductal adenocarcinoma (PDAC) is one of the most aggressive human cancer types and is currently the fourth leading cause of cancer-related deaths in both men and women [1]. Due to the difficulty of early diagnosis, the lack of effective treatments, the prevalence of tumor metastasis and relapse, and chemoresistance, the cure rate for pancreatic cancer is only 9% [2]. Furthermore, PDAC is expected to become the third most fatal cancer within decades [3]. Without treatment, the median survival time of patients with metastatic pancreatic cancer is only 3 months [2,4–7]. Although extensive research has been carried out in recent years, there have been only slight improvements in disease prognosis; the median survival is still less than 12 months, and the overall 5-year survival rate recently increased to only 10% [1].

The phosphoinositide 3-kinase (PI3K)/protein kinase B (AKT) pathway is an intracellular signaling pathway important in regulating the cell cycle. PI3Ks have been reported to be involved in several cell functions, such as cell growth, proliferation, differentiation and intracellular trafficking, which in turn contribute to cancer development [8]. Additionally, studies indicate that PI3Ks play important roles in cancer metastasis in several types of cancers, including colon cancers, breast cancers, and pancreatic cancers [9–11]. PI3Ks can be activated by growth factor stimulation, which results in the activation of AKTs. The activated AKTs affect cellular proliferation or survival through several downstream signaling pathways, such as activating the pathway for the nuclear factor kappa-light-chain-enhancer of activated B cells (NF-κB), or suppressing the p53 pathway [12]. Therefore, the PI3K/AKT pathway is directly related to cellular quiescence, proliferation, malignancy, and longevity. The activation of the PI3K/AKT pathway is implicated in human cancer and is perhaps the most commonly activated signaling pathway [13]. It is estimated that 60% of all PDAC patients have deregulation of the PI3K/AKT signaling pathway [14]. Increased activation of the PI3K/AKT pathway has been noted in more than 40% of PDAC cases and has been associated with a poorer prognosis [15,16]. Furthermore, several studies indicate that the PI3K/AKT pathway contributed to the chemoresistance of cancer cells by activating NF-κB [17,18].

Since the PI3K/AKT pathway plays a critical role in the development and prognosis of PDAC, inhibiting the activation of the PI3K/AKT pathway has become a focus for PDAC therapy. Furthermore, the inhibition of the PI3K/AKT pathway also enhances the chemosensitivity of PDAC cell lines in vitro and in vivo [19]. Key proteins such as PI3Ks and AKTs are considered therapeutic targets. A number of studies have shown that, whether used alone or in combination, PI3K and AKT inhibitors are reported to achieve promising effects in PDAC treatment [14]. Ihle et al. reported that the pan-PI3K inhibitor PX-866 displayed good antitumor activity against Kirsten rat sarcoma virus (*KRAS*) wild-type PDAC cell line BxPC-3 in vivo model, while PX-866 showed a slight effect against *KRAS* mutant PDAC cell lines Panc-1 and MIA Paca-2 [20]. Another study reported that the use of the AKT1/2/3 inhibitor GSK690693 to inhibit AKTs has also observed satisfactory anti-proliferative effects in PDAC cell lines [21]. Therefore, several PI3K inhibitors (e.g., the pan-PI3K inhibitors XL147, PX-866, Buparlisib, and GDC-0941, as well as the PI3Kδ-specific inhibitor CAL101) and AKT inhibitors (e.g., the ATP-competitive AKT inhibitor AZD5363 and the Allosteric AKT inhibitor MK-2206) have entered clinical trials, and some of them have achieved an acceptable response [22–24].

Due to the promising results shown by PI3K/AKT inhibition in PDAC experiments and clinical trials, we investigated the cytostatic/cytotoxic- and apoptosis/necrosis-inducing effects of the AKT1/2/3 inhibitor (MK-2206) and the pan-PI3K inhibitor (Buparlisib) in ten PDAC cell lines (AsPc-1, BxPc-3, Capan-1, Panc-1, PaTu8902, PaTu8988T, PaTu8988S, SU.86.86, T3M4, and Colo357). In addition, all cell lines were characterized by whole-exome sequencing (WES) and RNA-seq transcriptome analysis. *KRAS* and *TP53* are the two most important and most frequently mutated genes among all PDAC hotspot genes, and the mutation rates in PDAC are approximately 92% and 70%, respectively [25,26]. Both of them are not only involved in the tumorigenesis and development of PDAC but also play

an important role in tumor resistance and relapse [25,27]. Moreover, *KRAS* and *TP53* also interact to increase the malignancy of tumors, including immune evasion, which results in poor patient prognosis [28]. Here, we explore how these genes affect the response of PDAC cell lines to PI3K/AKT inhibitors. Further, we integrated these genetic data and the inhibitor response to explore their relationship.

2. Results

2.1. Analysis of the Cytotoxic Effects of MK-2206 and Buparlisib in PDAC Cell Lines

When treating the PDAC cell lines with the AKT1/2/3 inhibitor MK-2206 for 72 h, the cell proliferation and biomass of PDAC were significantly inhibited, starting at a concentration of 1 µM (Supplementary Figure S1 and Supplementary Table S1). However, the inhibition of cell metabolic activities was less pronounced than the inhibition of cell proliferation and biomass. The half-maximum inhibitory concentration (IC50) values ranged from 2.943 µM to 7.508 µM (proliferation), 7.233 µM to 12.15 µM (metabolic activity), and 2.024 µM to 7.340 µM (biomass) (Figures 1 and S2 and Supplementary Table S2).

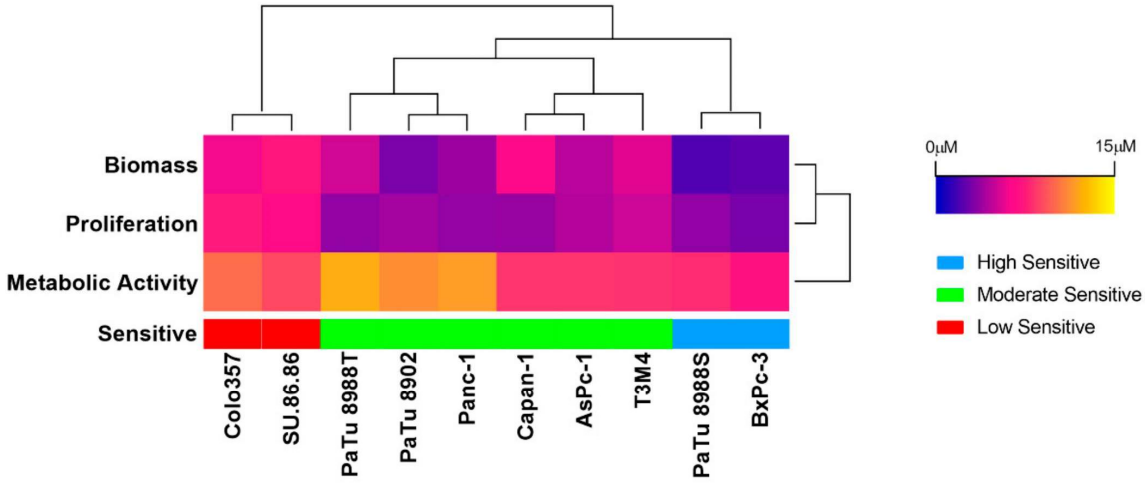

Figure 1. IC50 values when assessing proliferation, metabolic activity, and cell biomass after 72 h MK-2206 exposure in ten PDAC cell lines, as well as the classification of these cell lines by k-means++ (unsupervised machine learning algorithm) into low (red), moderate (green), and high (blue) groups.

These IC50 values were clustered by unsupervised machine learning into three sensitivity groups: low (Colo357 and SU.86.86), moderate (PaTu8988T, PaTu8902, Panc-1, Capan-1, AsPc-1, and T3M4), and high (PaTu8988S and BxPc-3) sensitivity groups (Figures 1 and S2).

When treating the cell lines with the Pan-PI3K inhibitor Buparlisib for 72 h, it significantly inhibited cell proliferation, metabolic activity, and cell biomass at a concentration of 0.5 µM (Supplementary Figure S3 and Supplementary Table S3). In the three viability assays, Buparlisib demonstrated a similarly efficient inhibition of cell proliferation and metabolic activity. The IC50 values ranged from 0.4741 µM to 2.469 µM (proliferation), 0.7471 µM to 4.098 µM (metabolic activity), and 0.5916 µM to 2.419 µM (biomass) (Figures 2 and S4 and Supplementary Table S4).

Based on the same method described above, ten PDAC cell lines were separated into three groups: low (Panc-1 and SU.86.86), moderate (AsPc-1, Capan-1, PaTu8902, and PaTu8988S), and high (BxPc-3, Colo357, PaTu8988T, and T3M4) sensitivity groups (Figures 2 and S4).

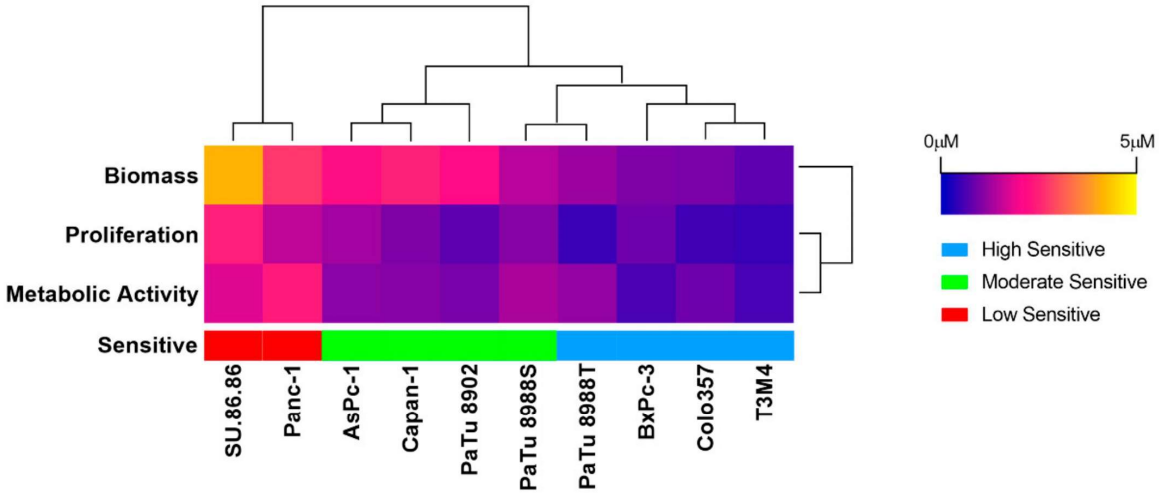

Figure 2. IC50 values when assessing proliferation, metabolic activity, and cell biomass after 72 h Buparlisib exposure in ten PDAC cell lines, as well as the classification of these cell lines by k-means++ (unsupervised machine learning algorithm) into low (red), moderate (green), and high sensitivity (blue) groups.

2.2. Analysis of MK-2206 and Buparlisib in Inducing Apoptosis/Necrosis of PDAC Cell Lines

MK-2206 induced a significant increase in cell death only in AsPc-1 (10 μM), BxPc-3 (1 μM), and Colo357 (10 μM). In addition, in all cell lines, even in AsPc-1, BxPc-3, and Colo357, the observed percentage of dead cells was less than 20% at all tested concentrations (Supplementary Figure S5 and Supplementary Table S5). Compared to the DMSO control group, the percentages of dead cells were decreased in all exposure groups of PaTu8988S.

Buparlisib induced apoptosis/necrosis in all tested PDAC cell lines. Compared with the DMSO control group, a significant induction effect was observed, starting at 1 μM. When Buparlisib concentrations reached 5 μM, more than 50% of AsPc-1, BxPc-3, and T3M4 cells were dead. However, although we observed a significant induction of cell death in Panc-1, SU.86.86, and PaTu8988T, the percentage of apoptotic/necrotic cells was still less than 20% even at the highest tested concentration (10 μM) (Supplementary Figure S6 and Supplementary Table S6).

2.3. Gene Expression and Genetic Variants of MK-2206 or Buparlisib Target Genes

The transcriptional activity of the target genes for each inhibitor (for MK-2206: *AKT1, AKT2, AKT3*; for Buparlisib: *PIK3CA, PIK3CB, PIK3CG, PIK3CD*) was evaluated in all cell lines by RNA-seq. The expression level was displayed as Log_2 (TPM + 1) (Figure 3). Specifically, *AKT2*, *AKT3*, *PIK3CG*, and *PIK3CD* demonstrated a lower expression than non-neoplastic control (Supplementary Table S7). These low-expressed genes and cell lines were as follows (expression minimum-maximum vs. control): *AKT2* in AsPc-1, PaTu8988S, PaTu8988T, PaTu8902, and T3M4 (4.32–4.91 vs. 5.13); *AKT3* in AsPC-1 and PaTu8988S (0.00–0.07 vs. 1.52); *PIK3CG* in AsPc-1, Colo357, Panc-1, PaTu8988T, PaTu8988S, PaTu8902, and T3M4 (0.00–0.10 vs. 0.12); and *PIK3CD* in AsPc-1, Colo357, and PaTu8988S (0.24–0.89 vs. 1.08). In addition, the expression of these target genes was higher in other PDAC cell lines than in the control. In particular, the expression of *AKT1* (6.66–8.96 vs. 5.13), *PIK3CA* (3.68–4.97 vs. 1.52), and *PIK3CB* (3.73–6.00 vs. 3.10) was higher than the control in all cell lines.

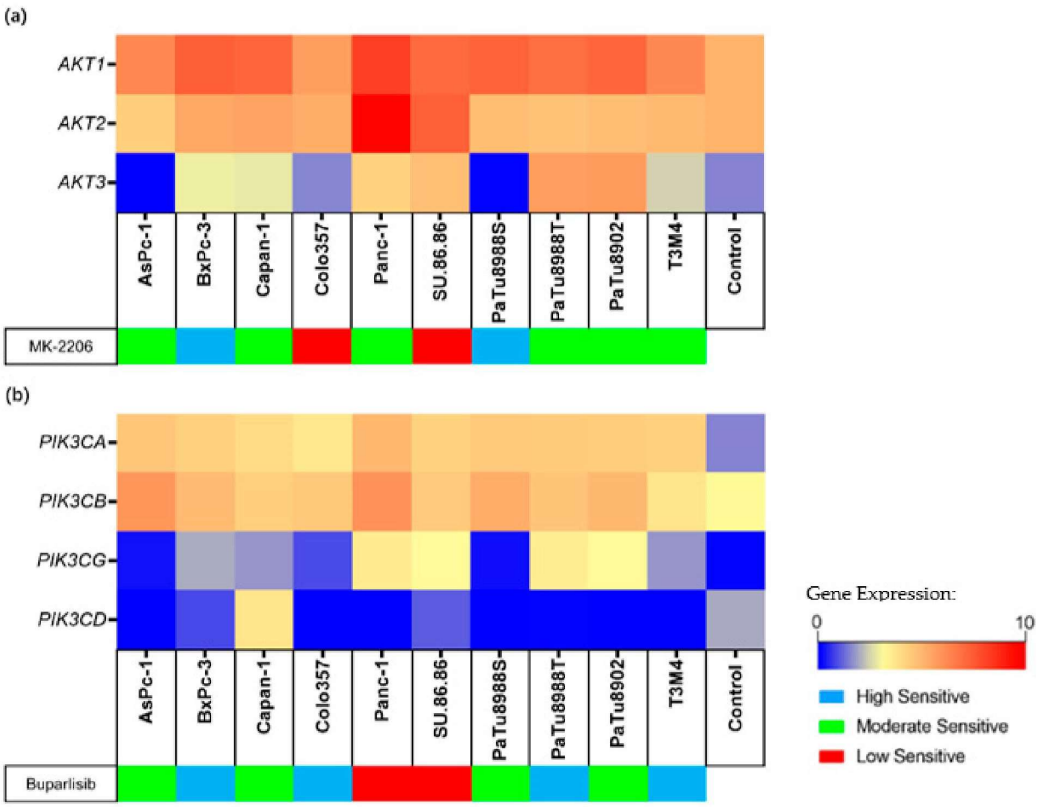

Figure 3. Gene expression levels of inhibitor target genes in cell lines and control. The different sensitivities to MK-2206 (**a**) and Buparlisib (**b**) are indicated for each cell line. Gene expression levels are displayed as Log_2 (TPM + 1). Control: non-neoplastic pancreatic tissue. Gene expression in normal pancreatic tissue comes from GTEx and TCGA databases.

The identical target genes for MK-2206 (*AKT1, AKT2, AKT3*) and Buparlisib (*PIK3CA, PIK3CB, PIK3CG, PIK3CD*) were selected to analyze transcript variants by WES.

When focusing on MK-2206 target genes, initially a total of nine variants, including four *AKT1* variants, two *AKT2* variants, and three *AKT3* variants, were identified in ten PDAC cell lines (Supplementary Table S8). Of these nine variants, one was identified in BxPc-3, Panc-1, PaTu8988T, and PaTu8902; two were identified in SU.86.86; and three were identified in PaTu8988S. Variant filtering according to Method 4.8 classified none of the identified variants as potentially affecting the protein-coding sequence leading to aberrant protein function.

When focusing on Buparlisib target genes, a total of 17 variants, including six *PIK3CA* variants, eight *PIK3CB* variants, one *PIK3CG* variant, and two *PIK3CD* variants, were identified (Supplementary Table S9). Of these seventeen variants, one was identified in Panc-1, PaTu8988T, PaTu8902, SU.86.86, and T3M4; two were identified in AsPc-1 and Capan-1; and eight were identified in Colo357. Variant filtering according to Method 4.8 classified that the missense variant *PIK3CG* c.2480C > G in Capan-1 and the splice region variant and synonymous variant *PIK3CA* c.1143C > G in Colo357 influenced the primary structure of the respective proteins; therefore, they were classified for further analysis (Figure 4a,b).

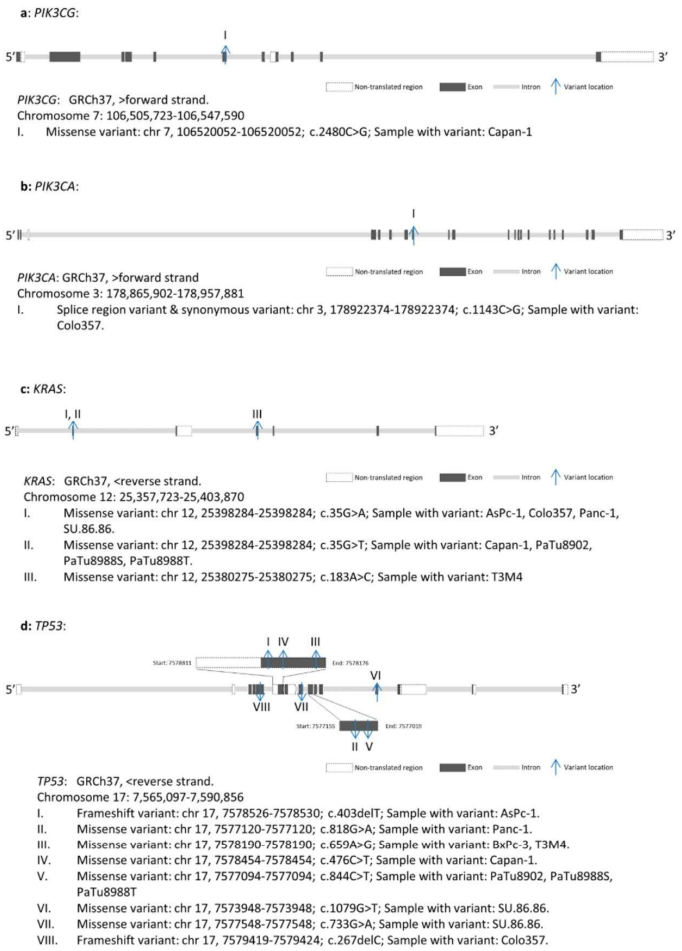

Figure 4. Gene maps indicating the variant positions of *PIK3CG* (**a**), *PIK3CA* (**b**), *KRAS* (**c**), and *TP53* (**d**) in different PDAC cell lines. GRCh37: Genome Reference Consortium Human Build 37, Chr: chromosome.

2.4. KRAS and TP53 Gene Variants Were Observed in PDAC Cell Lines

2.4.1. KRAS Variants and Expression in PDAC Cell Lines

WES demonstrated *KRAS* variants in nine of the ten tested PDAC cell lines (Figure 4c, Supplementary Table S10). Three different *KRAS* variants were identified, and all of them were missense variants. *KRAS* c.35G > A (p.Gly12Asp) was identified in AsPc-1 (Variant allele frequency (VAF): 100), Colo357 (VAF: 23.8), Panc-1 (VAF: 62.1), and SU.86.86 (VAF: 83.7). *KRAS* c.35G > T (p.Gly12Val) was identified in Capan-1 (VAF: 97.1), PaTu8902 (VAF: 100), PaTu8988S (VAF: 96.9), and PaTu8988T (VAF: 98). *KRAS* c.183A > C (p.Gln61His) was identified in T3M4 (VAF: 32.6).

The expression of *KRAS* in all PDAC cell lines was higher than in the control (4.16–7.09 vs. 2.14) (Figure 5a,b). Both the lowest and highest *KRAS* expressions were observed in the *KRAS* c.35G > A variant; they were identified in Colo357 (4.61) and SU.86.86 (7.09), respectively. The expression of all *KRAS* c.35G > T mutations, which were identified in Capan-1, PaTu8988S, PaTu8988T, and PaTu8902, was similar to wild type BxPc-3 (4.40, 4.65, 4.46, 4.51 vs. 4.53, respectively), and the expressions of *KRAS* c183A > C in T3M4 and *KRAS* c.35G > A in AsPc-1, Panc-1, and SU.86.86 were higher than wild type BxPc-3 (4.79–7.09 vs. 4.53).

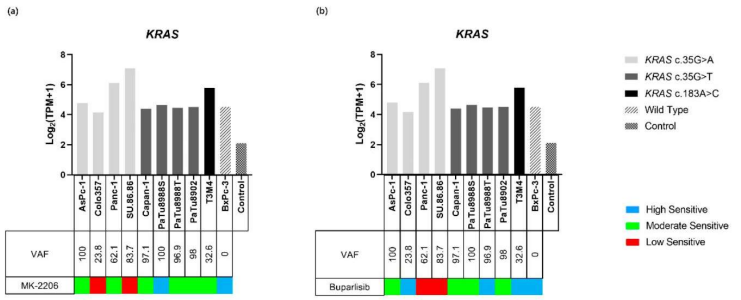

Figure 5. Gene expression of *KRAS* in ten PDAC cell lines and the control. The sensitivity to MK-2206 (**a**), Buparlisib (**b**), and the variants of *KRAS* are indicated for each cell line. Gene expressions are displayed as Log_2 (TPM + 1). Compared with the control group, expression levels of *KRAS* were increased in all cell lines.

2.4.2. KRAS and Inhibitor Response

A comprehensive comparison of the sensitivity and the *KRAS* status of all cell lines revealed that *KRAS* variants alone have no major influence on the inhibitory effect of Buparlisib, since cell lines harboring a *KRAS* mutation were classified into all sensitivity groups (Figure 5b). Moreover, the four cell lines in the highly sensitive group contained all three *KRAS* mutant and wild-type cell lines. For MK-2206, the results were different. The highly sensitive group contained only wild-type and one *KRAS* mutant cell line, while the rest of the *KRAS*-mutant-carrying cell lines were distributed in the moderate or low sensitivity groups, indicating that PDAC cell lines carrying the *KRAS* variant were less sensitive to MK-2206 (Figure 5a). *KRAS* gene expression and VAF did not affect the efficacy of the two inhibitors.

2.4.3. TP53 Variants and Expression in PDAC Cell Lines

Two different types of variants, including frameshift (fs) variants and missense variants of *TP53*, were identified in the PDAC cell lines (Figure 4d, Supplementary Table S11). The fs variants *TP53* c.403delT (p.Cys135fs) and *TP53* c.267delC (p.Ser90fs) were identified in AsPc-1 (VAF: 96.4) and Colo357 (VAF: 100), respectively. The missense variants *TP53* c.476C > T (p.Ala159Val) and *TP53* c.818G > A (p.Arg273His) were identified in Capan-1 (VAF: 100) and Panc-1 (VAF: 98.8), respectively. Double missense mutations, including *TP53* c.733G > A (p.Gly245Ser) and *TP53* c.1079G > T (p.Gly360Val), were identified in SU.86.86 (VAF: 100, 100, respectively). *TP53* c.659A > G (p.Tyr220Cys) was identified in BxPC-3 (VAF: 99) and T3M4 (VAF: 100). *TP53* c.844C > T (p.Arg282Trp) was identified in PaTu8902 (VAF: 100), PaTu8988S (VAF: 100), and PaTu8988T (VAF: 100).

The expression levels of *TP53* with fs variants were lower than that of missense variants (1.24–2.13 vs. 4.39–5.42) and normal controls (2.83) (Figure 6a,b).

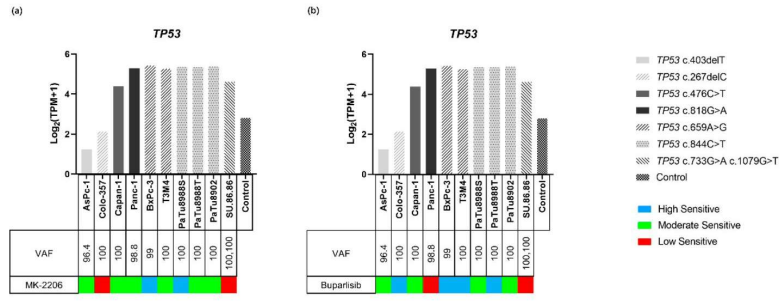

Figure 6. Gene expression of *TP53* in ten PDAC cell lines and the control. The sensitivity to MK-2206 (**a**), Buparlisib (**b**), and the variants of *TP53* are indicated for each cell line. Gene expressions are displayed as Log_2 (TPM + 1). Missense variants were related to overexpression, while frameshift variants were related to the inhibition of gene expression.

2.4.4. TP53 and Inhibitor Response

A comprehensive comparison of the sensitivity to both inhibitors and the *TP53* status of all cell lines revealed no obvious relationship between the status of this tumor suppressor gene and the efficacy of the inhibitors. Interestingly, SU.86.86, which carries two missense variants in *TP53*, was classified in the low-response group for both inhibitors (Figure 6a,b). Further, *TP53* gene expression and VAF did not affect the efficacy of the two inhibitors.

3. Discussion

Our study demonstrated that the proliferation, metabolic activity, and cell biomass of all PDAC cell lines decreased in a dose-dependent manner after Buparlisib exposure. It is reported that Buparlisib is a potent and highly specific oral pan-class I PI3K inhibitor in low concentrations: the IC50s of Buparlisib inhibit p110α/β/δ/γ with values of 52 nM/166 nM/116 nM/262 nM in cell-free assays, respectively [29]. In addition, at high concentrations (>5 μM), it might cause cell death by binding to tubulin, thus inhibiting tubulin polymerization [30]. However, in our study, significant inhibition mostly occurred at a concentration of 1 μM. In addition, the IC50 values of all cell viability assays were below 5 μM. These results suggest that Buparlisib can exert cytotoxic effects in PDAC cell lines by inhibiting PI3Ks. Furthermore, a comprehensive analysis of WES and RNA-seq transcriptome analysis revealed that the *PIK3CG* c.2480C > G variant was correlated with gene overexpression in the corresponding cell line, whereas *PIK3CA* c.1143C > G was associated with a corresponding decrease in gene expression in tumor cell lines, but at a level still higher than non-neoplastic controls (Figure 3b). However, the sensitivity grouping demonstrated that the cell lines carrying these two gene aberrations did not display a specific response to the inhibitory effect of Buparlisib. Therefore, these results suggest that the presence of mutations in these two genes alone does not affect the inhibitory effect of Buparlisib.

This study also confirmed that MK-2206 inhibited cell proliferation, metabolic activity, and biomass in a dose-dependent manner. However, the effects of apoptosis/necrosis induction were not distinct, and the percentage of dead cells was less than 20% at all tested concentrations in all cell lines. These results indicate that the efficacy of MK-2206 at inhibiting PDAC cell lines is not mainly caused by the induction of apoptosis/necrosis. Moreover, our experiments have also revealed that the anti-proliferative and cytotoxic effects of MK-2206 are similar to, but nevertheless differ from, the observed metabolic effects, especially in Panc-1, PaTu8902, and PaTu8988T. It has been reported that some inhibitors induce cellular stress that alters cellular metabolic activity, and we observed similar properties with MK-2206 [31,32]. This result suggests that conclusions based on metabolic activity assays (e.g., WST-1, CCK8, etc.) need to be validated with other assays when MK-2206 is used. In addition, we did not find any amino acid substitution of *AKT*s in PDAC. At the same time, transcriptomic analysis did not support the hypothesis that the expression level of *AKT*s affects the efficacy of MK-2206. However, *AKT2* expression seems to affect the efficacy of Buparlisib. Two cell lines with high *AKT2* expression, Panc-1 and Su.86.86, have low sensitivity to Buparlisib. As reported, not only does the overexpression of *AKT2* represent a biological indicator of PDAC aggressiveness, but also *AKT2* plays a critical role in the inhibitor resistance of PDAC [16,33,34]. Our data indicate that high expression of *AKT2* is related to reducing the efficacy of Buparlisib. However, further functional experiments are still needed to verify the relationship between high *AKT2* expression and Buparlisib resistance. Moreover, according to cBioPortal, although *AKT2* aberration occurred in only 3.99% (49/1228) of patients with PDAC, in 87.76% (43/49) of them, the overexpression of the genetic modulation of *AKT2* was observed [35]. An analysis of the functional relationship between AKT2 aberrations and Buparlisib efficacy remains to be completed.

We identified three different amino acid substitution variants of *KRAS* in nine of ten PDAC cell lines, including *KRAS* p.12Gly > Asp (c.35G > A), *KRAS* p.12Gly > Val (c.35G > T), and *KRAS* p.Gln61His (c.183A > C). In addition, it has been reported that *KRAS* mutations can be found in approximately 92% of pancreatic cancers, and patients

with *KRAS* mutations showed a bad response to first-line gemcitabine-based therapy and presented a poor prognosis [36,37]. However, relevant studies on *KRAS* variants and PDAC cell lines and on patients' responses to PI3K/AKT pathway inhibitors are currently lacking. A comprehensive analysis of the Buparlisib sensitivity groups and *KRAS* variants did not demonstrate any relationship. This is obvious, especially in the high sensitivity group, which included not only cell lines carrying *KRAS* variants but also a wild-type *KRAS*. These results suggest that the *KRAS* status alone does not influence the sensitivity to Buparlisib in PDAC cell lines. On the other hand, analysis of MK-2206 demonstrated that carrying the *KRAS* variant appeared to cause a decrease in the sensitivity of PDAC cell lines to this inhibitor. Consistent with these data, one study demonstrated that, in cell lines of colorectal cancer, lung cancer, breast cancer, and melanoma, *KRAS* mutations were associated with significant resistance to AKT1/2 inhibition [38]. This resistance is achieved through the activation of MEK/ERK by KRAS, which bypasses PI3K/AKT and directly activates 4E-BP1 [38]. The present study suggests that this mechanism also exists in PDAC cell lines. Therefore, it might be important to consider *KRAS* status before using MK-2206 to treat patients with PDAC.

We identified two *PI3K* variants (*PIK3CA* c.1143C > G and *PIK3CG* c.2480C > G) in PDAC cell lines. We further analyzed the response of cell lines carrying *PI3K* and *KRAS* double mutations and a *KRAS* single mutation to Buparlisib. In four cell lines carrying the *KRAS* c.35G > A mutation (AsPc-1, Colo357, Panc-1, and SU.86.86), we identified that Colo357 also carries the *PIK3CA* c.1143C > G variant. Interestingly, Colo357 was highly sensitive to Buparlisib, while the other three cell lines were less sensitive. This might indicate that there are unknown interactions between the *PIK3CA* c.1143C > G variant and the *KRAS* c.35G > A variant. This *PIK3CA* variant could reduce the negative effects of *KRAS* on the sensitivity to Buparlisib. However, we did not observe any interaction when analyzing another PI3K mutation (*PIK3CG* c.2480C > G) in cell lines bearing the *KRAS* c35G > T variant (Capan-1, PaTu8902, PaTu8988S, and PaTu8988T) when using either inhibitor. However, cBioPortal demonstrated that only 2.5% (31/1228) of patients with PDAC harbor *PIK3CA* and *KRAS* double aberrations, and 1.95% (24/1228) of patients harbor *PIK3CG* and *KRAS* double aberrations [35]. Moreover, no patients were found to carry the same specific *PIK3CA* and *KRAS* mutation in the cell line. For patients with the same gene aberration, further experiments are still needed to verify the efficacy of the inhibitor.

We also identified that in the tested ten PDAC cell lines, all carry only one *TP53* variant that can cause amino acid or RNA structure changes, except SU.86.86, which carries two *TP53* variants. It has been reported that patients with advanced PDAC who have two *TP53* mutations and who were treated with the EGFR-inhibitor Erlotinib demonstrated rapid disease progression, which suggests that multiple *TP53* mutations reduce the efficacy of specific inhibitors against PDAC [39]. In our study, a comprehensive analysis of the cell viability assays and the number of *TP53* variants revealed that SU.86.86 is in the low-sensitivity group when testing both inhibitors, suggesting that two *TP53* mutations are related to reducing the efficacy of PI3K/AKT pathway inhibitors (Figure 6). Therefore, when multiple *TP53* mutations are identified, the combination of inhibitors and drugs should be considered.

4. Materials and Methods

4.1. Kinase Inhibitors

The kinase inhibitors Buparlisib (Pan-PI3K inhibitor) and MK-2206 (AKT1/2/3 inhibitor) were purchased from Selleck Chemicals (Absource Diagnostics GmbH, Munich, Germany). According to the manufacturer's instructions, Buparlisib and MK-2206 were separately dissolved in dimethyl sulfoxide (DMSO) (Sigma-Aldrich Chemie GmbH, Steinheim, Germany) as a stock solution at a final concentration of 10 mM. The stock solutions were stored at −80 °C and diluted into corresponding working concentrations before each experiment.

4.2. Cell Lines and Cell Culture

PDAC cell lines AsPc-1, BxPc-3, Capan-1, Colo357, Panc-1, PaTu8902, PaTu8988T, PaTu8988S, SU.86.86, and T3M4 were kindly provided by the University of Greifswald. AsPc-1, BxPc-3, Colo357, Panc-1, SU.86.86, and T3M4 were cultured in RPMI1640 medium (PAN-Biotech, Aidenbach, Germany) supplemented with 10% heat-inactivated fetal calf serum (FCS) (PAN-Biotech, Aidenbach, Germany) and 1% Penicillin-Streptomycin (P/S) solution (10,000 U/mL Penicillin, 10 mg/mL Streptomycin) (PAN-Biotech, Aidenbach, Germany). PaTu8902, PaTu8988T, and PaTu8988S were cultured in DMEM/F12 medium (PAN-Biotech, Aidenbach, Germany) supplemented with 10% heated-inactivated FCS and 1% P/S solution. Capan-1 was cultured in RPMI1640 medium supplemented with 15% heat-inactivated FCS and 1% P/S solution. After verifying that all cell lines were not contaminated by mycoplasma, these PDAC cell lines were maintained in a 5% CO_2 humidified atmosphere incubator at 37 °C.

For all assays, the PDAC cell lines were seeded at a density of 3.3×10^4 cells per milliliter in 6-well plates (totaling 4.5 mL per well), 24-well plates (totaling 1.5 mL per well), and 96-well plates (totaling 150 µL per well). After 24 h, the supernatant was discarded, and media containing increasing concentrations (range from 1 µM–10 µM for MK-2206 and 0.5 µM–10 µM for Buparlisib) of the inhibitors or vehicle (DMSO, as control) were added to the corresponding PDAC cell lines. The treated cells were incubated for up to 72 h at 37 °C with 5% CO_2. At the indicated time points, cell proliferation, metabolic activities, cell biomass, and apoptosis/necrosis were evaluated in at least three biologically independent replicates.

4.3. Cell Viability Assays

4.3.1. Proliferation

Cell proliferation was evaluated by absolute cell counting and trypan blue (Sigma-Aldrich Chemie GmbH, Steinheim, Germany) staining. After inhibitor exposure in 24-well plates, the cells were harvested and washed with 1× PBS (PAN-Biotech, Aidenbach, Germany). In the following step, the cells were stained with trypan blue, and the numbers of viable cells were determined by counting with a hemocytometer. Proliferation was expressed as the percentage of viable cells treated with the inhibitor compared to the 100% DMSO control.

4.3.2. Metabolic Activity

Metabolic activity was tested by Water Soluble Tetrazolium—1 (WST-1) (TaKaRa Bio Inc., Kusatsu, Japan). After exposure to the corresponding inhibitor, the cells were incubated with 15 µL WST-1 for up to 2 h in 96-well plates. Absorbances at 450 nm and the reference wavelength of 620 nm were measured by Promega GloMax®-Multi Microplate Multimode Reader (Promega, Madison, WI, USA). The metabolic activity was calculated as recommended by the manufacturer. Metabolic activity is expressed as a percentage of the inhibitor-treated group compared to vehicle-treated controls (control = 100%).

4.3.3. Biomass Quantification

Biomass quantification was carried out by Crystal Violet (CV) (Sigma-Aldrich GmbH, Steinheim, Germany) staining. After exposure to the corresponding inhibitor in 96-well plates, the cells were washed once with PBS and stained with 50 µL of 0.2% CV solution on a shaker at room temperature for 10 min. Thereafter, the plates were washed twice with PBS. To elute bound CV, 100 µL 1% sodium dodecyl sulfate (SDS) (SERVA Electrophoresis GmbH, Heidelberg, Germany) was added to each well and incubated on a shaker at room temperature for 10 min. Finally, absorbances at 570 nm and a reference wavelength at 620 nm were measured by Promega GloMax®-Multi Microplate Multimode Reader. For background normalization, the absorbance of each group was subtracted from the absorbance of pure culture media. The amount of CV directly correlates to the cell biomass. The result is expressed as a percentage of the inhibitor-treated group compared to vehicle-treated controls (control = 100%).

4.4. Identification of IC50

IC50 values were calculated independently based on cell proliferation, metabolic activity, or biomass after 72 h of inhibitor exposure. GraphPad Prism Version 8.0.2 (GraphPad Software Inc., San Diego, CA, USA) was used to evaluate IC50. Briefly, after transforming concentrations and normalizing the results for the three vitality assays, a nonlinear regression model (dose-response-inhibition vs. normalized response—variable slope) was used to evaluate the IC50 values. We calculated the IC50 corresponding to the three vitality assays and applied these results to a response-based clustering analysis in order to evaluate the sensitivity of the cell lines to inhibitors.

4.5. Apoptosis and Necrosis Analyses

Apoptosis and necrosis were evaluated by YO-PRO-1 (Invitrogen, Darmstadt, Germany) and Propidium iodide (PI) (Sigma-Aldrich GmbH, Steinheim, Germany) double staining by flow cytometry. After exposure to the corresponding inhibitor, supernatants were collected, and cells were harvested and washed twice with cold PBS. Following that, cells were resuspended in 200 µL YO-PRO-1 (final concentration: 0.2 µM) solution. After incubating at room temperature for 20 min in the dark, cells were washed twice in cold PBS and resuspended in 400 µL cold PBS. Cells were then stained with PI (final concentration: 100 µg/mL) immediately before measurement. Unstained and single-stained cells were used as controls and measured in every single experiment. YO-PRO-1^-/PI^- cells are considered viable cells, YO-PRO-1^+/PI^- cells are considered apoptotic cells, and PI^+ cells are considered necrotic cells. Flow cytometry measurements were performed on FACSVerse (Becton, Dickinson and Company, Heidelberg, Germany), and data were analyzed by BD FlowJo software (Becton, Dickinson and Company, Heidelberg, Germany).

4.6. Nucleic Acid Extraction

Genomic DNA was extracted by NucleoSpin® Tissue Kit (MACHEREY-NAGEL GmbH, Dueren, Germany) according to the manufacturers' instructions. In brief, 5×10^6 cells were harvested from each continuous cultural cell line and washed twice with cold sterile PBS. Cell pellets were lysed, and then the lysis that contained genomic DNA was extracted and purified by a silica membrane of NucleoSpin column. Lastly, genomic DNA was eluted with 30 µM of nuclease-free water.

Total RNAs were extracted by miRNeasy Mini Kit (QIAGEN GmbH, Hilden, Germany) according to the manufacturers' instructions. In brief, 5×10^6 cells were harvested from each continuous cultural cell line and washed twice with cold sterile PBS. Cell pellets were resuspended in 700 µL QIAzol Lysis Reagent (QIAGEN GmbH, Hilden, Germany), and then the aqueous phase that contains the total RNA of the lysed cells was extracted and purified by a silica membrane of RNeasy Mini spin columns. Finally, total RNA was eluted in 30 µL of nuclease-free water.

After extraction, nucleic acid concentrations, as well as OD260/280 and OD260/230 ratios, were measured with a NanoDrop 1000 Spectrophotometer (Thermo Fisher Scientific Inc., Waltham, MA, USA).

4.7. Whole-Exome Sequencing

Barcoded sequencing libraries were generated after enrichment with the SureSelect Human All Exon kit (Agilent, Santa Clara, CA, USA), pooled and sequenced on a HiSeq4000 (Illumina Inc., San Diego, CA, USA) instrument using a 150 paired-end protocol to yield at least 20× coverage for >98% of the target region and an overall average depth of coverage above 100×. An in-house bioinformatics pipeline was used, including read alignment to human genome reference hg 19, variant calling (single nucleotide substitutions and small deletions/insertions), and variant annotation with publicly available databases.

4.8. Variant Calling Filtering Strategy

After WES, the sequencing data from ten PDAC cell lines were obtained and filtered in order to select variants with the expected highest impact on gene function. Briefly, variants were filtered based on quality (qual), variant allele frequency (VAF), depth of coverage (DP), and variant type. In order to exclude false positive variants, only variants with qual > 100, VAF > 20, and DP > 9 were included in our analysis. Germline mutations were excluded by comparison with COSMIC and dbSNP databases. Then, variant types were excluded if they were unable to cause amino acid substitution, RNA structure change, or base insertions/deletions (indels). These variant types include synonymous variants, intron variants, upstream or downstream variants, and 3 prime or 5 prime untranslated region (UTR) variants. After this filtering procedure, missense variants, splice region variants, inframe indels, frameshift variants, gene fusion, and start/stop gain or lost were chosen for further analysis (Figure 7).

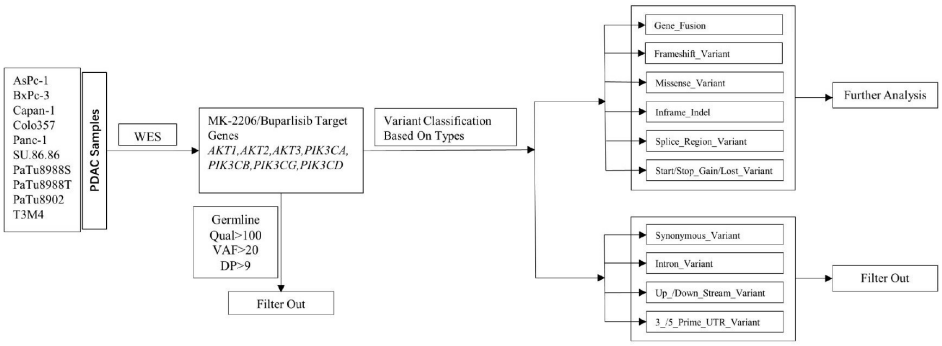

Figure 7. Filtering strategy of MK-2206 and Buparlisib target genes.

4.9. Gene Expression Analyses

Barcoded sequencing libraries were prepared with the TruSeq Stranded mRNA kit (Illumina Inc., San Diego, CA, USA), pooled and sequenced on a NextSeq 500 System (Illumina Inc., San Diego, CA, USA) using the 75 bp paired-end protocol. At least 30 million reads were obtained for each sample. The reads were aligned to reference genome GRCh37/Release 38 with STAR V.2.7.6a using the two-pass mode [40]. Transcript abundance and transcript per million estimates were calculated by counting the reads using featureCounts/subread V.2.0.1 [41].

The expression data of non-neoplastic pancreatic tissue from The Genotype-Tissue Expression (GTEx) and the Cancer Genome Atlas Program (TCGA) were chosen as controls.

4.10. Response-Based Clustering Strategy

The classification of cell lines into distinct sensitivity levels was performed by k-means++ clustering based on an unsupervised machine learning algorithm [42]. Briefly, cell proliferation, metabolic activity, and biomass were analyzed after treating the cells with various inhibitor concentrations and calculating the IC50 values. Then, all IC50 values were collected and applied to the Sci-kit learn package using the Python programming language to predict optimal clusters. The Silhouette score was used to detect the clustering density and the separation between the clusters. Ten cell lines were set to be divided into several clusters, and the cluster grouping was iterated a maximum of 100 times to test for the robustness of the classification. Finally, the ten cell lines were divided into different clusters identified as high, moderate, and low sensitivity groups based on their biological characteristics.

4.11. Statistical Analyses

Data have been replicated with at least three biologically independent experiments. GraphPad Prism Version 8.0.2 was used for statistical analysis. The results of proliferation, metabolic activity, biomass quantification, and apoptosis/necrosis analysis were expressed as mean ± standard deviation (SD). Statistical significance was determined by one-way ANOVA (after proving that the data within each group conformed to the Gaussian distribution) or the Kruskal-Willas-Test (for the data within each group that conformed to a non-Gaussian distribution) and displayed as *: $p < 0.033$, **: $p < 0.002$, ***: $p < 0.001$ versus the control group.

5. Conclusions

Our present study reveals distinct antitumor effects against PDAC cell lines when inhibiting the PI3K/AKT pathway. Exploring the inhibitor response and the corresponding target gene aberrations shows that neither *PIK3CA* nor *PIK3CG* aberration alone affect the inhibitor response of PDAC cell lines to Buparlisib or MK-2206. Moreover, in the relationship between the observed inhibitor response and aberrations of *KRAS* and *TP53*, *KRAS* point mutations (c.35C > T, c.35C > A, and c.183A > C) alone are not able to determine the level of sensitivity to Buparlisib, but they do appear to be related to the level of sensitivity to MK-2206. Cell line carrying a specific *PIK3CA* variant is associated with enhanced Buparlisib inhibition in *KRAS*-mutated cell lines. In addition, carrying two *TP53* missense variants appears to be associated with reduced sensitivity to PI3K/AKT pathway inhibitors. Thus, our study suggests that blocking the PI3K/AKT pathway is an optional strategy for the treatment of patients with PDAC but that it is still necessary to choose inhibitors based on genetic background.

Supplementary Materials: The following are available online at https://www.mdpi.com/article/10.3390/ijms23084295/s1.

Author Contributions: Conceptualization, H.M.E.; methodology, Y.M., S.S., A.S., N.A. and A.P.; software, Y.M., M.R. and A.P.; validation, Y.M., S.S. and H.M.E.; formal analysis, Y.M., S.S., N.A., R.A.-A. and A.P.; investigation, Y.M., S.S., A.S., P.B., N.A., S.K., R.A.-A. and M.R.; resources, F.U.W. and M.M.L.; data curation, Y.M.; writing—original draft preparation, Y.M.; writing—review and editing, W.K., S.S., N.A., D.Z., A.P. and H.M.E.; visualization, Y.M.; supervision, C.J. and H.M.E. All authors have read and agreed to the published version of the manuscript.

Funding: This research was funded by the PiCoP project (Funded by European Community, Europäischer Fonds für regionale Entwick-lung (EFRE), grant TBI-V-1-241-VBW-084/State Mecklenburg-Western-Pomerania, Germany).

Institutional Review Board Statement: Not applicable.

Informed Consent Statement: Not applicable.

Data Availability Statement: The data supporting the reported results can be found on the website listed in the article.

Acknowledgments: The authors gratefully thank the PiCoP project (Funded by European Community, Europäischer Fonds für regionale Entwicklung (EFRE), grant TBI-V-1-241-VBW-084/State Mecklenburg-Western-Pomerania, Germany) for supporting this research. We would like to express our appreciation for Patrick Brennan (Department of Medicine Clinic III, Hematology, Oncology and Palliative Medicine, Rostock University Medical Center, Germany) for his contribution to the improvement of the English language and style.

Conflicts of Interest: The authors declare no conflict of interest.

Abbreviations

Abbreviation	Meaning
AKT, AKT	Protein kinase B
Ala	Alanine
Arg	Arginine
Asp	Aspartate
CV	Crystal violet
Cys	Cysteine
DMSO	Dimethyl sulfoxide
DP	Reading depth
FCS	Fetal calf serum
fs	Frameshift
Gln	Glutamine
Gly	Glycine
GTEx	The Genotype-Tissue Expression
His	Histidine
IC50	Half maximal inhibitory concentration
indel	Insertion/deletion
KRAS, KRAS	Kirsten rat sarcoma viral oncogene homolog
mTOR	Mammalian target of rapamycin
NF-κB	Nuclear factor kappa-light-chain-enhancer of activated B cells
OD	Optical Density
PBS	Phosphate buffer saline
PDAC	Pancreatic ductal adenocarcinoma
PI	Propidium iodide
PI3K	Phosphatidylinositol-4,5-bisphosphate 3-kinase
P/S	Penicillin/streptomycin
qual	Variant confidence
RNA-seq	RNA sequencing
SD	Standard deviation
Ser	Serine
TCGA	The Cancer Genome Atlas Program
Thr	Threonine
TP53, p53	Tumor protein p53
TPM	Transcript per kilobase million
Trp	Tryptophan
Tyr	Tyrosine
VAF	Variant allele frequency
Val	Valine
UTR	Untranslated region
WES	Whole exome sequencing
WST-1	Water soluble tetrazolium—1

References

1. Siegel, R.L.; Miller, K.D.; Fuchs, H.E.; Jemal, A. Cancer Statistics, 2021. *CA Cancer J. Clin.* **2021**, *71*, 7–33. [CrossRef]
2. Tempero, M.A. NCCN Guidelines Updates: Pancreatic Cancer. *J. Natl. Compr. Cancer Netw.* **2019**, *17*, 603–605. [CrossRef]
3. Malvezzi, M.; Bertuccio, P.; Levi, F.; La Vecchia, C.; Negri, E. European cancer mortality predictions for the year 2014. *Ann. Oncol.* **2014**, *25*, 1650–1656. [CrossRef]
4. Klompmaker, S.; de Rooij, T.; Korteweg, J.J.; van Dieren, S.; van Lienden, K.P.; van Gulik, T.M.; Busch, O.R.; Besselink, M.G. Systematic review of outcomes after distal pancreatectomy with coeliac axis resection for locally advanced pancreatic cancer. *Br. J. Surg.* **2016**, *103*, 941–949. [CrossRef]
5. Kyriazanos, I.D.; Tsoukalos, G.G.; Papageorgiou, G.; Verigos, K.E.; Miliadis, L.; Stoidis, C.N. Local recurrence of pancreatic cancer after primary surgical intervention: How to deal with this devastating scenario? *Surg. Oncol.* **2011**, *20*, e133–e142. [CrossRef]
6. Xu, X.D.; Zhao, Y.; Zhang, M.; He, R.Z.; Shi, X.H.; Guo, X.J.; Shi, C.J.; Peng, F.; Wang, M.; Shen, M.; et al. Inhibition of Autophagy by Deguelin Sensitizes Pancreatic Cancer Cells to Doxorubicin. *Int. J. Mol. Sci.* **2017**, *18*, 370. [CrossRef]

7. Loveček, M.; Skalicky, P.; Chudacek, J.; Szkorupa, M.; Svebisova, H.; Lemstrova, R.; Ehrmann, J.; Melichar, B.; Yogeswara, T.; Klos, D.; et al. Different clinical presentations of metachronous pulmonary metastases after resection of pancreatic ductal adenocarcinoma: Retrospective study and review of the literature. *World J. Gastroenterol.* **2017**, *23*, 6420–6428. [CrossRef] [PubMed]
8. Yuan, T.L.; Cantley, L.C. PI3K pathway alterations in cancer: Variations on a theme. *Oncogene* **2008**, *27*, 5497–5510. [CrossRef] [PubMed]
9. Falasca, M.; Maffucci, T. Targeting p110γ in gastrointestinal cancers: Attack on multiple fronts. *Front. Physiol.* **2014**, *5*, 391. [CrossRef] [PubMed]
10. Attoub, S.; De Wever, O.; Bruyneel, E.; Mareel, M.; Gespach, C. The Transforming Functions of PI3-kinase-γ Are Linked to Disruption of Intercellular Adhesion and Promotion of Cancer Cell Invasion. *Ann. N. Y. Acad. Sci.* **2008**, *1138*, 204–213. [CrossRef]
11. Brazzatti, J.A.; Klingler-Hoffmann, M.; Haylock-Jacobs, S.; Harata-Lee, Y.; Niu, M.; Higgins, M.D.; Kochetkova, M.; Hoffmann, P.; McColl, S.R. Differential roles for the p101 and p84 regulatory subunits of PI3Kγ; in tumor growth and metastasis. *Oncogene* **2011**, *31*, 2350–2361. [CrossRef] [PubMed]
12. Wang, Y.; Kuramitsu, Y.; Baron, B.; Kitagawa, T.; Tokuda, K.; Akada, J.; Maehara, S.-I.; Maehara, Y.; Nakamura, K. PI3K inhibitor LY294002, as opposed to wortmannin, enhances AKT phosphorylation in gemcitabine-resistant pancreatic cancer cells. *Int. J. Oncol.* **2017**, *50*, 606–612. [CrossRef]
13. Liu, P.; Cheng, H.; Roberts, T.M.; Zhao, J.J. Targeting the phosphoinositide 3-kinase pathway in cancer. *Nat. Rev. Drug Discov.* **2009**, *8*, 627–644. [CrossRef] [PubMed]
14. Murthy, D.; Attri, K.S.; Singh, P.K. Phosphoinositide 3-Kinase Signaling Pathway in Pancreatic Ductal Adenocarcinoma Progression, Pathogenesis, and Therapeutics. *Front. Physiol.* **2018**, *9*, 335. [CrossRef]
15. Matthaios, D.; Zarogoulidis, P.; Balgouranidou, I.; Chatzaki, E.; Kakolyris, S. Molecular Pathogenesis of Pancreatic Cancer and Clinical Perspectives. *Oncology* **2011**, *81*, 259–272. [CrossRef] [PubMed]
16. Yamamoto, S.; Tomita, Y.; Hoshida, Y.; Morooka, T.; Nagano, H.; Dono, K.; Umeshita, K.; Sakon, M.; Ishikawa, O.; Ohigashi, H.; et al. Prognostic Significance of Activated Akt Expression in Pancreatic Ductal Adenocarcinoma. *Clin. Cancer Res.* **2004**, *10*, 2846–2850. [CrossRef]
17. Reddy, S.A.G.; Huang, J.H.; Liao, W.S.-L. Phosphatidylinositol 3-Kinase as a Mediator of TNF-Induced NF-κB Activation. *J. Immunol.* **2000**, *164*, 1355–1363. [CrossRef]
18. Madrid, L.V.; Wang, C.-Y.; Guttridge, D.C.; Schottelius, A.J.G.; Baldwin, A.S.; Mayo, M.W. Akt Suppresses Apoptosis by Stimulating the Transactivation Potential of the RelA/p65 Subunit of NF-κB. *Mol. Cell. Biol.* **2000**, *20*, 1626–1638. [CrossRef]
19. Mirjolet, J.-F.; Barberi-Heyob, M.; Didelot, C.M.; Peyrat, J.-P.; Abecassis, J.; Millon, R.; Merlin, J.-L. Bcl-2/Bax protein ratio predicts 5-fluorouracil sensitivity independently of p53 status. *Br. J. Cancer* **2000**, *83*, 1380–1386. [CrossRef]
20. Ihle, N.T.; Lemos, R.; Wipf, P.; Yacoub, A.; Mitchell, C.; Siwak, D.; Mills, G.B.; Dent, P.; Kirkpatrick, D.L.; Powis, G. Mutations in the Phosphatidylinositol-3-Kinase Pathway Predict for Antitumor Activity of the Inhibitor PX-866 whereas Oncogenic Ras Is a Dominant Predictor for Resistance. *Cancer Res.* **2009**, *69*, 143–150. [CrossRef]
21. Rhodes, N.; Heerding, D.A.; Duckett, D.R.; Eberwein, D.J.; Knick, V.B.; Lansing, T.J.; McConnell, R.T.; Gilmer, T.M.; Zhang, S.-Y.; Robell, K.; et al. Characterization of an Akt Kinase Inhibitor with Potent Pharmacodynamic and Antitumor Activity. *Cancer Res.* **2008**, *68*, 2366–2374. [CrossRef] [PubMed]
22. Conway, J.R.; Herrmann, D.; Evans, T.J.; Morton, J.; Timpson, P. Combating pancreatic cancer with PI3K pathway inhibitors in the era of personalised medicine. *Gut* **2019**, *68*, 742–758. [CrossRef] [PubMed]
23. McRee, A.J.; Sanoff, H.K.; Carlson, C.; Ivanova, A.; O'Neil, B.H. A phase I trial of mFOLFOX6 combined with the oral PI3K inhibitor BKM120 in patients with advanced refractory solid tumors. *Investig. New Drugs* **2015**, *33*, 1225–1231. [CrossRef] [PubMed]
24. Bedard, P.; Tabernero, J.; Janku, F.; Wainberg, Z.A.; Paz-Ares, L.; Vansteenkiste, J.; Van Cutsem, E.; Pérez-García, J.; Stathis, A.; Britten, C.D.; et al. A Phase Ib Dose-Escalation Study of the Oral Pan-PI3K Inhibitor Buparlisib (BKM120) in Combination with the Oral MEK1/2 Inhibitor Trametinib (GSK1120212) in Patients with Selected Advanced Solid Tumors. *Clin. Cancer Res.* **2015**, *21*, 730–738. [CrossRef]
25. Cicenas, J.; Kvederaviciute, K.; Meskinyte, I.; Meskinyte-Kausiliene, E.; Skeberdyte, A.; Cicenas, J. KRAS, TP53, CDKN2A, SMAD4, BRCA1, and BRCA2 Mutations in Pancreatic Cancer. *Cancers* **2017**, *9*, 42. [CrossRef]
26. Hwang, R.F.; Gordon, E.M.; Anderson, W.F.; Parekh, D. Gene therapy for primary and metastatic pancreatic cancer with intraperitoneal retroviral vector bearing the wild-type p53 gene. *Surgery* **1998**, *124*, 143–150. [CrossRef]
27. di Magliano, M.P.; Logsdon, C.D. Roles for KRAS in Pancreatic Tumor Development and Progression. *Gastroenterology* **2013**, *144*, 1220–1229. [CrossRef]
28. Hashimoto, S.; Furukawa, S.; Hashimoto, A.; Tsutaho, A.; Fukao, A.; Sakamura, Y.; Parajuli, G.; Onodera, Y.; Otsuka, Y.; Handa, H.; et al. ARF6 and AMAP1 are major targets of *KRAS* and *TP53* mutations to promote invasion, PD-L1 dynamics, and immune evasion of pancreatic cancer. *Proc. Natl. Acad. Sci. USA* **2019**, *116*, 17450–17459. [CrossRef]
29. Burger, M.T.; Pecchi, S.; Wagman, A.; Ni, Z.-J.; Knapp, M.; Hendrickson, T.; Atallah, G.; Pfister, K.; Zhang, Y.; Bartulis, S.; et al. Identification of NVP-BKM120 as a Potent, Selective, Orally Bioavailable Class I PI3 Kinase Inhibitor for Treating Cancer. *ACS Med. Chem. Lett.* **2011**, *2*, 774–779. [CrossRef]
30. Criscitiello, C.; Viale, G.; Curigliano, G.; Goldhirsch, A. Profile of buparlisib and its potential in the treatment of breast cancer: Evidence to date. *Breast Cancer Targets Ther.* **2018**, *10*, 23–29. [CrossRef]

31. Welch, W.J. How Cells Respond to Stress. *Sci. Am.* **1993**, *268*, 56–64. [CrossRef] [PubMed]
32. Berridge, M.V.; Herst, P.M.; Tan, A.S. Tetrazolium dyes as tools in cell biology: New insights into their cellular reduction. *Biotechnol. Annu. Rev.* **2005**, *11*, 127–152. [CrossRef] [PubMed]
33. Altomare, D.A.; Tanno, S.; De Rienzo, A.; Klein-Szanto, A.J.; Tanno, S.; Skele, K.L.; Hoffman, J.P.; Testa, J.R. Frequent activation of AKT2 kinase in human pancreatic carcinomas. *J. Cell. Biochem.* **2002**, *87*, 470–476. [CrossRef] [PubMed]
34. Banno, E.; Togashi, Y.; De Velasco, M.; Mizukami, T.; Nakamura, Y.; Terashima, M.; Sakai, K.; Fujita, Y.; Kamata, K.; Kitano, M.; et al. Clinical significance of Akt2 in advanced pancreatic cancer treated with erlotinib. *Int. J. Oncol.* **2017**, *50*, 2049–2058. [CrossRef]
35. Gao, J.; Aksoy, B.A.; Dogrusoz, U.; Dresdner, G.; Gross, B.E.; Sumer, S.O.; Sun, Y.; Jacobsen, A.; Sinha, R.; Larsson, E.; et al. Integrative Analysis of Complex Cancer Genomics and Clinical Profiles Using the cBioPortal. *Sci. Signal.* **2013**, *6*, pl1. [CrossRef] [PubMed]
36. Boeck, S.; Jung, A.; Laubender, R.P.; Neumann, J.; Egg, R.; Goritschan, C.; Ormanns, S.; Haas, M.; Modest, D.P.; Kirchner, T.; et al. KRAS mutation status is not predictive for objective response to anti-EGFR treatment with erlotinib in patients with advanced pancreatic cancer. *J. Gastroenterol.* **2013**, *48*, 544–548. [CrossRef]
37. Bailey, P.; Chang, D.K.; Nones, K.; Johns, A.L.; Patch, A.-M.; Gingras, M.-C.; Miller, D.K.; Christ, A.N.; Bruxner, T.J.C.; Quinn, M.C.; et al. Genomic analyses identify molecular subtypes of pancreatic cancer. *Nature* **2016**, *531*, 47–52. [CrossRef]
38. She, Q.-B.; Halilovic, E.; Ye, Q.; Zhen, W.; Shirasawa, S.; Sasazuki, T.; Solit, D.B.; Rosen, N. 4E-BP1 Is a Key Effector of the Oncogenic Activation of the AKT and ERK Signaling Pathways that Integrates Their Function in Tumors. *Cancer Cell* **2010**, *18*, 39–51. [CrossRef]
39. Ormanns, S.; Siveke, J.T.; Heinemann, V.; Haas, M.; Sipos, B.; Schlitter, A.M.; Esposito, I.; Jung, A.; Laubender, R.P.; Kruger, S.; et al. pERK, pAKT and p53 as tissue biomarkers in erlotinib-treated patients with advanced pancreatic cancer: A translational subgroup analysis from AIO-PK0104. *BMC Cancer* **2014**, *14*, 624. [CrossRef]
40. Liao, Y.; Smyth, G.K.; Shi, W. feature Counts: An efficient general purpose program for assigning sequence reads to genomic features. *Bioinformatics* **2014**, *30*, 923–930. [CrossRef]
41. Dobin, A.; Davis, C.A.; Schlesinger, F.; Drenkow, J.; Zaleski, C.; Jha, S.; Batut, P.; Chaisson, M.; Gingeras, T.R. STAR: Ultrafast universal RNA-seq aligner. *Bioinformatics* **2013**, *29*, 15–21. [CrossRef] [PubMed]
42. SKlearn. Available online: https://scikit-learn.org/stable/index.html (accessed on 25 November 2021).

8.2.3 Inhibition of KRAS, MEK and PI3K Demonstrate Synergistic Anti-Tumor Effects in Pancreatic Ductal Adenocarcinoma Cell Lines

cancers

MDPI

Article

Inhibition of KRAS, MEK and PI3K Demonstrate Synergistic Anti-Tumor Effects in Pancreatic Ductal Adenocarcinoma Cell Lines

Yixuan Ma [1], Benjamin Schulz [2], Nares Trakooljul [3], Moosheer Al Ammar [1], Anett Sekora [1], Sina Sender [1], Frieder Hadlich [3], Dietmar Zechner [2], Frank Ulrich Weiss [4], Markus M. Lerch [4,5], Robert Jaster [6], Christian Junhanss [1] and Hugo Murua Escobar [1,*]

[1] Department of Medicine Clinic III, Hematology, Oncology and Palliative Medicine, Rostock University Medical Center, 18057 Rostock, Germany
[2] Institute for Experimental Surgery, Rostock University Medical Center, 18057 Rostock, Germany
[3] Institute of Genome Biology, Research Institute for Farm Animal Biology (FBN), 18196 Dummerstorf, Germany
[4] Department of Medicine A, University Medicine Greifswald, 17475 Greifswald, Germany
[5] Ludwig Maximilian University Hospital, Ludwig Maximilian University of Munich, 81377 Munich, Germany
[6] Department of Medicine II, Division of Gastroenterology, Rostock University Medical Center, 18057 Rostock, Germany
* Correspondence: hugo.murua.escobar@med.uni-rostock.de; Tel.: +49-381494-7519 or +49-381494-7639; Fax: +49-381494-45803

Simple Summary: Small molecule inhibitors and targeted therapy are considered to have significant potential for pancreatic ductal adenocarcinoma therapies. Preclinical studies of novel inhibitors and inhibitor combinations can elucidate their acting mechanisms and provide valuable data for in vivo research and clinical trials. We explored the antitumor efficacy of KRAS inhibitors BI-3406 and sotorasib alone or in combination with the downstream inhibitors trametinib and buparlisib in PDAC cell lines, characterized by different *KRAS* mutational statuses. The two KRAS inhibitors demonstrated different anti-tumor efficacy and displayed synergistic or additive effects, when combined with downstream pathway inhibitors. These data emphasized the importance of KRAS as a therapeutic target for PDAC and indicate two distinct mechanisms of KRAS inhibition and their interactions with downstream pathway inhibitors.

Abstract: Kirsten rat sarcoma virus (*KRAS*) mutations are widespread in pancreatic ductal adenocarcinoma (PDAC) and contribute significantly to tumor initiation, progression, tumor relapse/resistance, and prognosis of patients. Although inhibitors against *KRAS* mutations have been developed, this therapeutic approach is not routinely used in PDAC patients. We investigated the anti-tumor efficacy of two KRAS inhibitors BI-3406 (KRAS::SOS1 inhibitor) and sotorasib (KRAS G12C inhibitor) alone or in combination with MEK1/2 inhibitor trametinib and/or PI3K inhibitor buparlisib in seven PDAC cell lines. Whole transcriptomic analysis of combined inhibition and control groups were comparatively analyzed to explore the corresponding mechanisms of inhibitor combination. Both KRAS inhibitors and corresponding combinations exhibited cytotoxicity against specific PDAC cell lines. BI-3406 enhance the efficacy of trametinib and buparlisib in BXPC-3, ASPC-1 and MIA PACA-2, but not in CAPAN-1, while sotorasib enhances the efficacy of trametinib and buparlisib only in MIA PACA-2. The whole transcriptomic analysis demonstrates that the two triple-inhibitor combinations exert antitumor effects by affecting related cell functions, such as affecting the immune system, cell adhesion, cell migration, and cytokine binding. As well as directly involved in RAF/MEK/ERK pathway and PI3K/AKT pathway affect cell survival. Our current study confirmed inhibition of KRAS and its downstream pathways as a potential novel therapy for PDAC and provides fundamental data for in vivo evaluations.

Keywords: pancreatic ductal adenocarcinoma; KRAS; kinase inhibitors; gene expression

Citation: Ma, Y.; Schulz, B.; Trakooljul, N.; Al Ammar, M.; Sekora, A.; Sender, S.; Hadlich, F.; Zechner, D.; Weiss, F.U.; Lerch, M.M.; et al. Inhibition of KRAS, MEK and PI3K Demonstrate Synergistic Anti-Tumor Effects in Pancreatic Ductal Adenocarcinoma Cell Lines. *Cancers* **2022**, *14*, 4467. https://doi.org/10.3390/cancers14184467

Academic Editors: Paola Ghiorzo, William Bruno and Lorenza Pastorino

Received: 26 August 2022
Accepted: 12 September 2022
Published: 14 September 2022

1. Introduction

Kirsten rat sarcoma viral oncogene homolog (*KRAS*) is one of the most frequently mutated oncogenes in human pancreatic ductal adenocarcinoma (PDAC); oncogenic *KRAS* mutations can be detected in approximately 92% of the PDAC genomes [1–6]. The *KRAS* gene encodes the protein KRAS, which is a guanosine triphosphatase (GTPase), and regulates signal transduction by cycling between active guanosine triphosphate (GTP) bound and inactive guanosine diphosphate (GDP) bound statuses [7]. *KRAS* point mutations downregulate the GTPase activity of RAS and prevent the GTPase from promoting the conversion of GTP to GDP. The status of permanent GTP-binding activates downstream signaling pathways, such as the PI3K/AKT pathway or RAF/MEK/ERK pathway, which in turn leads to the initiation and development of PDAC [8]. Moreover, *KRAS* cooperates with other common oncogenes, such as *TP53*, *CDKN2A*, *BRCA3*, *SMAD4*, etc., to cause the initiation and development of PDAC [9–13].

KRAS mutations not only cause the initiation and development of PDAC, but they also affect the efficacy of treatment routines and the long-term survival of patients. A considerable number of studies have revealed that *KRAS* mutations lead to a poor prognosis for patients, regardless of whether they undergo surgery [14]. At the same time, a study pointed out that *KRAS* activation plays an important role in the resistance to gemcitabine treatment and relapse after treatment [15]. Another study reported that specific *KRAS* mutation subtypes (G12V, G12D, and G12A) shortened the median overall survival of PDAC patients [16].

Due to the important role of *KRAS* in PDAC, a growing number of studies consider *KRAS* as a target for the treatment of PDAC. Sotorasib is the first small molecule inhibitor against KRAS G12C mutations and was approved by the FDA for the treatment of non-small cell lung cancer (NSCLC) in 2021. Studies have reported that it can effectively inhibit various cell lines that carry *KRAS* G12C mutations, including PDAC cell lines [17]. According to the recently disclosed CodeBreaK 100 clinical trial results, sotorasib displayed good efficacy in the treatment of advanced KRAS G12C-mutated PDAC, with 8 of the 38 patients having a partial response and 32 of 38 patients displaying disease control. The side effects of sotorasib are described as mild, as only a few patients were affected by grade 3 diarrhea, fatigue, and abdominal pain; no grade 4 side effects were observed in the patients [18]. Currently (2022), there are 18 clinical trials targeting KRAS by sotorasib in progress [19]. However, almost all the clinical trials target NSCLC and colorectal cancer and only a very small number of PDAC patients are enrolled. In addition, other reported KRAS G12C inhibitors (adagrasib, JNJ-74699157, and LY3499446) have also achieved distinct effects in cell experiments, and corresponding clinical trials are also ongoing [20,21]. At the same time, inhibitors that directly target other KRAS mutations (e.g., KS-58 targeting KRAS G12D) are under development.

Although the KRAS G12C inhibitors achieved satisfactory effects on its corresponding mutation, *KRAS* G12C mutations accounted for only 1.42% of all *KRAS* mutated PDAC patients. The specific inhibitors for *KRAS* G12D and G12V mutations, which currently represent the majority (40.45% and 32.14%, respectively), are still under development and have not yet entered any clinical trials [22]. Therefore, how to target other types of *KRAS* mutations is also an urgent problem to be solved. It is well known that there are dynamic positive feedback and negative feedback regulation loops in the RAS signaling pathway. A key role in this feedback regulation is the guanine exchange factor son of sevenless 1 (SOS1) [23]. In unstimulated cells, SOS1 hyperphosphorylation caused by mitogen-activated protein kinase (MAPK) activation catalyzes the activation of RAS. At the same time, SOS1 hyperphosphorylation in stimulated cells will cause it to separate from cytosolic glutathione reductase (GRC2) and cause RAS inactivation [23,24]. Moreover, down-regulation or loss of SOS1 lead to a decrease in the survival rate of tumor cells carrying *KRAS* mutations [25]. Based on these studies, Hoffman et al. developed an inhibitor BI-3406 that can block the interaction between SOS1 and KRAS. It can effectively inhibit a variety of *KRAS* mutant tumor cell lines in vivo and in vitro, including *KRAS*

G12C/V/S/A, and G13D, and also achieved excellent efficacy in the PDAC cell line MIA PACA-2. Moreover, the experimental animals displayed good tolerance to BI-3406 treatment [26]. Therefore, BI 1701963, another inhibitor closely related to BI-3406, has entered phase I clinical trials.

Although studies on the inhibition of *KRAS* have achieved encouraging results, there are still limitations that exist, especially for PDAC. At present, most studies still focus on NSCLS, while little attention has been paid to PDAC. There are also few studies that investigate the combined application of multiple inhibitors. In the existing studies on PDAC, only the MIA PACA-2 cell line was investigated. As a result, we were unable to evaluate the efficacy of these *KRAS* inhibitors on PDAC cells carrying other *KRAS* mutations. Therefore, we studied the efficacy of multiple *KRAS* mutation inhibitor BI-3406 and specific *KRAS* mutation inhibitor sotorasib in different *KRAS* mutations and wild-type *KRAS* PDAC cell lines. At the same time, we explored the efficacy of *KRAS* inhibitors and their downstream pathways (PI3K/AKT/mTOR pathway and RAF/MEK/ERK pathway) inhibitors in combination. RNA sequencing was performed after the combined application to explore the mechanism of the influence of the multi-inhibitor combination on the pathway.

2. Materials and Methods

2.1. Kinase Inhibitors

BI-3406 (KRAS::SOS1 inhibitor) was purchased from Chemietek (Chemietek, Indianapolis, IN, USA), sotorasib (KRAS G12C inhibitor), buparlisib (pan-PI3K inhibitor), and trametinib (MEK1/2 inhibitor) were purchased from Selleck Chemicals (Absource Diagnostics GmbH, Munich, Germany). According to the manufacturer's instructions, all inhibitors were separately dissolved in dimethyl sulfoxide (DMSO) (Sigma Aldrich Chemie GmbH, Steinheim, Germany) as a stock solution, at a final concentration of 10 mM. The stock solutions were stored at −80 °C and diluted into corresponding working concentrations before each experiment.

2.2. Cell Lines and Cell Culture

PDAC cell lines ASPC-1, BXPC-3, CAPAN-1, COLO357, PATU8902, and T3M4 were kindly provided by the University Medicine Greifswald and MIA PACA-2 was kindly provided by Prof. Robert Jaster from Rostock University Medical Center. ASPC-1, BXPC-3, COLO357, and T3M4 were cultured in RPMI1640 medium (PAN-Biotech, Aidenbach, Germany), supplemented with 10% heat-inactivated fetal calf serum (FCS) (PAN-Biotech) and 1% penicillin-streptomycin solution (P/S) (10,000 U/mL penicillin, 10 mg/mL streptomycin) (PAN-Biotech). CAPAN-1 was cultured in RPMI1640 medium, supplemented with 15% heat-inactivated FCS and 1% P/S solution. MIA PACA-2 was cultured in DMEM medium (PAN-Biotech), supplemented with 1% heated-inactivated FCS and 1% P/S solution. PATU8902 was cultured in DMEM/F12 medium (PAN-Biotech), supplemented with 10% heated-inactivated FCS and 1% P/S solution. After verifying that all cell lines were not contaminated by mycoplasma, these PDAC cell lines were maintained in a 5% CO_2 incubator with a humidified atmosphere at 37 °C.

2.3. Inhibitor Application Experiments

For the single inhibitor application experiments, the PDAC cell lines were seeded at a density of 3.3×10^4 cells per milliliter in a 24-well plate (in total, 1.5 mL per well, for cell proliferation assay) or a 96-well plate (in total, 150 µL per well, for biomass quantification assay). After 24 h, the supernatant was discarded and media containing increasing concentrations (range from 0.1 to 10 µM for BI-3406, 0.001 to 10 µM for sotorasib) of inhibitors or vehicle (DMSO, as control) were added to the corresponding PDAC cell lines.

The results of single inhibitor application and related experiments were comprehensively analyzed, and specific PDAC cell lines and inhibitor concentrations were selected for further combined application experiments and the concentrations are listed in Table 1 (the results of the buparlisib inhibition assay are detailed in a previously published paper, and the

results of the trametinib inhibition assay are detailed in the Supplementary Table S14) [27]. Inhibitor concentrations are displayed in Table 1. The PDAC cell lines were seeded in 6-well plates (for RNA isolation), 24-well plates (for proliferation assay, morphological examination, and apoptosis/necrosis analysis), or 96-well plates (for biomass quantification assay). After 24 h, the supernatant was discarded and media containing different combinations of inhibitors were added to the corresponding PDAC cell lines.

Table 1. Inhibitor concentrations used for combined application.

Cell Lines	BI-3406	Sotorasib	Trametinib	Buparlisib
ASPC-1	4 µM	4 µM	0.001 µM	0.3 µM
BXPC-3	4 µM	4 µM	0.001 µM	1 µM
CAPAN-1	4 µM	4 µM	0.005 µM	0.3 µM
MIA PACA-2	4 µM	0.005 µM	0.0025 µM	0.6 µM

The treated cells were incubated for 72 h at 37 °C with 5% CO_2. At the indicated time points, all cell experiments evaluated at least three biologically independent replicates.

2.4. Cell Viability Assays

2.4.1. Proliferation

Proliferation was evaluated by absolute counting, which was determined by trypan blue (Sigma-Aldrich Chemie GmbH, Steinheim, Germany) staining. After inhibitor exposure in 24-well plates, the cells were harvested and washed with 1× PBS (PAN-Biotech). Following the cells being stained with trypan blue, the number of viable cells was determined by counting with a hemocytometer. Proliferation was expressed as a percentage of viable cells treated with the inhibitor to the vehicle-treated control (control = 100%).

2.4.2. Biomass Quantification

Biomass quantification was carried out by crystal violet (CV) staining. After exposure to the corresponding inhibitors, cells in 96-well plates were washed once with PBS and stained with 50 µL 0.2% CV solution on a shaker at room temperature for 10 min. Thereafter, the plates were washed twice with PBS. To elute bound CV, 100 µL 1% sodium dodecyl sulfate (SDS) was added to each well and incubated on a shaker at room temperature for 10 min. Finally, absorbances at a measuring wavelength of 570 nm and at the reference wavelength of 620 nm were measured by a Promega GloMax®-Multi Microplate Multimode Reader. The absorbance value of the reference wavelength was subtracted from that of the corresponding measuring wavelength. The value of cells exposed to the vehicle was used as a control and the value of culture media was used as the background. The background value was subtracted from the control and experimental values. The amount of CV directly correlates to cell biomass. The result is expressed as a percentage of the inhibitor-treated group to vehicle-treated controls (control = 100%).

2.5. Apoptosis and Necrosis Analyses

Apoptosis and necrosis were evaluated by Annexin V FITC (Becton, Dickinson and Company, Heidelberg, Germany) and propidium iodide (PI) (Sigma-Aldrich Chemie GmbH) double staining by flow cytometry. After exposure to the vehicle control, and both single and combined inhibitors, cells were harvested and washed twice with cold PBS. After the washing step, the cell pellet was resuspended in 100 µL Annexin V binding buffer (1×) (Becton, Dickinson and Company), and incubated with 5 µL of Annexin V FITC for 15 min at room temperature in the dark. Then, cells were stained with PI (final concentration: 20 µg/mL) straightway before measurement. Unstained and single-stained cells were used to determine the negative and positive boundaries and measured in each experiment. Annexin V^-/PI^- cells were considered to be viable cells, Annexin V^+/PI^- cells were considered to be early apoptotic cells, and Annexin V^+/PI^+ cells were considered to be late apoptotic/necrotic cells. Flow cytometry measurement was performed on FACSVerse™

(Becton, Dickinson and Company) and all data were analyzed by BD FlowJo™ software (Becton, Dickinson and Company).

2.6. Evaluation of Combined Inhibitor Application

The interaction among the inhibitors was evaluated by the Bliss independent model. The interaction of the inhibitor combination was determined by the difference between the observed (E_O) and predicted (E_P) inhibition of the combination therapy.

In double inhibitor application, E_P was calculated with the following equation:

$$E_P = E_A + E_B - E_A \times E_B,$$

where E_A and E_B are the relative inhibition of single-inhibitors A and B.

In triple inhibitor application, E_P was calculated with the following equation:

$$E_P = E_A + E_B + E_C - E_A \times E_B - E_A \times E_C - E_B \times E_C - E_A \times E_B \times E_C,$$

where E_A, E_B, and E_C are the relative inhibition of single-inhibitors A, B, and C.

$E_O > E_P$ indicated a synergistic effect, $E_O = E_P$ indicated an additional effect; $E_O < E_P$ indicated an antagonistic effect. Bliss values for inhibitor combinations were calculated based on the results of proliferation and cell biomass of PDAC cell lines [28].

2.7. Examination of Cell Morphology Changes

Examination of PDAC cell line morphology changes was carried out by Pappenheim staining. After 72 h of exposure to the vehicle control, single inhibitor, or combined inhibitor, supernatants were collected and cells were harvested. After counting the cells, we resuspended the cell pellet and adjusted the cell density of the control group and each experimental group to 5×10^4 cells/200 µL. Then, 200 µL of the cell suspension was fixed on a glass slide using Shandon Cytospin 3 centrifuge (Shandon, Frankfurt/Main, Germany), and two cell slides were made for each group. After 24 h of air-drying, the slides were stained with May–Grünwald solution (Merck, Darmstadt, Germany) for 6 min, washed with phosphate buffer solution (pH = 7.2) (Merck) three times for 1 min, then stained with Giemsa solution (1:10) (Merck) for 20 min, and washed with phosphate buffer solution three times for 1 min again. After the slides were air-dried for 24 h, the morphology of cells was examined and visualized with Evos XL Core Imaging System (Life Technologies, Darmstadt, Germany), magnified 100 times. Each experiment was repeated 3 times to eliminate random errors.

2.8. RNA Extraction

Total RNAs were extracted using the miRNeasy Mini Kit (QIAGEN GmbH, Hilden, Germany) according to the manufacturer's instructions. For each cell line, only the RNA of the DMSO control group and the triple inhibitor application group were extracted. In brief, at least 5×10^6 cells were harvested and washed twice with cold sterile PBS. Cell pellets were resuspended in 700 µL QIAzol Lysis Reagent (QIAGEN GmbH), then the aqueous phase that contains the total RNA of the lysed cells was extracted and purified by a silica membrane of RNeasy Mini spin columns. At last, total RNA was eluted by 30 µL of RNAse-free water.

After extraction, RNA concentrations, as well as OD 260/280 and OD 260/230 ratios, were measured with the NanoDrop 1000 Spectrophotometer (Thermo Fisher Scientific Inc., Waltham, MA, USA).

2.9. RNA Sequencing Analysis

The RNA quality was assessed using the Agilent RNA 6000 Nano Kit (Agilent Technologies Inc., Waldbronn, Germany) on the 2100 Bioanalyzer system (Agilent Technologies Inc.). Only samples with an RNA integrity number (RIN) >8 were proceeded to DNA library preparation using the Illumina Stranded mRNA Sample Preparation Kit (Illumina Inc., San Diego, CA, USA). Briefly, 800 ng of total RNA was enriched for mRNA via poly-T oligo-coated magnetic beads, and chemically fragmented under elevated temperature. The RNA fragments were then reverse-transcribed into the first- and second-strand cDNA using random hexamers. Double-stranded cDNA fragments were ligated with anchor primers and PCR-amplified for 10 rounds, using 10bp unique dual index primers (UDIs). The quality of the libraries was evaluated for fragment length distribution on the Agilent DNA-1000 Chip (Agilent Technologies Inc.). The library concentration was quantified using a Qubit dsDNA HS Assay kit (Life Technologies), normalized to 2 nM and equally pooled. The multiplexing library pool was sequenced for 2 × 101 bp paired-end reads at a final loading concentration of 750 pM on the NextSeq 2000 system and P3 Flow Cell at the sequencing facility of Research Institute for Farm Animal Biology (FBN), Dummerstorf, Germany.

2.10. Data Pre-Processing and Differentially Expressed Genes (DEGs) Analysis

Sample de-multiplexing and FASTQ generation of raw sequencing reads were conducted using on-board DRAGEN BCL Convert analysis workflow (Illumina). The data were quality-checked pre- and post-processing using FastQC version 0.11.9 [29]. Data pre-processing was performed using Trim Galore v.0.6.7 with the following options: -q 20—paired—stringency 3—length 20—illumine [29]. The remaining high quality paired reads were then aligned to the reference genome, Homo_sapiens.GRCh38 from Ensembl release 106 using Hisat2 version 2.2.1 [30]. The number of reads uniquely mapped to each gene was extracted from the HISAT2 mapping results using HTSeq version 2.0.1, with the following options: -f bam -r name—stranded = reverse -t exon -i gene_id -m union [31]. The resulting gene count data were further analyzed for DEGs using DESeq2 package [32]. DEGs that passed a threshold of $|\mathrm{Log_2}(\text{Fold Change})| > 1$ and adjusted p value (padj) < 0.05 were considered analytically valuable and proceeded to Gene Ontology (GO) and Kyoto Encyclopedia of Genes and Genomes (KEGG) enrichment analysis.

The GO and KEGG enrichment analysis were applied for the functional annotation and pathway analysis using the gene set enrichment analysis (GSEA) [33,34]. The functional enrichment analyses of DEGs were explored by R package clusterProfiler4.0 and Pathview [35,36]. GO and KEGG enrichment analysis with a p-value < 0.05 and q-value < 0.25 were considered to have a significant impact and were selected for further analysis.

2.11. Statistical Analyses

Each experiment was performed in at least 3 biologically independent repetitions. Results of proliferation, biomass quantification, and apoptosis/necrosis analysis were expressed as mean ± standard deviation (SD). Statistical significance was determined by one-way ANOVA (after proving the data within each group conformed to the Gaussian distribution) or Kruskal–Wallis test (the data within each group conformed to the non-Gaussian distribution) and displayed as follows: *: $p < 0.033$, **: $p < 0.002$, ***: $p < 0.001$ versus the control group.

3. Results

3.1. KRAS Status of the PDAC Cell Lines

The analyzed seven PDAC cell lines were characterized by the following *KRAS* mutational statuses: one *KRAS* wild-type cell line (BXPC-3), one *KRAS* G12C (c.34G>T) cell line (MIA PACA-2), one *KRAS* Q61H (c.183A>C) cell line (T3M4), two *KRAS* G12D (c.35G>A) cell lines (ASPC-1and COLO357), and two *KRAS* G12V (c.35G>T) cell lines (CAPAN-1 and PATU8902). The information about each cell line includes the chromosomal location (#Chr), the zygosity (hom: homozygous, het: heterozygous), reference base (Ref), observed base

(Obs), allele frequency (VAF), base change, and amino acid substitution, which are listed in Table 2. Thereby, COLO357 and T3M4 represent the only two cell lines characterized by a heterozygotic *KRAS* genotype.

Table 2. *KRAS* status of PDAC cell lines.

Cell Line	#Chr	Start	End	Ref	Obs	Zygosities	VAF	Gene	Base Change	AA Change
BXPC-3	chr12	25398284	25398284	G	G	hom	100	*KRAS*	-	-
ASPC-1	chr12	25398284	25398284	G	A	hom	100	*KRAS*	NM_033360.2:c.35G>A	G12D
COLO357	chr12	25398284	25398284	G	A	het	23.8	*KRAS*	NM_033360.2:c.35G>A	G12D
CAPAN-1	chr12	25398284	25398284	G	T	hom	97.1	*KRAS*	NM_033360.2:c.35G>T	G12V
PATU8902	chr12	25398284	25398284	G	T	hom	100	*KRAS*	NM_033360.2:c.35G>T	G12V
MIA PACA-2	chr12	25398285	25398285	G	T	hom	99.6	*KRAS*	NM_004985.5:c.34G>T	G12C
T3M4	chr12	25380275	25380275	A	C	het	32.6	*KRAS*	NM_033360.2:c.183A>C	Q61H

3.2. Single Application of KRAS Inhibitors BI-3406 and Sotorasib to PDAC Cell Lines

The *KRAS* G12C inhibitor sotorasib had almost no inhibitory effect on the *KRAS* Q61H cell line T3M4 (Figure 1). At the highest tested concentration of 10 µM, cell proliferation and biomass were reduced by only 6% and 0%, respectively. In addition, sotorasib displayed similar inhibitory effects on *KRAS* wild-type and *KRAS* G12V cell lines, and the biomass of cell proliferation decreases ranged from 25% to 38% at the concentration of 10 µM. Notably, the inhibitory effects of sotorasib on ASPC-1 (VAF: 100) and COLO357 (VAF: 23.8), which both carry *KRAS* G12D, are quite different; cell proliferation decreased by 50% and 37%, and biomass decreased by 41% and 27%, respectively. Sotorasib appears to be more effective against *KRAS* G12D mutations with high VAF.

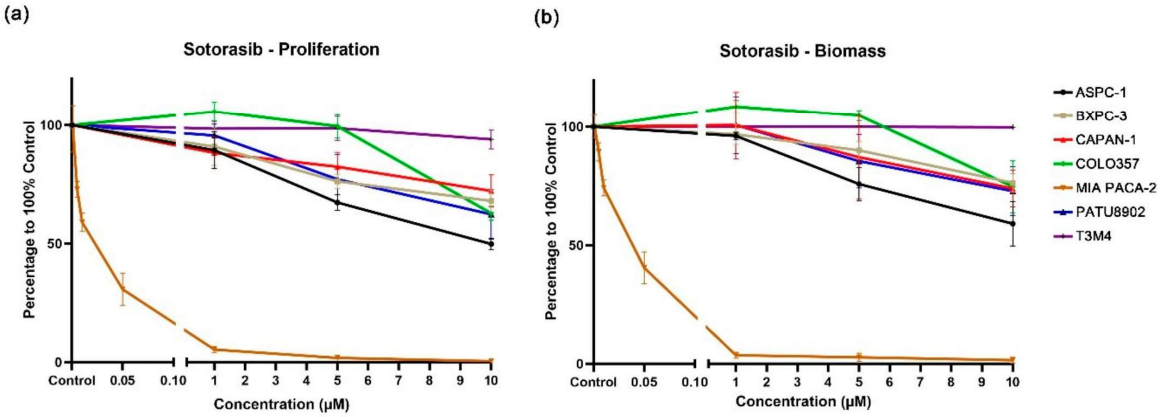

Figure 1. Proliferation (**a**) and biomass (**b**) changes in PDAC cell lines after exposure to different concentrations of sotorasib.

As expected, sotorasib showed a very strong inhibitory effect on MIA PACA-2, which carry a *KRAS* G12C mutation. A significant inhibitory effect can be observed at a concentration of 0.005 µM, while at 0.05 µM, cell proliferation and biomass were reduced by 69% and 60%, respectively (Figures 1 and S1, Supplementary Table S1).

Compared with the DMSO control group, the KRAS::SOS1 inhibitor BI-3406 demonstrated a weak inhibitory effect on PDAC cell lines carrying KRAS G12V (CAPAN-1 and PATU8902). At the highest test concentration of 10 µM, cell proliferation only decreased by 11% and 17%, and the biomass decreased by 12% and 21%, respectively (Supplementary Table S2). In addition, the inhibitory effect of BI-3406 on the cell proliferation and biomass of the KRAS wild-type cell line BXPC-3 is similar to the inhibition observed in the KRAS G12V cell lines. The cell proliferation and biomass of BXPC-3 were reduced by only 15% and

27% at the concentration of 10 µM. BI-3406 demonstrated an increased, but still limited, inhibitory effect on the cell lines carrying the other three KRAS mutations (ASPC-1 and COLO357, KRAS G12D; MIA PACA-2, *KRAS* G12C; T3M4, *KRAS* Q61H). At the highest tested concentration, cell proliferation and biomass were only reduced between 30 and 50% (Figures 2 and S2, Supplementary Table S2).

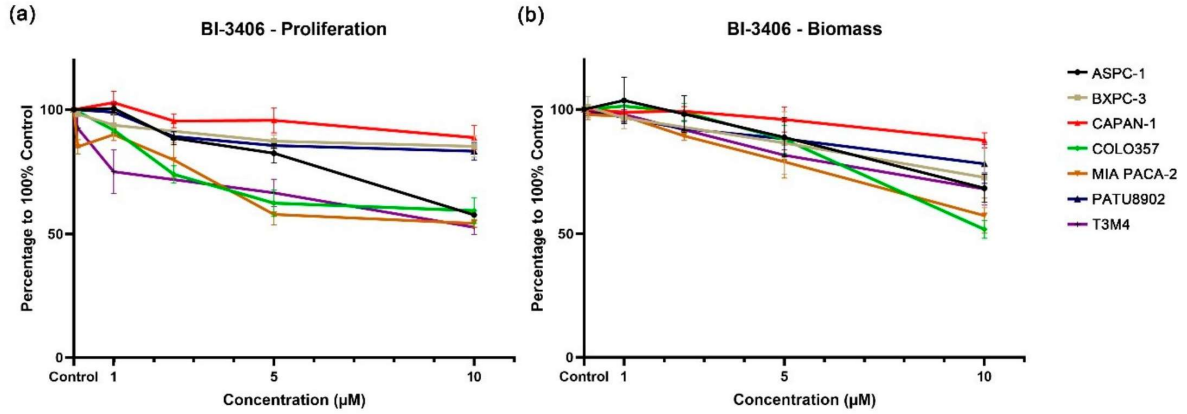

Figure 2. Proliferation (**a**) and biomass (**b**) changes in PDAC cell lines after exposure to different concentrations of BI-3406.

3.3. Combined Applications of KRAS, PI3K, and MEK1/2 Inhibitors Enhance Inhibition of PDAC Cell Lines

For BI-3406 in combination with trametinib and buparlisib, a significant increase in the inhibition of cell proliferation and biomass was observed when compared with the DMSO control group, regardless of whether double-inhibitor combinations or triple-inhibitor combinations were tested (Figure 3 and Supplementary Tables S3 and S4). When comparing the effect of the triple-inhibitor with the effects of the double-inhibitor, a significantly increased inhibition in cell proliferation can also be observed in ASPC-1, BXPC-3, and MIA PACA-2. In CAPAN-1, a significant increase was only observed when comparing the triple therapy with the combination of BI-3406 and buparlisib. As for the other two combinations (BI-3406 + trametinib, trametinib + buparlisib), no significant increase could be observed. Moreover, we also observed similar inhibitory effects in the biomass quantification assay.

For the combination of sotorasib with trametinib and buparlisib, significant inhibition of cell proliferation and biomass was observed in the triple combination compared to the DMSO control group (Figure 4 and Supplementary Tables S5 and S6). The addition of sotorasib significantly improved inhibition in ASPC-1 and MIA PACA-2 compared with a single application of trametinib or buparlisib. In addition, when focusing on the efficacy of the triple combination (sotorasib + trametinib + buparlisib) versus the double combination (trametinib + buparlisib), a significant increase in inhibitory effect was only observed in ASPC-1 and MIA PACA-2.

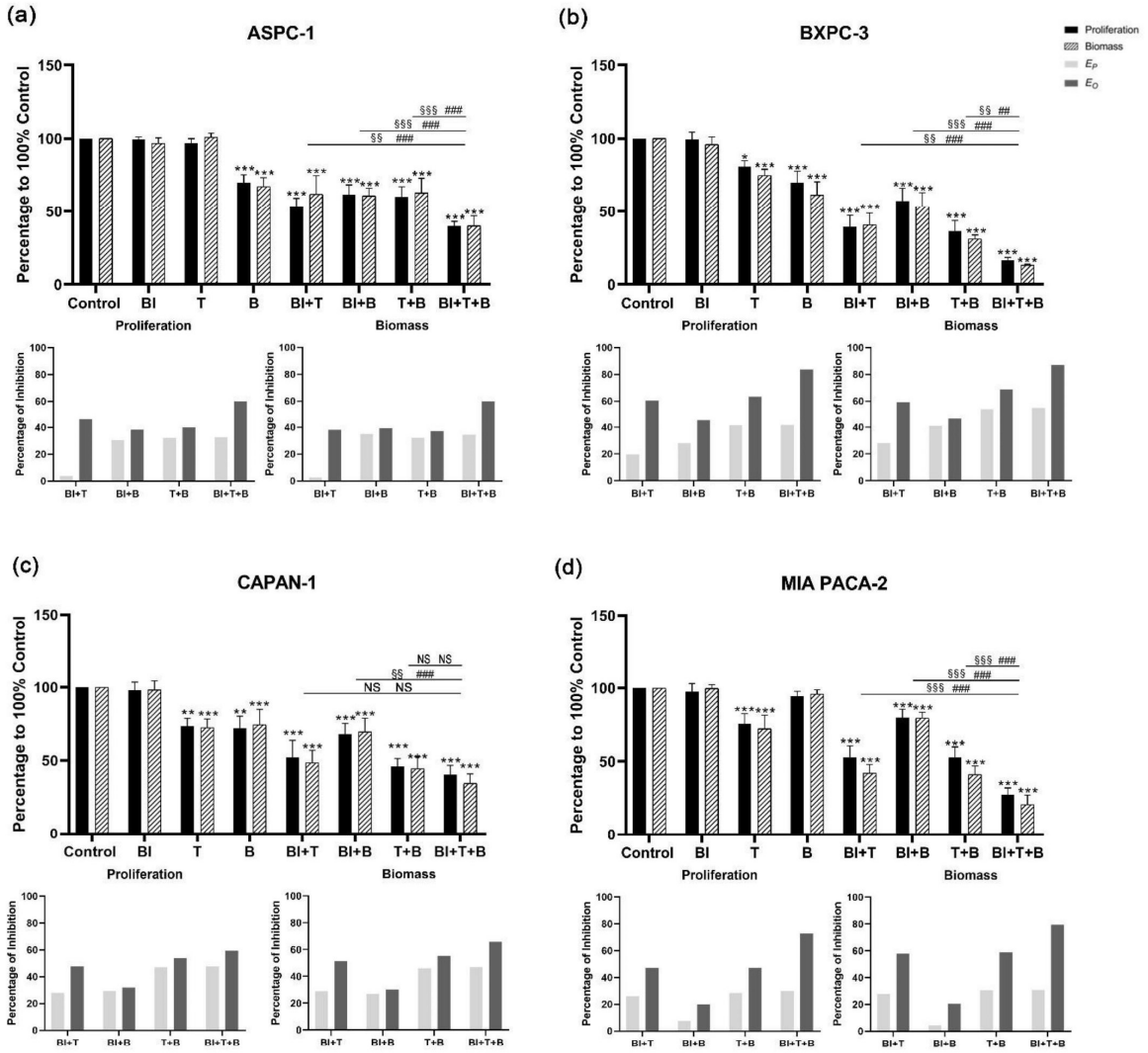

Figure 3. Cell proliferation and biomass of ASPC-1 (**a**), BXPC-3 (**b**), CAPAN-1 (**c**), and MIA PACA-2 (**d**) after 72 h BI-3406, trametinib, buparlisib or inhibitor combination exposure, as well as analysis of synergistic effect using Bliss independent model. Data are presented as mean ± SD. Significance of a treatment effect compared to the DMSO control was determined by one-way ANOVA and displayed as *: $p < 0.033$, **: $p < 0.002$, ***: $p < 0.001$ ($n \geq 3$). The significance of the treatment effect for double inhibition compared to triple inhibition was determined by one-way ANOVA and was shown as # (proliferation), § (biomass): $p < 0.033$; ##, §§: $p < 0.002$, ###; §§§: $p < 0.001$. BI: BI-3406; T: trametinib; B: buparlisib; NS: not significant; E_P: predicted inhibition by Bliss independent model; E_O: observed inhibition.

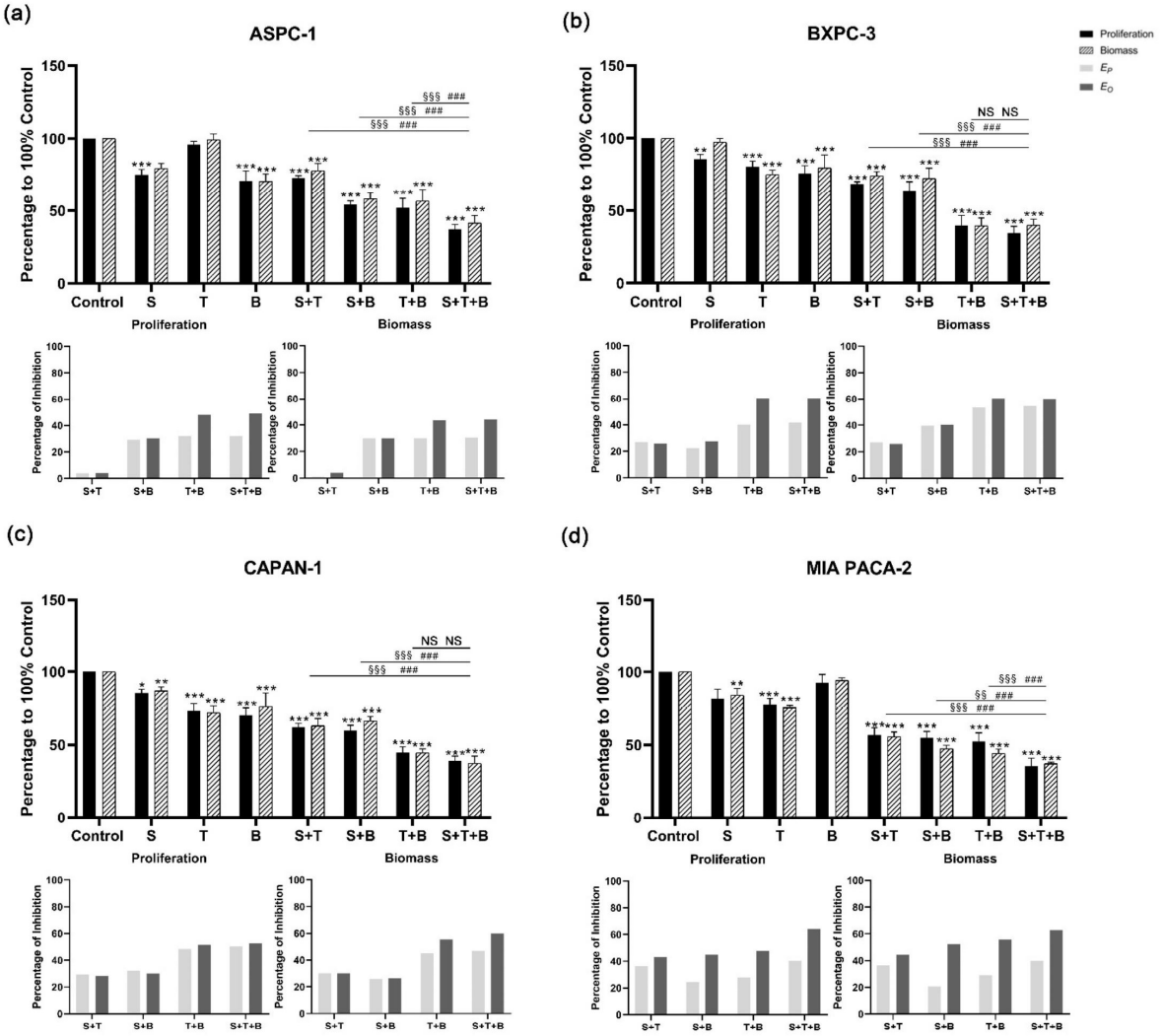

Figure 4. Cell proliferation and biomass of ASPC-1 (**a**), BXPC-3 (**b**), CAPAN-1 (**c**), and MIA PACA-2 (**d**) after 72 h sotorasib, trametinib, buparlisib or inhibitor combination exposure, as well as analysis of synergistic effect using Bliss independent model. Data are presented as mean ± SD. Significance of a treatment effect compared to the DMSO control was determined by one-way ANOVA and displayed as *: $p < 0.033$, **: $p < 0.002$, ***: $p < 0.001$ ($n \geq 3$). The significance of the treatment effect for double inhibition compared to triple inhibition was determined by one-way ANOVA and was shown as # (proliferation), § (biomass): $p < 0.033$; §§: $p < 0.002$, ###; §§§: $p < 0.001$. S: sotorasib; T: trametinib; B: buparlisib; NS: not significant; E_P: predicted inhibition by Bliss independent model; E_O: observed inhibition.

3.4. Bliss Analysis Revealed the Synergistic Effects of Double- and Triple-Application

The Bliss prediction effects were calculated based on the results of proliferation and biomass inhibition. For the BI-3406-based triple inhibitor combination, the Bliss predicted that inhibition (E_P) is lower than the observed inhibition results (E_O) in all cell lines (Figure 3). When focusing on comparing the double combination of trametinib + buparlisib and the triple combination of BI-3406 + trametinib + buparlisib, ASPC-1, BXPC-3, and MIA PACA-2 showed significantly higher inhibitory efficacy. However, this significant improvement did not appear in CAPAN-1, suggesting that BI-3406 was not able to enhance the inhibitory efficacy of trametinib + buparlisib in CAPAN-1. For the sotorasib-based triple inhibitor combination, E_P was observed to be lower than E_O in all cell lines. When focusing on comparing the double combination of trametinib + buparlisib and the triple combination of sotorasib + trametinib + buparlisib, only MIA PACA-2 demonstrated a significant improvement in inhibitory efficacy. Furthermore, in the other three cell lines, the inhibitory effects were not affected by the addition of sotorasib. These data indicated that the sotorasib-based triple inhibitor combination is synergistic in MIA PACA-2 cells that express the KRAS G12C mutant (using 0.005 µM sotorasib).

In the BI-3406-based double inhibitor combination, the combination of BI-3406 + trametinib demonstrated a significantly increased inhibitory effect in all four cell lines (Figure 3). The differences from E_O and E_P were between 20 and 43% (proliferation) and 23 and 36% (biomass) (Supplementary Table S4). The combination of BI-3406 + buparlisib also demonstrated a synergistic effect in all four cell lines; the differences between E_O and E_P were between 3 and 15% (proliferation) and 4 and 16% (biomass) (Supplementary Table S6). In addition, for sotorasib, either in combination with trametinib or in combination with buparlisib, synergistic effects were only observed in MIA PACA-2, with differences between E_O and E_P of 7%, 21% (proliferation) and 8%, 32% (biomass), respectively (Supplementary Figure S6). In the other cell lines that do not harbor the KRAS G12C variant, the difference between E_P and E_O was almost 0, suggesting that sotorasib does not act synergistically in these cell lines when combined with trametinib or buparlisib.

3.5. Combined Application of KRAS, PI3K, and MEK1/2 Inhibitors Induce Apoptosis and Necrosis of PDAC Cell Lines

Apoptosis/necrosis assays were performed on ASPC-1, BXPC-3, CAPAN-1, and MIA PACA-2 cells after exposure to BI-3406-based inhibitor combinations and MIA PACA-2 after exposure to sotorasib-based inhibitor combinations. Compared to the DMSO control group, Annexin V/propidium iodide (PI) double staining revealed a significant increase in induced apoptosis/necrosis, when using the triple-inhibitor combinations (Supplementary Figures S3 and S4, Supplementary Table S7). These triple-inhibitor combinations also significantly increased cell death when compared with all double-inhibitor combinations. In addition, most of the double-inhibitor combinations caused a significant increase in cell death when compared to the control group. Only in MIA PACA-2 cells, the combination of BI-3406 and buparlisib was not able to significantly increase cell death.

Furthermore, the microscopic evaluation at 100× magnification of Pappenheim stained samples indicated that the cells clearly demonstrated signs of cell death, including numerous vacuoles in the cytoplasm, splitting or breaking up of the nucleoli (karyorrhexis), protrusions of the plasma membrane, and apoptotic bodies, as well as morphological deformation (Figures 5 and S5). These morphological changes were also observed in the samples that have been exposed to the double inhibitor combinations. However, there was more evidence after the application of the triple inhibitor combination.

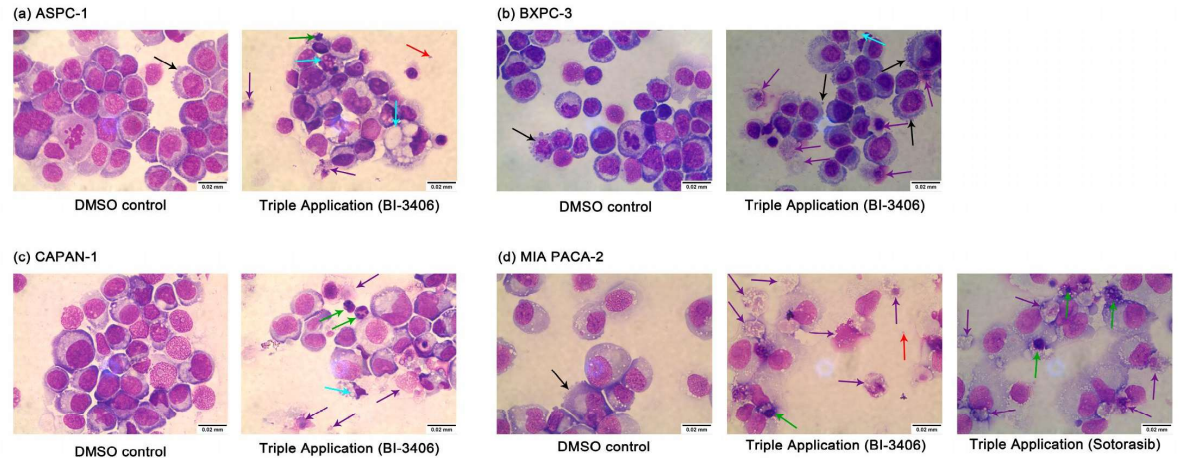

Figure 5. Morphology changes in ASPC-1 (**a**), BXPC-3 (**b**), CAPAN-1 (**c**), and MIA PACA-2 (**d**) after DMSO or triple inhibitor combination exposure. Magnification: 100×. ↑ membrane bubbles, membrane bound apoptotic body, ↑ vacuolization, ↑ apoptotic body, ↑ nuclear condensation/fragmentation; ↑ rupture of the plasma membrane.

3.6. Comparative Analysis of Differentially Expressed Genes (DEGs) between BI-3406 Combination-Treated and Non-Exposed PDAC Cell Lines

Differential expression analysis revealed several genes that were differentially regulated in triple combination-treated cells, when compared with the DMSO control exposed cells. For the combination of BI-3406 with trametinib and buparlisib, 587 DEGs were identified in ASPC-1 cells, 423 DEGs in BXPC-3 cells, 1191 DEGs in CAPAN-1 cells, and 1259 DEGs were identified in MIA PACA-2 cells (Supplementary Figures S6 and S7, Supplementary Table S8). Of these DEGs, only 12 DEGs were shared among all the tested PDAC cell lines (Figure 6a). In addition, in the top 25 up- and down-regulated genes identified in the 4 cell lines (Figure 6b), no gene was shared by all cell lines.

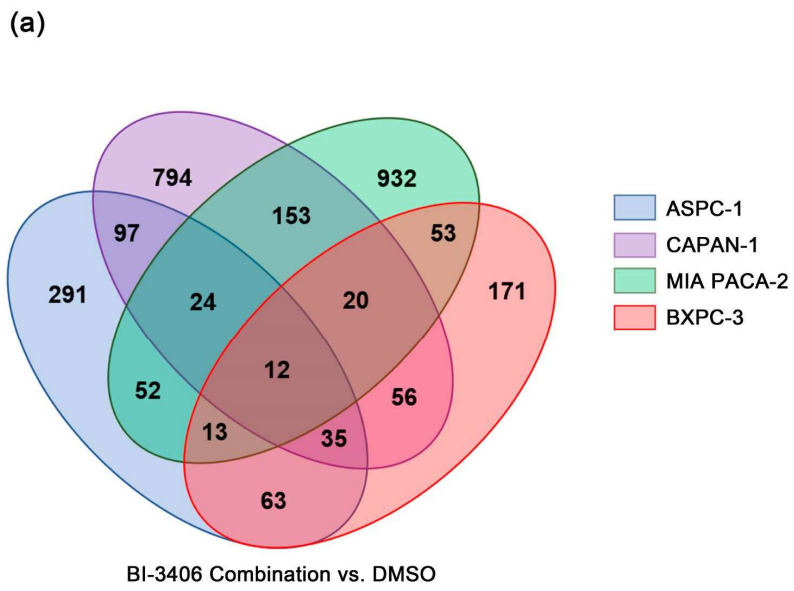

Figure 6. *Cont.*

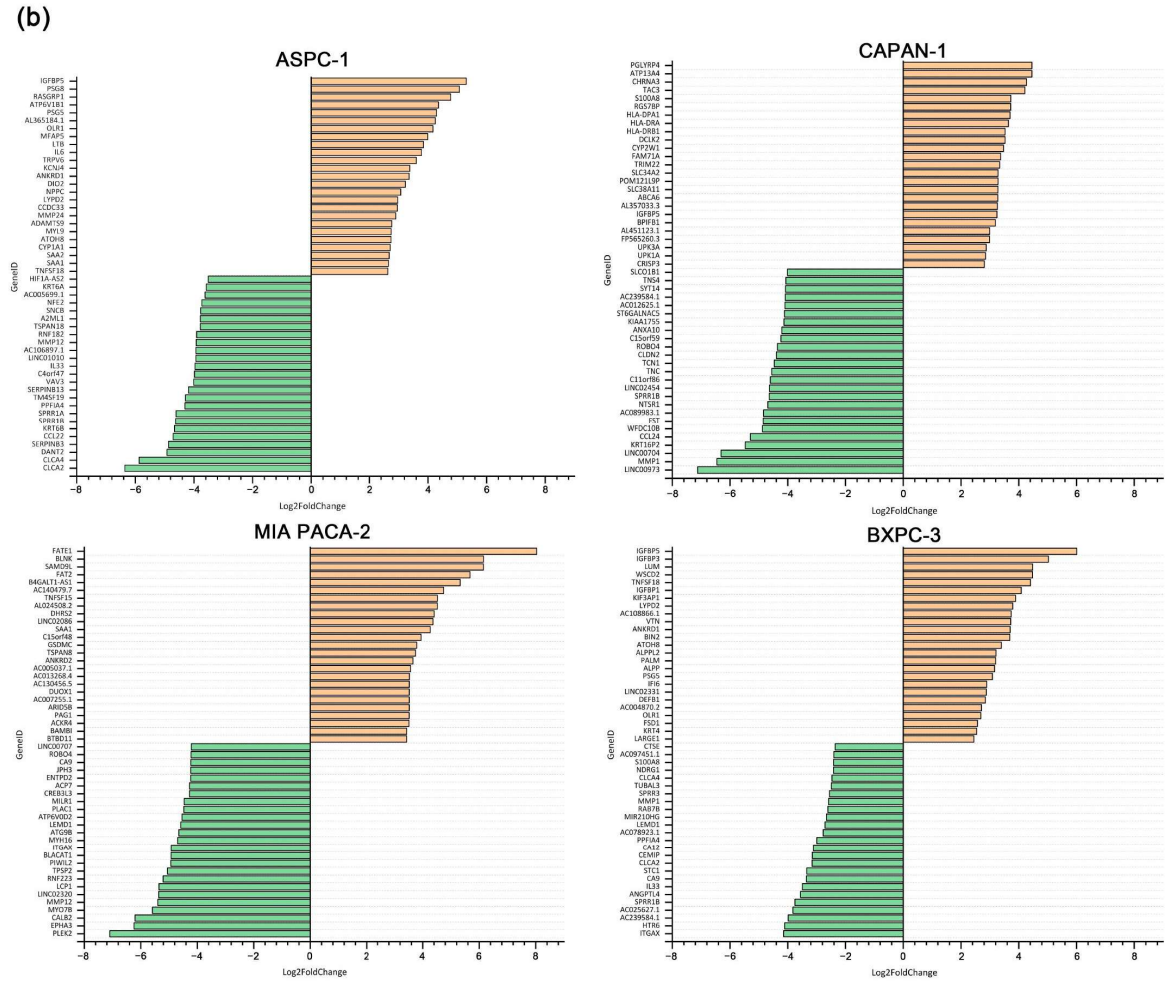

Figure 6. Number and overlap of DEGs in ASPC-1, BXPC-3, CAPAN-1 and MIA PACA-2 cell lines after exposure to BI-3406 combination (**a**) and the top 25 up- and down-regulated genes before and after BI-3406 combination exposure (**b**).

3.7. Comparative Analysis of DEG Changes Induced by BI-3406 Combination-Treated and Sotorasib Combination-Treated in MIA PACA-2 Cell Line

For the sotorasib triple combination, only MIA PACA-2 cells were analyzed. Compared to the DMSO control group, 928 DEGs were identified in MIA PACA-2 (Supplementary Figure S7, Supplementary Table S9). Comprehensive analysis of DEG changes in MIA PACA-2 using BI-3406 or sotorasib triple therapy revealed 778 DEGs that were up- or down-regulated by both inhibitor combinations (Figure 7a). In the top 25 up- and down-regulated genes, 17 overlapping up-regulated genes and 15 overlapping down-regulated genes were observed (Figure 7b).

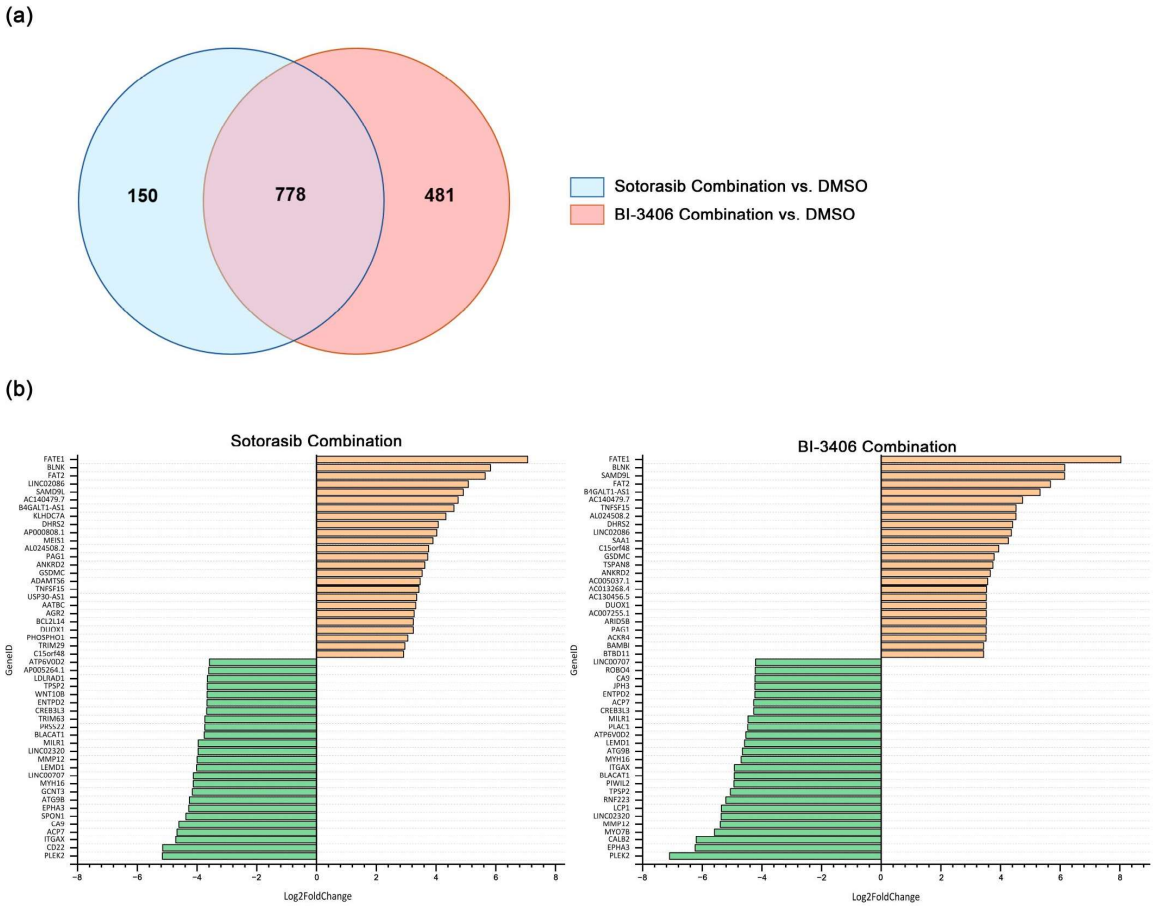

Figure 7. Number and overlap of DEGs in MIA PACA-2 cell lines after exposure to sotorasib combination or BI-3406 combination (**a**) and the top 25 up- and down-regulated genes before and after inhibitor combination exposure (**b**).

3.8. Functional and Pathway Enrichment Analysis of DEGs Induced by Combination-Treated PDAC Cell Lines

In order to assess the effect of inhibitor combinations on PDAC cell lines, GO and KEGG pathway analysis was performed on all of the DEGs selected in result 3.6 for each cell line.

For the BI-3406 triple inhibitor combination, GO and KEGG enrichment analysis demonstrated different results in different PDAC cell lines. The number of GO terms, including the biological process (BP), the cellular component (CC), and the molecular function (MF), as well as the number of KEGG pathways caused by BI-3406 triple inhibitor combination treatment, are displayed in Table 3. Detailed information is displayed in Supplementary Figures S7–S11 and Supplementary Tables S10 and S11.

Table 3. GO term and KEGG pathway enrichment analysis of DEGs induced by BI-3406 triple inhibitor combination treatment.

PDAC Cell Line	KRAS Mutation	GO Term			KEGG Pathway
		Biological Process	Cellular Components	Molecular Functions	
BXPC-3	Wild Type	847	49	96	24
ASPC-1	KRAS G12D	744	80	96	48
CAPAN-1	KRAS G12V	1447	116	168	59
MIA PACA-2	KRAS G12C	1053	76	120	66

Further analysis of the GO term function revealed that in the PDAC cell lines, DEGs were involved in regulating the immune system, cell adhesion, cell migration, localization, locomotion, and response to stimulus in biological process, cell membrane, and extracellular functions in cellular components, as well as cytokine binding in molecular functions. KEGG pathway enrichment analysis identified nine overlapping pathways, which were involved in cancer, cellular community, cardiovascular disease, and immune regulation and directly acting on PI3K/AKT and TNF pathways (Supplementary Table S11). Furthermore, the expected RAS signaling pathway was not observed to be affected in all of the tested cell lines. The KEGG pathway results revealed that the RAS pathway was affected in ASPC-1, BXPC-3, and MIA PACA-2, but not in CAPAN-1.

For the sotorasib combination, 928 DEGs in MIA PACA-2 were involved in 849 BP, 39 CC, and 63 MF; KEGG analysis revealed that DEGs were enriched in 58 pathways, which are mainly associated with cancer, signal transduction, and the immune system (Supplementary Figure S12 and Supplement Tables S12 and S13).

Comparing the GO terms and KEGG pathway enrichment analysis of MIA PACA-2 in the two inhibitor combinations did not reveal major differences. The GO term demonstrated that both inhibitor combinations were involved in similar cellular functions in MIA PACA-2. KEGG analysis revealed that both inhibitor combinations were involved in immune regulation, signal transduction (especially PI3K/AKT, TNF, and JAK-STAT signaling pathways), metabolic activity, and cancer pathways (especially proteoglycans in cancer). The BI-3406 triple combination additionally participated in the MAPK pathway; however, this effect was not observed in the sotorasib triple combination (Supplementary Tables S11 and S13).

4. Discussion

KRAS mutations are the most common mutations in PDAC patients and are characterized by poor prognosis and resistance to general treatment [6,14]. Although a series of targeted inhibitors have been developed for PDAC, so far, these inhibitors are still not routinely used in clinical treatment. In our study, sotorasib, which targets the *KRAS* G12C mutation, exhibited the expected inhibitory efficacy in MIA PACA-2, and significantly inhibited cell proliferation and biomass even at very low concentrations (0.005 μM). At the same time, sotorasib at 10 μM exhibited a partial inhibitory effect on other tested PDAC cell lines, except for T3M4 (KRAS Q61H). The cell proliferation and biomass decreased by 32–50% and 24–41%, respectively. However, in T3M4, minimal inhibition of cell proliferation and biomass was observed at all the concentrations tested. This may be due to the fact that the Q61H mutation has the lowest intrinsic GTPase activity and requires less upstream signaling to maintain a GTP-bound status [37]. In a previous report, the maximum plasma concentration of sotorasib was 7.5 μg/mL (13.4 μM) [38]. The results of this study demonstrated that sotorasib had inhibitory effects on KRAS G12D, G12V, and wild-type PDAC cell lines at a concentration of 10 μM, which can be achieved in clinical trials [38]. The incidence of serious adverse reactions at this concentration in clinical trials is low, suggesting that sotorasib can potentially become an interesting option for the development of novel approaches for the above-mentioned PDAC types [18,38]. Although sotorasib is currently only approved for the treatment of KRAS G12C-mutated NSCLC, the CodeBreaK100 study has confirmed its potential for the treatment of advanced KRAS G12C

mutated PDAC with low side effects. At the same time, the clinical trials demonstrated that the maximum plasma concentration is higher than 10 μM [18]. Combined with our findings, sotorasib may also have inhibitory effects on KRAS G12D and G12V mutated PDAC in vivo, suggesting that sotorasib may have further potential to treat KRAS wild type and other KRAS G12-mutated PDACs besides KRAS G12C.

Using the multi-KRAS mutation inhibitor BI-3406, our results were comparable to those previously reported in 2D cultures [26]. The biological response of cell lines carrying the KRAS G12V mutation (CAPAN-1 and PATU8902) was similar to that of the wild-type cell line BXPC-3, showing a decrease of only about 15% at 10 μM. In the cell lines carrying KRAS G12C and G12D mutations, the inhibition of cell proliferation and biomass at 10 μM concentration was higher than 30%, up to 48.18%. In the previously reported in vivo studies, the BI-3406 single-inhibitor demonstrated a good inhibitory effect on KRAS G12C-mutated MIA PACA-2 cells, and the tumor volume of the two different doses of the experimental group was significantly reduced compared with the control group. However, even at the highest dose, BI-3406 was only able to inhibit tumor growth, but could not reduce tumor volume below the baseline [26]. It is suggested that a single application of BI-3406 does not have a strong inhibitory effect on PDAC cell lines both in vivo and in vitro. Nonetheless, it demonstrated a distinct synergistic effect with downstream pathway inhibitors in combination inhibition, especially with the MEK1/2 inhibitor trametinib. The combination of BI-3406 and trametinib demonstrated a synergistic effect in both *KRAS*-mutated and wild-type PDAC cell lines, which is in agreement with previous reports, both confirming the synergistic effect of BI-3406 and trametinib [26]. This is probably because BI-3406 combined with trametinib can block the negative feedback regulatory mechanism by reducing phosphorylated (p)-MEK and p-ERK levels, resulting in a strong synergistic effect [26]. Since this regulatory mechanism exists both in *KRAS*-mutated and wild-type cell lines, this double-inhibitor combination was also effective in the BXPC-3 cells. For the combination of BI-3406 and buparlisib, a synergistic effect was only observed in MIA PACA-2. Since buparlisib does not reduce p-MEK and p-ERK levels, it is highly likely that it fails to activate the negative feedback loop, resulting in a small synergistic effect [26].

The double-inhibitor combination based on sotorasib also displayed a synergistic effect, but mainly in MIA PACA-2 cells. Since RAS directly forms a complex with PI3K to further activate the PI3K signaling pathway, inhibition of these two proteins greatly reduces the activation of this pathway and might explain the synergistic effect of these two inhibitors [39–42]. Additive effects were observed in ASPC-1, BXPC-3, and CAPAN-1 cells, indicating that sotorasib might target an unknown target protein at a high concentration and the inhibition of this target protein does not synergistically interact with inhibitors of MEK and PI3K.

The efficacy of the triple-inhibitor combination of BI-3406, trametinib, and buparlisib was significantly stronger than that of the double-inhibitor combination in ASPC-1, BXPC-3, and MIA PACA-2 cells. However, in CAPAN-1 cells, there was no significant improvement in the triple-inhibitor combination versus the double-inhibitor combination of buparlisib and trametinib. Moreover, the KEGG pathway enrichment analysis revealed that in CAPAN-1, the RAS pathway was not affected by the triple therapy, while the enrichment of DEGs in the RAS pathway was observed in the other three cell lines. In addition, a single application of BI-3406 did not significantly inhibit the proliferation and biomass of CAPAN-1. Although BI-3406 has previously been reported to achieve good inhibitory effects on KRAS G12V-mutated NSCLC cell lines, this antitumor effect appears to be poor for PDAC cell lines [26]. This suggests that in PDAC cell lines, BI-3406 is less able to block the interaction between KRAS G12V and SOS1, at least not causing changes at the gene expression level. This may account for the low response of the KRAS G12V cell lines to BI-3406 and the inability of the BI-3406 to enhance the efficacy of downstream inhibitors in CAPAN-1. Moreover, the triple inhibitor combination of sotorasib demonstrated only an additive effect in ASPC-1, BXPC-3 and CAPAN-1, further confirming that the inhibition

of non-KRAS G12C mutant cell lines by sotorasib is not affected by the changes in the RAS/RAF/MEK/ERK pathway or PI3K/AKT pathway.

The BI-3406 triple inhibitor combination modulated immunity, cell adhesion, migration, and targeted cancer pathways in all four cell lines. This indicates that this inhibitor combination can directly influence the pathophysiology of tumor cells, but might also indirectly inhibit the growth of PDAC cells by modulating the immune system, as well as cell-to-cell interactions. Furthermore, we observed that in all four cell lines, both triple inhibitor combinations regulated DEGs, which are involved in the response to hypoxia. These genes (*ALDOA*, *IL6*, *IL6R*, *EGF*, *VEFG*, *PDK-1*, *ENO1*, etc.) were all associated with the hypoxia inducible factor-1 (HIF-1) pathway, suggesting that both combinations can act on the HIF-1 pathway. Several studies have shown that HIF-1 is associated with tumor growth in a variety of cancers, including PDAC [43]. Inhibition of mTOR blocks the translation of HIF-1 mRNA, and inhibition of ERK can also lead to inhibition of HIF-1 [44,45]. The combination of the two inhibitors in this experiment affected both mTOR and ERK, leading to changes in the downstream HIF-1 pathway, which seems to be another mechanism of this inhibitor combination.

Altogether, our current study demonstrates the antiproliferative effects of KRAS inhibitors alone or in combination with downstream inhibitors in PDAC cell lines in vitro. Moreover, the dose of each inhibitor was greatly reduced when used in combination, thereby reducing the side effects of the inhibitor. The KRAS::SOS1 inhibitor BI-3406 was able to enhance the antiproliferative effect of downstream inhibitors in the KRAS wild-type, KRAS G12C, and KRAS G12D mutant cell lines, but not for the KRAS G12V mutant cell lines. The KRAS G12C inhibitor sotorasib mainly enhanced the anti-proliferative effect of downstream inhibitors in KRAS G12C mutant cell lines.

5. Conclusions

Our current study demonstrates the effects of two KRAS inhibitors, BI-3406 and sotorasib, as monotherapy for PDAC. This provides evidence for a potential extended application of sotorasib in non-KRAS G12C mutated PDAC and the application of BI-3406 as a multi-KRAS mutated inhibitor in PDAC. In addition, these two KRAS inhibitors act synergistically or additively with downstream pathway inhibitors, when reducing cell proliferation and biomass in PDAC cell lines with different *KRAS* statuses. The two triple combinations also demonstrated extraordinary effects in enhancing inhibitor efficacy and reducing inhibitor dose. These data emphasize the importance of KRAS as a therapeutic target for PDAC and validate two different mechanisms of KRAS inhibition and its interaction with downstream pathway inhibitors. The current study provides novel ideas for the drug treatment of PDAC; however, in vivo experiments and clinical trials are still needed to observe the real efficacy and adverse reactions of these inhibitors and inhibitor combinations for the treatment of PDAC.

Supplementary Materials: The following supporting information can be downloaded at: https://www.mdpi.com/article/10.3390/cancers14184467/s1, Figure S1: Cell Viability after 72 Hours Sotorasib Exposure in PDAC Cell Lines; Figure S2: Cell Viability after 72 Hours BI-3406 Exposure in PDAC Cell Lines; Figure S3: PDAC Cell Death Induction after 72 Hours BI-3406, Sotorasib, Trametinib, Buparlisib or Inhibitors Combination Exposure; Figure S4: Apoptosis/necrosis Dot Plot of PDAC Cell Lines after 72 Hours BI-3406, Trametinib, Buparlisib and Inhibitor Combination Exposure; Figure S5: Morphology Changes of PDAC Cell Lines after 72 Hours BI-3406, Sotorasib, Trametinib, Buparlisib and Inhibitor combination exposure; Figure S6: DEGs after PDAC Cell Lines Exposed to the Combination of BI-3401, Trametinib and Buparlisib; Figure S7: DEGs after MIA PACA-2 Exposed to the Combination of BI-3401, Trametinib and Buparlisib or Sotorasib, Trametinib and Buparlisib; Figure S8: GO and KEGG Enrichment Analysis of ASPC-1 after BI-3406+Trametinib+Buparlisib Exposure; Figure S9: GO and KEGG Enrichment Analysis of BXPC-3 after BI-3406+Trametinib+Buparlisib Exposure; Figure S10: GO and KEGG Enrichment Analysis of CAPAN-1 after BI-3406+Trametinib+Buparlisib Exposure; Figure S11: GO and KEGG Enrichment Analysis of MIA PACA-2 after BI-3406+Trametinib+Buparlisib Exposure; Figure S12: GO and KEGG

Enrichment Analysis of MIA PACA-2 after Sotorasib + Trametinib + Buparlisib Exposure. Table S1: Cell Viability Sotorasib; Table S2: Cell Viability BI-3406; Table S3: Combination Inhibition (BI-3406 + Trametinib + Buparlisib); Table S4: Bliss Independent Model (BI-3406 + Trametinib + Buparlisib); Table S5: Combination Inhibition (Sotorasib + Trametinib + Buparlisib); Table S6: Bliss Independent Model (Sotorasib + Trametinib + Buparlisib); Table S7: Combination Cell Death; Table S8: DEGs of PDAC Cell Lines after Exposure to the Combination of BI-3406, Trametinib and Buparlisib; Table S9: DEGs of MIA PACA-2 after Exposure to the Combination of Sotorasib, Trametinib and Buparlisib; Table S10: GO Enrichment Analysis after PDAC Cell Lines Exposure to the Combination of BI-3406, Trametinib and Buparlisib; Table S11: KEGG Pathway Enrichment Analysis after PDAC Cell Lines Exposure to the Combination of BI-3406, Trametinib and Buparlisib; Table S12: GO Enrichment Analysis after MIA PACA-2 Exposure to the Combination of Sotorasib, Trametinib and Buparlisib; Table S13: KEGG Pathway Enrichment Analysis after MIA PACA-2 Exposure to the Combination of Sotorasib, Trametinib and Buparlisib; Table S14: Cell Viability Trametinib.

Author Contributions: Conceptualization, B.S., C.J. and H.M.E.; Data curation, Y.M.; Formal analysis, Y.M., M.A.A. and S.S.; Funding acquisition, C.J. and H.M.E.; Investigation, Y.M., M.A.A. and A.S.; Methodology, Y.M., N.T., M.A.A. and A.S.; Project administration, H.M.E.; Resources, F.U.W., M.M.L. and R.J.; Software, Y.M., N.T. and F.H.; Supervision, C.J. and H.M.E.; Validation, Y.M., N.T. and H.M.E.; Writing—original draft, Y.M.; Writing—review and editing, S.S., D.Z., F.U.W., R.J. and H.M.E. All authors have read and agreed to the published version of the manuscript.

Funding: This research was funded by the PiCoP project (funded by European Community, Europäischer Fonds für regionale Entwicklung (EFRE), grant TBI-V-1-241-VBW-084/State Mecklenburg-Western-Pomerania, Germany).

Institutional Review Board Statement: Not applicable.

Informed Consent Statement: Not applicable.

Data Availability Statement: The data supporting the reported results can be found on the website in detail in the article.

Acknowledgments: The authors gratefully acknowledge the PiCoP project (funded by European Community, Europäischer Fonds für regionale Entwicklung (EFRE), grant TBI-V-1-241-VBW-084/state Mecklenburg. Western Pomerania, Germany) for supporting this research. We would like to appreciate Patrick Brennan (Department of Medicine Clinic III, Hematology, Oncology and Palliative Medicine, Rostock University Medical Center, Germany) for his contribution to the improvement of English language and style.

Conflicts of Interest: The authors declare no conflict of interest.

Abbreviations

A	Alanine
AKT	Protein kinase B
BP	Biological process
BRCA3	Breast cancer 3
C	Cysteine
CC	Cellular components
CDKN2A	Cyclin dependent kinase inhibitor 2A
CV	Crystal violet
D	Aspartic acid
DEG	Differentially expressed gene
DMSO	Dimethyl sulfoxide
E_O	Observed inhibition
E_P	Bliss predicted inhibition
ERK	Extracellular signal-regulated kinase
FCS	Fetal calf serum
G	Glycine

GDP	Guanosine diphosphate
GO	Gene Ontology
GRC2	Cytosolic glutathione reductase
GSEA	Gene set enrichment analysis
GTP	Guanosine triphosphate
H	Histidine
HIF-1	Hypoxia inducible factor-1
KEGG	Kyoto Encyclopedia of Genes and Genomes
KRAS	Kirsten rat sarcoma virus
MEK	Mitogen-activated protein kinase kinase
MF	Molecular function
mTOR	Mammalian target of rapamycin
NSCLC	Non-small cell lung cancer
P-	Phosphorylated-
P/S	Penicillin-streptomycin solution
PDAC	Pancreatic ductal adenocarcinoma
PI	Propidium iodide
PI3K	Phosphoinositide 3-kinase
Q	Glutamine
RAS	Rat sarcoma virus
RIN	RNA integrity number
SD	Standard deviation
SMAD4	Mothers against decapentaplegic homolog 4
SOS1	Son of sevenless 1
TP53	Tumor protein P53
V	Valine

References

1. Jones, S.; Zhang, X.; Parsons, D.W.; Lin, J.C.; Leary, R.J.; Angenendt, P.; Mankoo, P.; Carter, H.; Kamiyama, H.; Jimeno, A.; et al. Core signaling pathways in human pancreatic cancers revealed by global genomic analyses. *Science* **2008**, *321*, 1801–1806. [CrossRef]
2. Campbell, P.J.; Yachida, S.; Mudie, L.J.; Stephens, P.J.; Pleasance, E.D.; Stebbings, L.A.; Morsberger, L.A.; Latimer, C.; McLaren, S.; Lin, M.L.; et al. The patterns and dynamics of genomic instability in metastatic pancreatic cancer. *Nature* **2010**, *467*, 1109–1113. [CrossRef] [PubMed]
3. Biankin, A.V.; Waddell, N.; Kassahn, K.S.; Gingras, M.C.; Muthuswamy, L.B.; Johns, A.L.; Miller, D.K.; Wilson, P.J.; Patch, A.M.; Wu, J.; et al. Pancreatic cancer genomes reveal aberrations in axon guidance pathway genes. *Nature* **2012**, *491*, 399–405. [CrossRef] [PubMed]
4. Waddell, N.; Pajic, M.; Patch, A.M.; Chang, D.K.; Kassahn, K.S.; Bailey, P.; Johns, A.L.; Miller, D.; Nones, K.; Quek, K.; et al. Whole genomes redefine the mutational landscape of pancreatic cancer. *Nature* **2015**, *518*, 495–501. [CrossRef] [PubMed]
5. Witkiewicz, A.K.; McMillan, E.A.; Balaji, U.; Baek, G.; Lin, W.C.; Mansour, J.; Mollaee, M.; Wagner, K.U.; Koduru, P.; Yopp, A.; et al. Whole-exome sequencing of pancreatic cancer defines genetic diversity and therapeutic targets. *Nat. Commun.* **2015**, *6*, 6744. [CrossRef]
6. Bailey, P.; Chang, D.K.; Nones, K.; Johns, A.L.; Patch, A.M.; Gingras, M.C.; Miller, D.K.; Christ, A.N.; Bruxner, T.J.; Quinn, M.C.; et al. Genomic analyses identify molecular subtypes of pancreatic cancer. *Nature* **2016**, *531*, 47–52. [CrossRef]
7. Simanshu, D.K.; Nissley, D.V.; McCormick, F. RAS Proteins and Their Regulators in Human Disease. *Cell* **2017**, *170*, 17–33. [CrossRef]
8. Di Magliano, M.P.; Logsdon, C.D. Roles for KRAS in pancreatic tumor development and progression. *Gastroenterology* **2013**, *144*, 1220–1229. [CrossRef]
9. Hingorani, S.R.; Wang, L.; Multani, A.S.; Combs, C.; Deramaudt, T.B.; Hruban, R.H.; Rustgi, A.K.; Chang, S.; Tuveson, D.A. Trp53R172H and KrasG12D cooperate to promote chromosomal instability and widely metastatic pancreatic ductal adenocarcinoma in mice. *Cancer Cell* **2005**, *7*, 469–483. [CrossRef]
10. Bardeesy, N.; Cheng, K.H.; Berger, J.H.; Chu, G.C.; Pahler, J.; Olson, P.; Hezel, A.F.; Horner, J.; Lauwers, G.Y.; Hanahan, D.; et al. Smad4 is dispensable for normal pancreas development yet critical in progression and tumor biology of pancreas cancer. *Genes Dev.* **2006**, *20*, 3130–3146. [CrossRef]
11. Bardeesy, N.; Aguirre, A.J.; Chu, G.C.; Cheng, K.H.; Lopez, L.V.; Hezel, A.F.; Feng, B.; Brennan, C.; Weissleder, R.; Mahmood, U.; et al. Both p16(Ink4a) and the p19(Arf)-p53 pathway constrain progression of pancreatic adenocarcinoma in the mouse. *Proc. Natl. Acad. Sci. USA* **2006**, *103*, 5947–5952. [CrossRef] [PubMed]

12. Aguirre, A.J.; Bardeesy, N.; Sinha, M.; Lopez, L.; Tuveson, D.A.; Horner, J.; Redston, M.S.; DePinho, R.A. Activated Kras and Ink4a/Arf deficiency cooperate to produce metastatic pancreatic ductal adenocarcinoma. *Genes Dev.* **2003**, *17*, 3112–3126. [CrossRef] [PubMed]
13. Guerra, C.; Barbacid, M. Genetically engineered mouse models of pancreatic adenocarcinoma. *Mol. Oncol.* **2013**, *7*, 232–247. [CrossRef] [PubMed]
14. Bournet, B.; Buscail, C.; Muscari, F.; Cordelier, P.; Buscail, L. Targeting KRAS for diagnosis, prognosis, and treatment of pancreatic cancer: Hopes and realities. *Eur. J. Cancer* **2016**, *54*, 75–83. [CrossRef]
15. Zhao, H.; Wu, S.; Li, H.; Duan, Q.; Zhang, Z.; Shen, Q.; Wang, C.; Yin, T. ROS/KRAS/AMPK Signaling Contributes to Gemcitabine-Induced Stem-like Cell Properties in Pancreatic Cancer. *Mol. Oncolytics* **2019**, *14*, 299–312. [CrossRef]
16. Kawesha, A.; Ghaneh, P.; Andren-Sandberg, A.; Ograed, D.; Skar, R.; Dawiskiba, S.; Evans, J.D.; Campbell, F.; Lemoine, N.; Neoptolemos, J.P. K-ras oncogene subtype mutations are associated with survival but not expression of p53, p16(INK4A), p21(WAF-1), cyclin D1, erbB-2 and erbB-3 in resected pancreatic ductal adenocarcinoma. *Int. J. Cancer* **2000**, *89*, 469–474. [CrossRef]
17. Canon, J.; Rex, K.; Saiki, A.Y.; Mohr, C.; Cooke, K.; Bagal, D.; Gaida, K.; Holt, T.; Knutson, C.G.; Koppada, N.; et al. The clinical KRAS(G12C) inhibitor AMG 510 drives anti-tumour immunity. *Nature* **2019**, *575*, 217–223. [CrossRef]
18. Strickler, J.H.; Satake, H.; Hollebecque, A.; Sunakawa, Y.; Tomasini, P.; Bajor, D.L.; Schuler, M.H.; Yaeger, R.; George, T.J.; Garrido-Laguna, I.; et al. First data for sotorasib in patients with pancreatic cancer with KRAS p.G12C mutation: A phase I/II study evaluating efficacy and safety. *J. Clin. Oncol.* **2022**, *40*, 360490. [CrossRef]
19. ClinicalTrials.gov. Available online: https://www.clinicaltrials.gov/ (accessed on 25 August 2022).
20. Nagasaka, M.; Li, Y.; Sukari, A.; Ou, S.I.; Al-Hallak, M.N.; Azmi, A.S. KRAS G12C Game of Thrones, which direct KRAS inhibitor will claim the iron throne? *Cancer Treat Rev.* **2020**, *84*, 101974. [CrossRef]
21. Hallin, J.; Engstrom, L.D.; Hargis, L.; Calinisan, A.; Aranda, R.; Briere, D.M.; Sudhakar, N.; Bowcut, V.; Baer, B.R.; Ballard, J.A.; et al. The KRAS(G12C) Inhibitor MRTX849 Provides Insight toward Therapeutic Susceptibility of KRAS-Mutant Cancers in Mouse Models and Patients. *Cancer Discov.* **2020**, *10*, 54–71. [CrossRef]
22. Gao, J.; Aksoy, B.A.; Dogrusoz, U.; Dresdner, G.; Gross, B.; Sumer, S.O.; Sun, Y.; Jacobsen, A.; Sinha, R.; Larsson, E.; et al. Integrative analysis of complex cancer genomics and clinical profiles using the cBioPortal. *Sci. Signal.* **2013**, *6*, 1. [CrossRef] [PubMed]
23. Cherniack, A.D.; Klarlund, J.K.; Conway, B.R.; Czech, M.P. Disassembly of Son-of-sevenless proteins from Grb2 during p21ras desensitization by insulin. *J. Biol. Chem.* **1995**, *270*, 1485–1488. [CrossRef] [PubMed]
24. Waters, S.B.; Yamauchi, K.; Pessin, J.E. Insulin-stimulated disassociation of the SOS-Grb2 complex. *Mol. Cell. Biol.* **1995**, *15*, 2791–2799. [CrossRef] [PubMed]
25. Jeng, H.H.; Taylor, L.J.; Bar-Sagi, D. Sos-mediated cross-activation of wild-type Ras by oncogenic Ras is essential for tumorigenesis. *Nat. Commun.* **2012**, *3*, 1168. [CrossRef] [PubMed]
26. Hofmann, M.H.; Gmachl, M.; Ramharter, J.; Savarese, F.; Gerlach, D.; Marszalek, J.R.; Sanderson, M.P.; Kessler, D.; Trapani, F.; Arnhof, H.; et al. BI-3406, a Potent and Selective SOS1-KRAS Interaction Inhibitor, Is Effective in KRAS-Driven Cancers through Combined MEK Inhibition. *Cancer Discov.* **2021**, *11*, 142–157. [CrossRef]
27. Ma, Y.; Sender, S.; Sekora, A.; Kong, W.; Bauer, P.; Ameziane, N.; Al-Ali, R.; Krake, S.; Radefeldt, M.; Weiss, F.U.; et al. The Inhibitory Response to PI3K/AKT Pathway Inhibitors MK-2206 and Buparlisib Is Related to Genetic Differences in Pancreatic Ductal Adenocarcinoma Cell Lines. *Int. J. Mol. Sci.* **2022**, *23*, 4295. [CrossRef]
28. Goldoni, M.; Johansson, C. A mathematical approach to study combined effects of toxicants in vitro: Evaluation of the Bliss independence criterion and the Loewe additivity model. *Toxicol. Vitr.* **2007**, *21*, 759–769. [CrossRef]
29. Babraham Bioinformatics. Available online: http://www.bioinformatics.babraham.ac.uk/ (accessed on 1 May 2022).
30. Kim, D.; Paggi, J.M.; Park, C.; Bennett, C.; Salzberg, S.L. Graph-based genome alignment and genotyping with HISAT2 and HISAT-genotype. *Nat. Biotechnol.* **2019**, *37*, 907–915. [CrossRef]
31. Anders, S.; Pyl, P.T.; Huber, W. HTSeq—A Python framework to work with high-throughput sequencing data. *Bioinformatics* **2015**, *31*, 166–169. [CrossRef]
32. Love, M.I.; Huber, W.; Anders, S. Moderated estimation of fold change and dispersion for RNA-seq data with DESeq2. *Genome Biol.* **2014**, *15*, 550. [CrossRef]
33. Mootha, V.K.; Lindgren, C.M.; Eriksson, K.F.; Subramanian, A.; Sihag, S.; Lehar, J.; Puigserver, P.; Carlsson, E.; Ridderstrale, M.; Laurila, E.; et al. PGC-1alpha-responsive genes involved in oxidative phosphorylation are coordinately downregulated in human diabetes. *Nat. Genet.* **2003**, *34*, 267–273. [CrossRef] [PubMed]
34. Subramanian, A.; Tamayo, P.; Mootha, V.K.; Mukherjee, S.; Ebert, B.L.; Gillette, M.A.; Paulovich, A.; Pomeroy, S.L.; Golub, T.R.; Lander, E.S.; et al. Gene set enrichment analysis: A knowledge-based approach for interpreting genome-wide expression profiles. *Proc. Natl. Acad. Sci. USA* **2005**, *102*, 15545–15550. [CrossRef] [PubMed]
35. Luo, W.; Brouwer, C. Pathview: An R/Bioconductor package for pathway-based data integration and visualization. *Bioinformatics* **2013**, *29*, 1830–1831. [CrossRef] [PubMed]
36. Wu, T.; Hu, E.; Xu, S.; Chen, M.; Guo, P.; Dai, Z.; Feng, T.; Zhou, L.; Tang, W.; Zhan, L.; et al. clusterProfiler 4.0: A universal enrichment tool for interpreting omics data. *Innovation* **2021**, *2*, 100141. [CrossRef]

37. Hunter, J.C.; Manandhar, A.; Carrasco, M.A.; Gurbani, D.; Gondi, S.; Westover, K.D. Biochemical and Structural Analysis of Common Cancer-Associated KRAS Mutations. *Mol. Cancer Res.* **2015**, *13*, 1325–1335. [CrossRef]
38. Hong, D.S.; Fakih, M.G.; Strickler, J.H.; Desai, J.; Durm, G.A.; Shapiro, G.I.; Falchook, G.S.; Price, T.J.; Sacher, A.; Denlinger, C.S.; et al. KRAS(G12C) Inhibition with Sotorasib in Advanced Solid Tumors. *N. Engl. J. Med.* **2020**, *383*, 1207–1217. [CrossRef]
39. Rodriguez-Viciana, P.; Warne, P.H.; Dhand, R.; Vanhaesebroeck, B.; Gout, I.; Fry, M.J.; Waterfield, M.D.; Downward, J. Phosphatidylinositol-3-OH kinase as a direct target of Ras. *Nature* **1994**, *370*, 527–532. [CrossRef]
40. Rodriguez-Viciana, P.; Warne, P.H.; Vanhaesebroeck, B.; Waterfield, M.D.; Downward, J. Activation of phosphoinositide 3-kinase by interaction with Ras and by point mutation. *EMBO J.* **1996**, *15*, 2442–2451. [CrossRef]
41. Rubio, I.; Rodriguez-Viciana, P.; Downward, J.; Wetzker, R. Interaction of Ras with phosphoinositide 3-kinase gamma. *Biochem. J.* **1997**, *326 Pt 3*, 891–895. [CrossRef]
42. Vanhaesebroeck, B.; Welham, M.J.; Kotani, K.; Stein, R.; Warne, P.H.; Zvelebil, M.J.; Higashi, K.; Volinia, S.; Downward, J.; Waterfield, M.D. P110delta, a novel phosphoinositide 3-kinase in leukocytes. *Proc. Natl. Acad. Sci. USA* **1997**, *94*, 4330–4335. [CrossRef]
43. Semenza, G.L. Defining the role of hypoxia-inducible factor 1 in cancer biology and therapeutics. *Oncogene* **2010**, *29*, 625–634. [CrossRef] [PubMed]
44. Laughner, E.; Taghavi, P.; Chiles, K.; Mahon, P.C.; Semenza, G.L. HER2 (neu) signaling increases the rate of hypoxia-inducible factor 1alpha (HIF-1alpha) synthesis: Novel mechanism for HIF-1-mediated vascular endothelial growth factor expression. *Mol. Cell. Biol.* **2001**, *21*, 3995–4004. [CrossRef] [PubMed]
45. Pages, G.; Pouyssegur, J. Transcriptional regulation of the Vascular Endothelial Growth Factor gene—A concert of activating factors. *Cardiovasc. Res.* **2005**, *65*, 564–573. [CrossRef] [PubMed]

8.3 Curriculum Vitae

Personal Details

Name:	Ma, Yixuan
Gender:	Male
Date of Birth:	24 June 1991
Place of Birth:	Zhumadian, Henan, China

Education

Since Oct. 2018	**Doctor** Department of Medicine Clinic III, Hematology, Oncology and Palliative Medicine, Rostock University Medical Center, Rostock, Germany Working group: PD Dr. rer. nat. Hugo Murua Escobar Clinical management: Prof. Dr. med. Christian Junghanß
Sep. 2015 - Jul. 2017	**Master's Study** Zhengzhou University, Zhengzhou, Henan, China Master of Clinical Medicine Topic of the master thesis: "Relationship Between White Blood Cell Count and the Prognosis of Patients with Chronic Myelogenous Leukaemia" Department of Hematology, Henan Cancer Hospital, Zhengzhou, China Working group & clinical management: Prof. Dr. Xudong Wei
Sep. 2010 - Jul. 2015	**Bachelor's Study** Zhengzhou University, Zhengzhou, Henan, China Bachelor of Clinical Medicine

8.4 Publication as Co-Author

1. Kong, W.; Sender, S.; Taher, L.; Villa-Perez, S.; **Ma, Y.**; Sekora, A.; Ruetgen, B.C.; Brenig, B.; Beck, J.; Schuetz, E.; Junghanss, C.; Nolte, I.; Murua Escobar, H. BTK and PI3K Inhibitors Reveal Synergistic Inhibitory Anti-Tumoral Effects in Canine Diffuse Large B-Cell Lymphoma Cells. *Int. J. Mol. Sci.* **2021**, 22, 12673.

8.5 Posters

1. Kong. W., Sender S., Sekora A., **Ma Y.**, Rütgen B., Nolte I., Taher L., Brenig B., Beck J., Schuetz E., Junghanss C., Murua Escobar H.. Combined inhibition of BTK and PI3K acts synergistically in a canine B-cell lymphoma in vitro model. Oncol Res Treat 2019;42(suppl.4)1-336. P428. Presented at the Annual Meeting of the German Society for

Hematology and Medical Oncology 2019

2. **Ma Y.**, Sender S., Sekora A., Bauer P., Krake S., Radefeld M., Lerch M., Weiss F.W., Junghanss C., Murua Escobar H.. Evaluation of PI3K/AKT and CDK pathway inhibitors MK-2206, Buparlisib, Silmitasertib, and Dinaciclib in eleven pancreatic cancer cell lines. Oncol Res Treat 2020; 43 (suppl 4): 248, P554. Presented at the Annual Meeting of the German Society for Hematology and Medical Oncology 2020.
3. Kong W., Sender S., Villa Perez S., Sekora A., **Ma Y.**, Rütgen B., Nolte I., Junghanß C., Murua Escobar H.. Comparative analyses of pan- and isoform-specific BET inhibition and evaluation of synergistic potential by SYK inhibitor addition in a canine DLBCL in vitro model. Oncol Res Treat 2020;43(suppl 4):1-288. 495. Presented at the Annual Meeting of the German Society for Hematology and Medical Oncology 2020.
4. **Ma Y.**, Sender S., Sekora A., Kong W., Bauer P., Krake S., Ameziane N., Radefeld M., Weiss F.U., Lerch M., Junghanss C., Murua Escobar H.. Evaluation of pathway specific inhibitors MK-2206, Buparlisib, Silmitasertib and Dinaciclib in ten pancreatic cancer cell lines. Oncol Res Treat 2021;44(suppl 4): 220, ep438. Presented at the Annual Meeting of the German Society for Hematology and Medical Oncology 2021.

9 List of Figures and Tables

10 Eidesstattliche Erklärung

Ich versichere hiermit, dass ich die eingereichte Dissertation selbstständig und ohne fremde Hilfe verfasst, keine anderen als die angegebenen Quellen und Hilfsmittel verwendet und wörtlich oder inhaltlich entnommene Stellen der benutzen Quellen als solche kenntlich gemacht habe.

Rostock, den 26 September 2022

Yixuan Ma

11 Acknowledgement

During the past four years, I have spent a meaningful time in Rostock. Sincerely, I would give many thanks to person who helped me for accomplishing my doctoral dissertation.

First of all, I am particularly grateful to my supervisors Prof. Dr. med. Christian Junghanss for providing me with the opportunity to study in Germany, for the warm welcome, support and trust over the past four years.

My greatest gratitude goes to my supervisor PD Dr. rer. nat. Hugo Murua Escobar. Thank you for the provision of the study topic, the supervision during the doctoral working and the support, the trust and constructive criticism and the always positive words. Also, thank you so much for your help in my life and entertainment in Germany.

Many thanks to Sina Sender, Weibo Kong, Anett Sekora and Anna Richter for their help in experimental techniques, methods, data analysis and manuscripts; thanks to Gudrun Knübel and Saskia Krohn for their support in sequencing technology; thanks to my lab colleagues Simón Villa Pérez, Catrin Roolf, Carolin Gabler, Lisa-Madeleine Sklarz, Annika Eichhorst, Andrea Hobeck, Leon Eggers, Xin Shu, Claudia Maletzki, Inken Salewski, and Nina Schönewälder for their help and the happy times we spent together.

I would like to thank my cooperation partners for the great cooperation. A special thanks to Prof. Dr. Peter Bauer, Dr. Najim Ameziane, Dr. Ruslan Al-Ali, PD Dr. Frank Ulrich Weiss, Prof. Dr. Markus M. Lerch, PD Dr. Dietmar Zechner, Dr. Alisha Parveen, and Dr. Nares Trakooljul for their professional and prompt support.

Special thanks to the PiCoP project for financial, technical, and coordination support of this research.

Particularly, I would like to thank my family for their support in continuing my studies, their support has brought me to where I am today. Especially the endless encouragement in times of difficulty, the admiration for the highlight moments, and the surprises in my ordinary life, these things supported me to live and study alone far away from home.